SUPRAMOLECULAR CHEMISTRY OF CUCURBIT[N]URIL HOMOLOGUES WITH A DITOPIC GUEST AND LIGHT EMITTING CONJUGATED POLYMERS

A THESIS

SUBMITTED TO THE DEPARTMENT OF CHEMISTRY
AND THE GRADUATE SCHOOL OF ENGINEERING AND SCIENCE
OF BILKENT UNIVERSITY

IN PARTIAL FULFILLMENT OF THE REQUIREMENTS
FOR THE DEGREE OF
MASTER OF SCIENCE

By
MÜGE ARTAR
NOVEMBER 2011

I certify that I have read this thesis and in my opinion it is fully adequate, in scope and in quality, as a thesis of the degree of Master of Science

_____

Assoc. Prof. Dr. Donus Tuncel (Supervisor)

I certify that I have read this thesis and in my opinion it is fully adequate, in scope and in quality, as a thesis of the degree of Master of Science

_____

Prof. Dr. Engin Umut Akkaya

I certify that I have read this thesis and in my opinion it is fully adequate, in scope and in quality, as a thesis of the degree of Master of Science

_____

Prof. Dr. Özdemir Doğan

I certify that I have read this thesis and in my opinion it is fully adequate, in scope and in quality, as a thesis of the degree of Master of Science

Assoc. Prof. Dr. Hilmi Volkan Demir

I certify that I have read this thesis and in my opinion it is fully adequate, in scope and in quality, as a thesis of the degree of Master of Science

Asst. Prof. Dr. Emrah Özensoy

Approved for the Graduate School of Engineering and Science:

Prof. Dr. Levent Onural

Director of Graduate School of Engineering and Science

ABSTRACT

MÜGE ARTAR

M.S. in Chemistry

Supervisor: Assoc. Prof. Dr. Dönüş Tuncel

November 2011

The general objective of this thesis is to explore the ability of cucurbit[n]uril (CB[n]) (n= 6,7,8) homologues to form nano-structured supramolecular assemblies with various organic guests through self-sorting, self-assembly and recognition.

In the first part of the thesis, the selectivity and recognition properties of CB[n] homologues towards a ditopic guest have been investigated. The guest was synthesized through Cu(I)-catalyzed click reaction between the salts of N,N'-bis-(2-azido-ethyl)-dodecane-1,12-diamine and propargylamine and contain two chemically and geometrically distinct recognition sites, namely, a flexible and hydrophobic dodecyl spacer and a five-membered triazole ring terminated with ammonium ions. Complex formation between the guest and CB[6], CB[7] and CB[8] in the ratios of 1:2, 1:1 and 1:1, respectively, was confirmed by ^{1}H NMR spectroscopy and mass spectrometry. It was also revealed that CB[n] homologues have ability to self-sort and recognise the guests according to their chemical nature, size and shape. Kinetic formation of a hetero[4]pseudorotaxane via sequence-specific self-sorting was confirmed and controlled by the order of the addition.

In the second part, the effect of CB[n] homologues on the dissolution and the photophysical properties of non-ionic conjugated polymers in water were investigated. A fluorene-based polymer, namely, poly[9,9-bis{6(N,N dimethylamino)hexyl}fluorene-co-2,5-thienylene (PFT) was synthesized via Suzuki coupling and characterization was performed by spectroscopic techniques including 1D and 2D NMR(Nuclear Magnetic Resonans), UV–vis, fluorescent spectroscopy, and matrix-assisted laser desorption mass spectrometry (MALDI-MS)(Matrix Assisted Laser Desorption/Ionization Mass Spectroscopy). The interaction of CB[6], CB[7] and CB[8] with PFT have been investigated and it was observed that only

CB[8] among other CB homologues forms a water-soluble inclusion complex with PFT. Furthermore, upon complex formation a considerable enhancement in the fluorescent quantum yield of PFT in water was observed. The structure of resulting PFT@CB[8] complex was characterized through ^{1}H-NMR and selective 1D-NOESY(The Nuclear Overhauser Enhancement Spectroscopy) and further investigated by imaging techniques (e.g. AFM(Atomic Force Microscopy), SEM(Scanning Electron Microscopy), TEM(Transmission Electron Microscopy) and fluorescent optical microscopy) to reveal the morphology. The results suggested that through CB[8]-assisted self-assembly of PFT polymer chains vesicle-like nanostructures formed. The sizes of nanostructures were also determined using dynamic light scattering (DLS(Dynamic Light Scattering)) measurements.

Keywords: Cucurbituril, rotaxanes, self-recognition, self-sorting supramolecular chemistry, conjugated polymers, self-assembly, water-soluble polymers

ÖZET

MÜGE ARTAR

Kimya Bölümü Yüksek Lisans Tezi

Tez Yöneticisi: Doç. Dr. Dönüş Tuncel

Kasım 2011

Bu tezin genel amacı kükürbit[n]uril (CB[n]) (n= 6,7,8) homologlarının çeşitli organik misafir moleküller ile kendiliğinden sıralanma, bir araya gelme ve tanıma yoluyla nano-yapılar oluşturma yeteneklerini keşfetmekti.

Tezin ilk kısmında, CB[n] homologlarının iki ucunda fonksiyonel grup taşıyan bir zincir moleküle karşı gösterdiği seçicilik ve tanıma özellikleri araştırıldı. Misafir zincir molekül, bir N'-bis-(2-azido-etil)-dodekan-1,12-diamin tuzu ve propargilaminin Cu(I) kataliziyle girdiği klik reaksiyon sonucunda sentezlendi; bu misafir molekül kimyasal ve geometrik açıdan farklı olan, esnek ve hidrofobik bir dodesil grubu ve amonyum grubu ile sonlandırılmış iki adet beş üyeli triazol halkası taşır. Misafir molekül ve CB[6], CB[7], CB[8 homologları arasındaki sırasıyla 1:2, 1:1 ve 1:1 oranlarında kompleks oluşumu ^{1}H NMR ve kütle spektrometrisi ile doğrulandı. Bunun yanında kükürbituril 6, 7 ve 8 türevlerinin kimyasal doğaları, hacim ve şekillerine göre tanıma ve kendiliğinden sıralanma kabiliyetleri doğrulandı. Sıralanmaya özgü, kükürbityuril 6 ve 8 taşıyan, kinetik açıdan kontrol edilebilen ve oluşumu mikrodaire ekleme rejimine dayalı bir hetero[4]psödorotaksan oluşumu gözlendi.

Çalışmanın ikinci bölümünde ise, kükürbityuril türevlerinin iyonik olmayan konjüge polimerlerin sudaki çözünürlüklerine ve fotofiziksel özelliklerine olan etkisi araştırıldı. Floren bazlı bir konjüge polimerin, poli[9,9-bis{6(N,N-dimetilamino)hexil}floreneko-2,5-tiyonilen (PFT), Suzuki eşleşmesine bağlı sentezlenmesinin ardından 1D and 2D NMR, UV–vis, floresans spektroskopi ve matriks-destekli lazer salınım spektroskopisi (MALDI-MS) kullanılarak karakterizasyonu yapıldı. PFT polimerinin CB[6], CB[7] ve CB[8] homologları ile ilişkisi araştırıldı ve sadece CB[8] homoloğunun suda çözünür bir katılma kompleksi oluşturduğu gözlendi. Ayrıca, kompleks oluşumuna bağlı olarak floresan kuantum veriminde önemli oranda bir artma gözlendi. PFT@CB[8] kompleksinin yapısını

araştırmak için ^{1}H-NMR ve selektif 1D-NOESY yöntemleri, morfoloji tayini için ise çeşitli görüntüleme teknikleri (AFM, SEM, TEM, floresans optik mikroskopi vb.) kullanıldı. Sonuçlar kendiliğinden bir araya gelme yoluyla kükürbituril 8 güdümlü keseciklerin oluştuğunu gösterdi. Bu nanoyapıların boyutları ise dinamik ışık saçılımı (DLS) ölçümleri ile tayin edildi.

Anahtar kelimeler: Kükürbituril, rotaksanlar, kendiliğinden tanıma, kendiliğinden sıralanan süpramoleküler sistemler, konjüge polimerler, kendiliğinden bir araya gelme, suda çözünen polimerler

ACKNOWLEDGEMENT

"Becoming a scientist" is a never ending way and I am glad to have ...

A father who has started my journey via pushing me to find out number pi by using my cup for milk and a tapeline,

A mother who regave me my left eye and spread first seeds of humanism,

A brother who has educated me in the field of anger management,

All people who have been taking great pains for the world peace,

An advisor as Assoc. Prof. Dr. Dönüş Tuncel who guided me with great patience starting from my second year in the chemistry department and presented a brilliant example of being a scientist.

I owe many thanks to thesis juries Prof. Dr. Engin Umut Akkaya, Asst. Prof. Dr. Emrah Özensoy, Assoc. Prof. Dr. Hilmi Volkan Demir, Prof. Dr. Özdemir Doğan for reading my thesis and their valuable feedbacks.

I want to send my sincere thanks all present and former members of Bilkent University Chemistry Department, especially D.T. Laboratory members for their supports during my study; and also thanks to Mahmut Burak Şenol for his endless support.

LIST OF FIGURES

Figure 1. Schematic illustrating the difference between a cavitate and a clathrate: (a) synthesis and conversion of a cavitand into a cavitate by inclusion of a guest into the cavity of the host molecule; (b) inclusion of guest molecules in cavities formed between the host molecules in the lattice resulting in conversion of a clathrand into a clathrate; (c) synthesis and self-assembly of a supramolecular aggregate that does not correspond to the classical host-guest description.[7].....2

Figure 2. (a)Rigid lock and key and (b) induced fi t models of enzyme–substrate binding.[7].....4

Figure 3. Examples of cryptands, katapinands and calixarene.[7].....7

Figure 4. . α-, β-, γ- Cylodextrin derivatives.....8

Figure 5. First illustration of CB[6] by Mock et al.[20 b].....10

Figure 6. Top and side views of the X-ray crystal structures of CB[5],[7] CB[6],[2] CB[7],[7] CB[8],[7] and CB[5]@CB[10].[9] The various compounds are drawn to scale.[38].....12

Figure 7. (a) Representation of the different binding regions of CB[6], (b) Endo- and exocyclic methylene protons bearing magnetic non-equivalence.....13

Figure 8. Electrostatic Potential map for (a) α-CD and (b) CB[6][38].....14

Figure 9. Dependence of strength of binding to CB[6] upon chain length *n*-alkyl ammonium ions (o-o) and *n*-alkanediammonium ions (Δ-- Δ). Vertical axis proportional to free energy of binding (log K_d).[38].....16

Figure 10. Representation of a rotary molecular machine.....20

Figure 11. Schematic rep. of various types of main chain polyrotaxanes.....21

Figure 12. Schematic representation of types of side chain polyrotaxanes....22

Figure 13. (a) Excitation with 448 nm light induces the dynamic wagging motion of the nano impellers, but the nano valves remain shut the contents are contained. (b) Addition of NaOH opens the nanovalves, but the static nanoimpellers are able to keep the contents contained. (c) Simultaneous excitation with 448 nm light AND addition of NaOH causes the contents to be released.[148].....28

Figure 14. Conjugated polymer examples: A) Polyacetylene, B) Polypyrrole C) Polythiophene D) Poly (phenylene vinylene) E) Polyfluorene.....31

Figure 15. A model OLED.[120].....32
Figure 16. Suggested structures after the formation of complexes of CB homologues with **Axle A**……...……37

Figure 17. ^{1}H-NMR spectra of Axle A.....37

Figure 18. COSY spectra of Axle A.....39

Figure 19. ^{1}H NMR (400 MHz, D_2O, 25 °C) spectra of **Axle A**; the addition of (a) 0 equiv of CB[6] (b) 0.5 equiv of CB[6], (c) 1 equiv of CB[6], (d) 2.2 equiv of CB[6] (* denotes impurities).....40
Figure 20. Structure of CB[8]-Axle A and ^{1}H NMR (400 MHz, D_2O, 25 °C) spectra of Axle A; the addition of (a) 0 equiv of CB[8] (b) 0.5 equiv of CB[8], (c) 1.2 equiv of CB[8].....41
Figure 21. MALDI-mass spectrum of CB[8]-Axle A.....42
Figure 22. Proposed structure of CB[7]-Axle A and 1H NMR (400 MHz, D_2O, 25 °C) spectra of Axle A; the addition of (a) 0 equiv of CB[7] (b) 0.4 equiv of CB[7], (c) 0.9 equiv of CB[7], (c) 1.3 equiv of CB[7] 43
Figure 23. MALDI-mass spectrum of CB[7]-Axle A.....44
Figure 24. The 1H NMR spectra (400 MHz, 25 8C, D_2O) of a) Axle A+ CB[8]; b) 10 min later after addition of 2 equiv CB[6] to (a); c) 2 h later after addition of 2 equiv CB[6] to (a); d) 24 h later after addition of 2 equiv CB[6] to (a); e) 96 h later after addition of 2 equiv CB[6] to (a). Rectangle and sphere denote protons from hetero[4]pseudorotaxane and [3]pseudorotaxane respectively; the peak at d=3.25 ppm is assigned to MeOH residue.....45
Figure 25. MALDI-mass spectrum of Axle A+ 1 C B[8]+ 2 C B[6] 46

Figure 26. ^{1}H-NMR spectrum of PFT in $CDCl_3$.....49
Figure 27. FT-IR spectrum of PFT 49

Figure 28. MALDI-TOF mass spectrum of PFT from a trihydroxy acetophenone (THAP) matrix 49
Figure 29. ^{1}H-NMR (400 MHz, 298 K) spectrum of protonated PFT in D_2O (3mM) …….....50

Figure 30. 1H-NMR (400 MHz, 298 K) spectra of (a) PFT $CDCl_3$, (b) PFT@CB[8] (3 mM) in D_2O, and (c) 1D-NOESY spectrum of PFT@CB[8] in D_2O, proton Hx at 5,73 ppm was irradiated, mixing time D: 100 ms (* for $CHCl_3$) 51
Figure 31. ^{1}H-NMR (400 MHz, 298 K) spectra of (a) M2 in $CDCl_3$, (b) protonated M2 (M2H) in D_2O, (c) M2H (4 mM) in the presence of 1 equiv CB[8] in D_2O, and (d) M2 (4 mM) in the presence of 1 equiv CB[8] in D_2O.....52
Figure 32. Selective 1D-NOESY NMR spectra of M2H@CB[8] (400 Mz, D_2O, 25 °C)…….....53

Figure 33. Selective 1D-NOESY NMR spectra of PFT@CB[8] (400 Mz, D_2O, 25 °C), Mixing time D: 100 ms…….....….....54

Figure 34. Suggested structure based on the 1H and 1D-NOESY NMR data for the PFT@CB[8] complex formation.....54

Figure 35. (a) UV–vis absorption, (b) emission spectra of PFT in methanol, protonated PFT in water and PFT@CB[8] in water.....55
Figure 36. DLS results of PFT@CB[8] before and after filtration…….....57

Figure 37. AFM image of PFT@CB[8].....58

Figure 38. SEM image of PFT@CB[8].....58

Figure 39. TEM image of PFT@CB[8].....58

Figure 40. FOM (40x magnification) image of PFT@CB[8].....59
Figure 41. Suggested structure for the vesicles formation.....60

LIST OF SCHEMES

Scheme 1. The equilibrium between a host-guest complex and the free species.....5

Scheme 2. The selectivity between GUEST1 and GUEST2.....5

Scheme 3. Pedersen's first synthesis of dibenzo[18]crown-6.....6

Scheme 4. Synthesis of CB[6] from 1a under forcing conditions and a mixture of CB[n] under milder conditions. a) CH_2O, HCl, heat; b) H_2SO_4; c) CH_2O, HCl, 100°C, 18 h. [38].....11

Scheme 5. Catalysis of a [3+2] dipolar cycloaddition inside CB[6].[38].....17

Scheme 6. A 4-component self-sorting system that owes its high fidelity to the following facts: (*i*) benzo-21-crown-7 (**C7**) is not able to pass over a phenyl group under the conditions of the experiment. Thus, the formation of a pseudorotaxane with **1**-H_PF6 is kinetically hindered; (*ii*) the complexation of **2**-H_PF6 with **C7** is thermodynamically more stable than that with dibenzo-24-crown-8 (**C8**); (*iii*) **C8** thermodynamically prefers **1**-H_PF6 over **2**-H_PF6.[80].....19

Scheme 7. Chemical conversion method.....22

Scheme 8. Schematic representation of the methods for the synthesis of rotaxanes polyrotaxanes[101].....22

Scheme 9. CB[6]-based molecular switch.[38].....24

Scheme 10. pH driven states of a porphyrin-based molecular switch.[123].....24

Scheme 11. pH and heat driven CB[6]-based bi-stable molecular switch.[[124].....26

Scheme 12. The π-π stacking can be easily tuned through the addition of the macrocyclic hosts CB[7] and CB[8] as well as select small molecule competitive guests.[40] 29

Scheme 13. Yamamoto(A), Suzuki(B) and Stille(C) coupling for polyfluorene synthesis.[120]
.....32

Scheme 14. (a) 2 equivalents of propargylamine, $CuSO_4.5H_2O$, sodium ascorbate,room temperature, 24h, in ethanol-water mixture, % 92; (b) Diluted HCl (aq.), room temperature, 24h, %
95.....36

Scheme 15. (a) $Br(CH_2)_6Br$, 50% wt. NaOH (aq.), DMSO, 64 % (b) THF, 94% (c) $PdCl_2$(dppf), K_2CO_3, H_2O/THF,
77%.....47

LIST OF TABLES

Table 1. Summary of supramolecular interactions[7].....1

Table 2. [a] The values quoted for a, b, and c for CB[n] take into account the van der Waals radii of the relevant atoms. [b] Determined from the X-ray structure of the CB[5]@CB[10] complex.[38].....12

Table 3. Photophysical Data of PFT in MeOH, Proton-PFT, PFT@CB[8].....62

Table 4. Photophysical data for PFT in methanol, protonated PFT and PFT@CB[8].....63

ABBREVIATIONS

CB	Cucurbituril
MALDI-TOF	Matrix Assisted Laser Desorption/Ionization Time-Of Flight
FT-IR	Fourier Transform-Infrared
^{1}H-NMR	Proton-Nuclear Magnetic Resonance
^{13}C-NMR	Carbon13-Nuclear Magnetic Resonance
D_2O	Deuterated Water
THAP	2,4,6-trihydroxy acetophenone
MeOH	Methanol
EtOH	Ethanol
DLS	Dynamic Light Scattering
TEM	Transmission Electron Microscopy
AFM	Atomic Force Microscopy
SEM	Scanning Electron Microscopy
NOESY	The Nuclear Overhauser Enhancement Spectroscopy) and further
PFT	Poly[9,9-bis{6(N,N dimethylamino)hexyl}fluorene-co-2,5-thienylene

TABLE OF CONTENTS

Chapter 1.Introduction.....1

1.1 Supramolecular Chemistry.....1

1.1.1 Host-guest Chemisty.....3

1.1.1.1 Driving Forces in Host-Guest Chemistry.....4

1.1.1.2 Examples of Hosts for Guest Binding.....6

1.1.1.2.1 Cation Binding Hosts.....6

1.1.1.2.2 Neutral Molecule Binding Hosts 8

1.1.1.3 Cucurbiturils.....9

1.1.1.3.1 Synthesis of CB[n] 10

1.1.1.3.2 Dimensions and Structure.....12

1.1.1.3.3 Physical Properties.....15

1.1.1.3.4 Host-guest Chemistry of CB[n].....15

1.1.1.3.5 The Ability of CB Homologues to Catalyze 1,3-Dipolar Cycloaddition.....17

1.1.2 Self-Sorting 18

1.1.3 Molecular Machines.....19

1.1.4 CB[n] Containing Materials.....20

1.1.4.1 Mechanically Interlocked Complexes.....20

1.1.4.2 Rotaxanes, Pseudorotaxanes, Polyrotaxanes.....20

1.1.4.3 Other Examples of CB[n] Containing Materials.....28

1.1.4.3.1 In Frameworks.....28

1.1.4.3.2Controlling Supramolecular Aggregates by Using CB[n].28

1.1.5 Fluorene Based Conjugated Polymers.....29

Chapter 2. RESULTS AND DISCUSSION.....34

Section 1.....35

2.1.1 Synthesis and Characterization of the Axle A.....37

2.1.2 Hetero[4]Pseudorotaxane formation via complexation of Axle A with both CB[6] and CB[8] Homologues Simultaneously.....42

Section 2.....53

2.2.1 Synthesis and Characterization of poly[(9,9-bis (Dimethylamino-hexyl)-9H-fluorene)-benzene] (PFT) 53

2.2.2 Synthesis and Characterization of PFT@CB[8] Complex.....47

Chapter 3. CONCLUSION.....61

Chapter 4. EXPERIMENTAL SECTION.....62

4.1 Materials.....62

4.2 Instrumentation.....62

4.3 Synthesis 63

4.3.1 Synthesis of N,N'-Bis-[1-(2-amino-ethyl)-1H-[1,2,3]triazol-4-ylmethyl]-dodecane-1,12-diamine.....64

4.3.2 Synthesis of (9,9-bis (3-bromo-hexyl)-9H-fluorene).....64

4.3.3 Synthesis of (poly[(9,9-bis (Dimethylamino-hexyl)-9H-fluorene)-benzene]).....65

4.3.4 Synthesis of PFT@CB[8] Complex:.....66

REFERENCES.....68

Chapter 1

Introduction

1.1 Supramolecular Chemistry

Supramolecular chemistry is a relatively new field of chemistry that came of age with Nobel Prize awarded (1987) studies of Donald J. Cram[1], Jean-Marie Lehn[2], and Charles J. Pedersen[3]. If the atoms are the letters, if the molecules are the words, and if the supermolecules are the phrases, as J.F. Stoddart suggested[4] then supramolecular chemistry is the branch that aims to understand the structure, function, and properties of these phrases made up of molecules that are bound together with non-covalent forces as hydrogen bonding, metal coordination, hydrophobic forces, pi-pi interactions, van der Waals forces, ionic and dipolar forces.[5] These non-covalent forces are considerably weaker than covalent bonding as seen in Table 1 but in a supramolecular system, non-covalent interactions are designed in a co-operative way that yields a stable complex.[6]

Interaction	**Strength (kJ mol^{-1})**
Ion-ion	200-300
Ion-dipole	50-200
Dipole-dipole	5-50
Hydrogen bonding	4-120
Cation- π	5-80
π –π	0-50
Van der Waals	< 5 kJ mol^{-1} but variable depending on surface area
Hydrophobic	Related to solvent-solvent interaction energy

Table 1. Summary of non-covalent interactions[7] Reproduced with permission from ref. 7. Copyright 2009 John Wiley and Sons.

However, definition of a supermolecule is enlarged by supramolecular photo chemists with covalently bounded systems in which different parts as chromophores, spacers and a redox centre contribute their own properties in a systematic way yielding one output. Although supramolecular chemistry was originally described as the non-covalent interaction between host and guest, a modern approach to supramolecular chemistry consists also processes as molecular recognition, molecular devices and machines.[7]

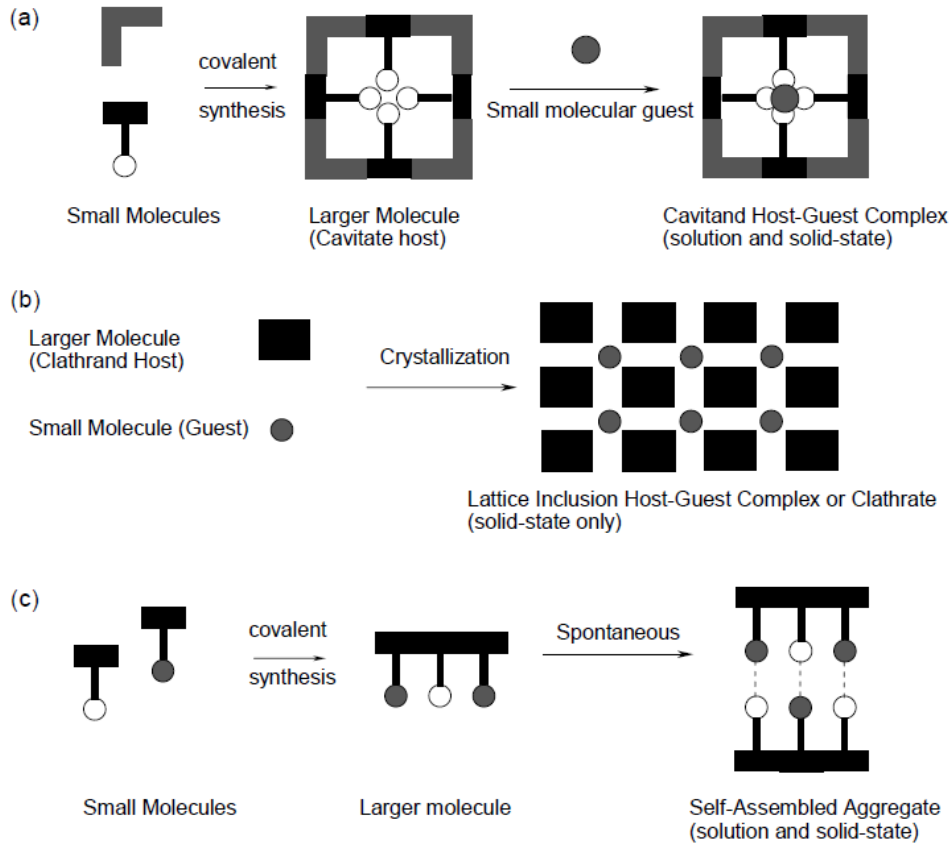

Figure 1. Schematic illustrating the difference between a cavitate and a clathrate: (a) synthesis and conversion of a cavitand into a cavitate by inclusion of a guest into the cavity of the host molecule; (b) inclusion of guest molecules in cavities formed between the host molecules in the lattice resulting in conversion of a clathrand into a clathrate; (c) synthesis and self-assembly of a supramolecular aggregate that does not correspond to the classical host-guest description.[7] Reproduced with permission from ref. 7. Copyright 2009 John Wiley and Sons.

Supramolecular chemistry can be classified in two broad categories as host-guest chemistry and self assembly, in which classification is done in terms of size and shape comparison among interacting molecules. Host-guest condition occurs for two molecules which differ from each other in a way that one can host the other one by providing a hole or can wrap around the guest. [6] However in self-assembly case, building blocks do not differ in size and shape as one of them can serve as host or guest.[7]

Supramolecular chemistry has set its goal as the synthesis of supramolecular assemblies possessing new functions that cannot appear from a single molecule or ion, based on light responsiveness, novel magnetic properties, catalytic activity, fluorescence, redox properties, etc.[2] New materials that are bearing aforementioned functions can help enhancing the performance of materials present, decrease undesired properties of the materials present or yield a brand new approach that is intimately related to nanotechnology.

1.1.1 Host-guest Chemisty

Host-guest chemistry as being a fruitful branch of supramolecular chemistry, investigates complexes consisting two or more molecules or ions that are formed through interactions that aforementioned non-covalent forces result in. Before further explanation on driving forces for these complexes, different types of host-guest interactions need to be clarified from a topological point of view. The first example of host-guest structures was given by H.M.Powell[8] from Oxford University in 1948 as clathrates that are inclusion complexes composed of two or more components that are associated without ordinary chemical union, but through complete enclosure of one set of molecules in a suitable structure formed by another. In the cavitand case, host bears a permanent intramolecular cavity for the guest in both solid state and in solution.[9] Moreover, the fact that guest should bear binding sites which diverge in the complex while binding sites of the host that converge, can be considered as the difference between host-guest and self-assembly case in which complexing agents cannot be distinguished as in the previous case.[6] Another subdivision should be made among the terms “cavitate”, “clathrate” and “complex”; if host-guest interaction is built through primarily electrostatic interactions, complex is used as

description and in the case less specific and non-directional interactions “cavitand” or “clathrate” is used.[7]

1.1.1.1 Driving Forces in Host-Guest Chemistry

For a better understanding of how the field of supramolecular and particularly host-guest chemistry have been established, some essential concepts that are introduced independently and even do not follow each other in a chronological manner should be addressed. In 1906, concept of a biological receptor was introduced by Paul Ehrlich from the study on molecules that do not act if they do not bind. Emil Fischer introduced the fact that binding must be selective in the means of having a guest that is complementary to host by size and shape, in 1894. Fischer’s recognition of lock and key model which would be developed by Daniel Koshland’s induced fit theory later, built a basis for molecular recognition.[Figure 2] In 1893, mutual attraction between host and guest has been already enlightened with the recognition of dative bond concept in coordination chemistry by Alfred Werner.[7]

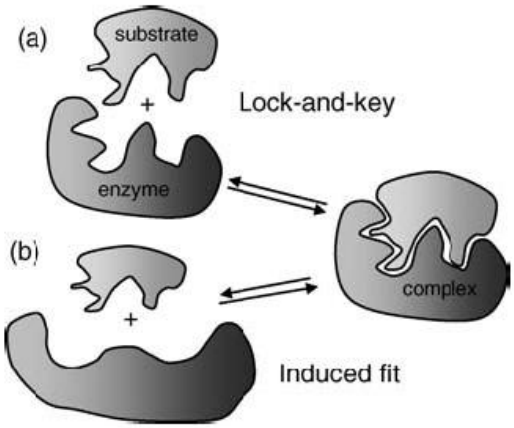

Figure 2. (a)Rigid lock and key and (b) induced fit models of enzyme–substrate binding.[7] Reproduced with permission from ref. 44. Reproduced with permission from ref. 7. Copyright 2009 John Wiley and Sons.

All of aforementioned concepts like selectivity, complementarity and additionally preorganization and macrocyclic effect bear vital importance in host design. Selectivity plays an important role in the case of having various kinds of guests; selectivity occurs if binding of one guest or guests of same kind is significantly

stronger than others. It should be noted that there are two kinds of selectivity that can be called as thermodynamic and kinetic selectivity. Thermodynamic selectivity can be described as ratio of binding constants for a host binding two different guests as following;

If equilibrium between a host-guest complex is defined as,

$$\text{Host} + \text{Guest} \Leftrightarrow \text{Host.Guest}$$

$$K = \frac{[H.G]}{[H].[G]}$$

Scheme 1. The equilibrium between a host-guest complex and the free species.

selectivity can be defined as,

$$\text{Selectivity} = \frac{\text{KGUEST 1}}{\text{K GUEST 2}}$$

Scheme 2. The selectivity between GUEST1 and GUEST2.

and kinetic selectivity is determined by the rate at which substrates that are competing for transformation upon guest binding in an enzyme-based process. Complementarity is a key concept for selectivity in other words it determines the affinity of a host for a guest and as Cram stated, for complexation, hosts must bear binding sites that can cooperatively interact and attract binding sites of guest without bonding covalently.[1]

If the scope is moved on host itself, it can be stated that as a host undergoes less conformational change upon guest binding, it is more preorganised. Preorganisation enables macrocycles to pay in advance for unfavourable repulsion and desolvation effects during macrocycle synthesis yielding more stable complexes in either enthalpic (a result of unfavourable interactions due to being in close proximity) and entropic (being conformationally less flexible that lose fewer degrees of freedom upon complexation) terms.

1.1.1.2 Examples of Hosts for Guest Binding

Once the guest molecule is known, one can design artificial hosts by using tools of complementarity and preorganisation. These artificial host molecules can be further optimised through adjusting their interaction abilities like solubility properties in working media and addition of other functional groups for a better selectivity.

1.1.1.2.1 Hosts for Cationic Guest Binding

Some common neutral cation binding hosts are crown ethers, cryptands, podands, cyclophanes and calixarenes; these molecules complex with guests through hydrogen bonding, cation-π or π-π interactions.[6]

Discovery of crown ethers was introduced by Pedersen[3] in 1967 in a fortious way as a side product of a bis(phenol) derivative (Scheme 2). After first synthesis, investigation of the extent of binding with various metal cations were performed by Pedersen and subsequently selectivity of different analogues bearing various combinations of donor atoms towards alkali metals were also studied.[10] Ammonium, arenediazonium, guanidium, tropylium and pyridinium complexes of crown ethers were also investigated. Some open-chained structures also serves as hosts like podands that was further developed as dendrimers.[11]

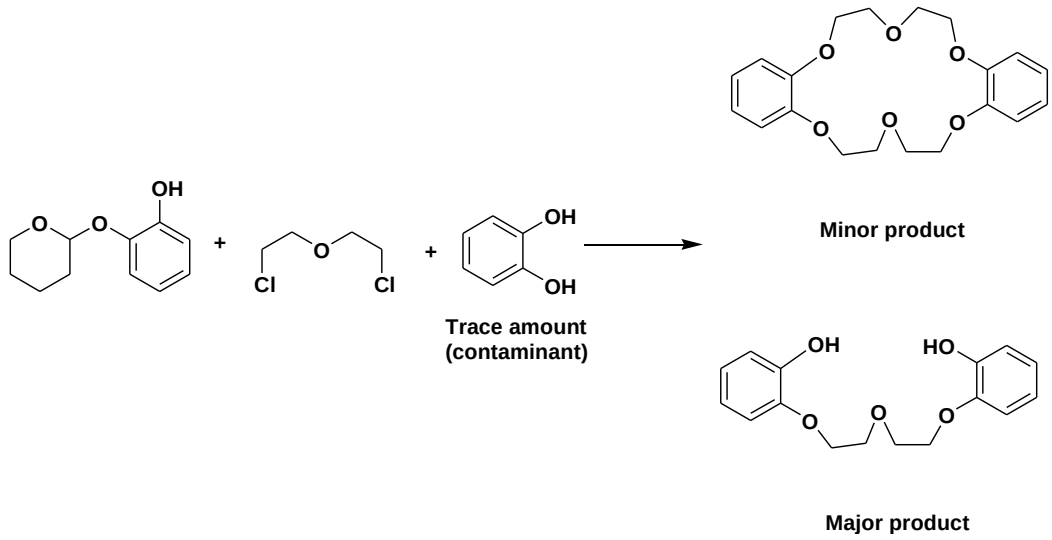

Scheme 3. Pedersen's first synthesis of dibenzo[18]crown-6

Study of Pedersen on crown ethers was followed by J.M.Lehn[2] with the synthesis of a three-dimensional structure for the complete encapsulation of ions from solution and this structure was called as cryptand which implies to bury the guest. Their complexes with various metals were also studied.

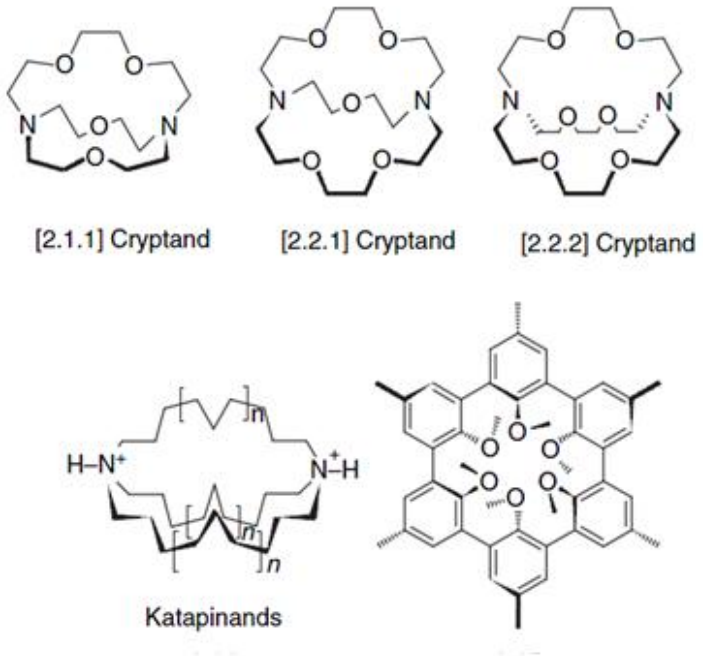

Figure 3. Examples of cryptands, katapinands and calixarene.[7] Reproduced with permission from ref. 7. Copyright 2009 John Wiley and Sons.

Cyclophanes are another type of host molecules that bear bridged aromatic rings and cavities for guest accomodation.[7] Beside cations, neutral molecules also can be encapsulated by these host molecules.[12]

Calixarenes are products of condensation reaction between a *p*-substituted phenol and formaldehyde and its name comes from a Greek name “calix crater” meaning vase like its shape in which an upper and a lower rim exist.[7] Due to the advantage of being easily functionalised from both upper and lower rims their various derivatives are used in enzyme mimicing applications and also alkali, alkali earth and other metal ions.[13-15]

1.1.1.2.2 Hosts for Neutral Guest Binding

Cyclodextrins are cyclic oligosaccharides that are produced from starch via enzymatic conversion. In 1891, A.Villiers[16] firstly described them as "cellulosine" and then F.Schardinger described three naturally occurring cyclodextrin derivatives –α, -β, -γ.[Figure 5] Like calixarene family, cyclodextrines also bear upper and lower rims that are decorated with secondary and primary hydroxyl groups, respectively, and their hydrophobic cavity enables water soluble inclusion complexes in aqueous media. Like calixarenes, cyclodextrins can also be easily functionalised in order to adjust solubility properties, optimise the affinity for a particular guest and yield in catalytic functions.[17]

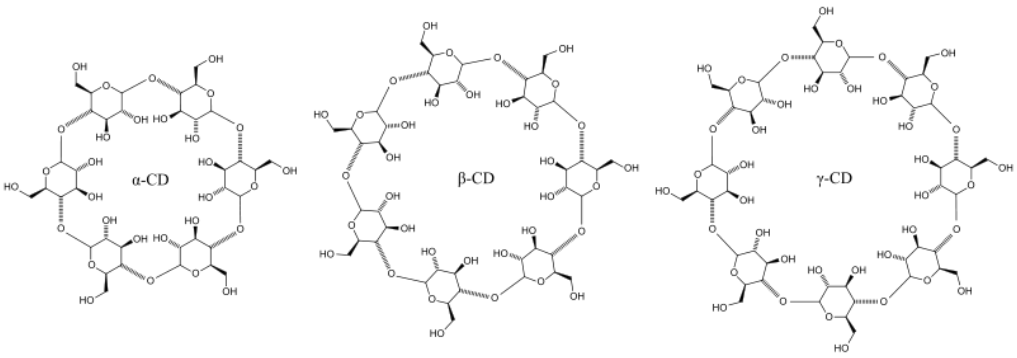

Figure 4. α-, β-, γ- Cylodextrin derivatives.[51]

1.1.2.3 Cucurbiturils

Since Cucurbit[n]uril derivatives employed as macrocycle in the supramolecular systems taking part in this thesis, this family of molecules is discussed in more detail. Story of cucurbiturils has taken a start unknowingly as "a mysterious white material", a product of acid-catalyzed condensation of glycouril and excess formaldehyde, in 1905. Robert Behrend[18], a German chemist known as the father of this remarkable macrocycles, recognized complex formation ability of these cross-linked aminal-type polymer with metal salts like $KMnO_4$, $AgNO_3$, H_2PtCl_6, $NaAuCl_4$ or organic dyes like congo red or methylene blue and also water-solubility in the presence of protons or alkali ions. This macrocycle, also known as Behrend's

polymer, was not constitutionally identified until reinvestigation of Mock et al. 1981; investigation yielded in a macrocyclic structure consisting six glycouril units and twelve methylene bridges. [19] Figure 6 below was the first depiction of this macrocycle and Mock et al. cited that magnetic non-equivalence of the methylene protons arises from endo- and exocyclic orientations as the reason for a closed, center symmetric depiction of this polymeric material. The name, cucurbituril was given to this macrocycle by Mock and co-workers due to its resemblance of a gourd or pumpkin, the most prominent member of the cucurbitaceae family. It should be also note that Mock et al. have found the name cucurbituril reasonable due to existence of similarly shaped and named alembic of the early chemists.

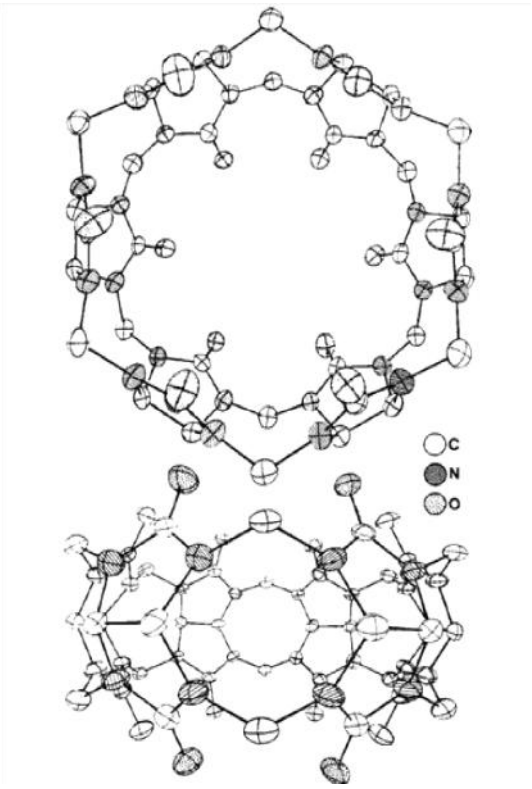

Figure 5. First illustration of CB[6] by Freeman et al.[20 b] Reproduced with permission from ref. 19 1981 American Chemical Society.

Cucurbituril chemistry can be classified as a new field of chemistry that was mainly established after Behrend discovery by Mock, Buschmann and co-workers, Kim and co-workers and Steinke after 1980. However, today applications of these molecules are leading supramolecular chemistry in the fields of pH-responsive molecular switches[21], rotaxanes-polyrotaxanes[22-25], catalysis[23-25], self-assemblies with polymeric materials[26,27], biology[28,29], drug binding and delivery[30,31], molecular

sensing[32-34] and surface functionalisation of materials[35,36]. Cucurbituril family employs as a key molecule for all of those aforementioned fields related strongly to nanotechnology due to synthetic control over size, shape and functionalisation, selectively binding properties, high chemical stability, low toxicity, controllable kinetics via stimuli and commercial availability.[26]

1.1.1.2.3.1 Synthesis of CB[n]

Original discovery of cucurbiturtil by Behrend et al.[18] in 1905 and further investigation on this macrocycle's structure by Mock et al.[19] in 1981 has not been followed by report of other homologues of cucurbituril family until groups of Kimoon Kim[23] and Anthony Day[37] report on the synthesis and isolation of CB[5]-CB[8] and research group Anthony Day also isolated CB[5]@CB[10] homologue as products under milder, kinetically controlled conditions (100°C, conc. HCl, or 75°C, 9M H_2SO_4).[38] Both of the research groups exploited advantage of the differences in solubility of the different homologues in water and aqueous acidic solution during isolation process. From the work of Kim et al. and Day et al., it is known that odd-numbered analogues like CB[5] and CB[7] bears a better solubility over other analogues of the family in different solvent mixtures. Isaacs et al.[39] reported another isolation technique consisting column chromatography with a harsh acidic eluent (HCO_2H-HCl mixture).

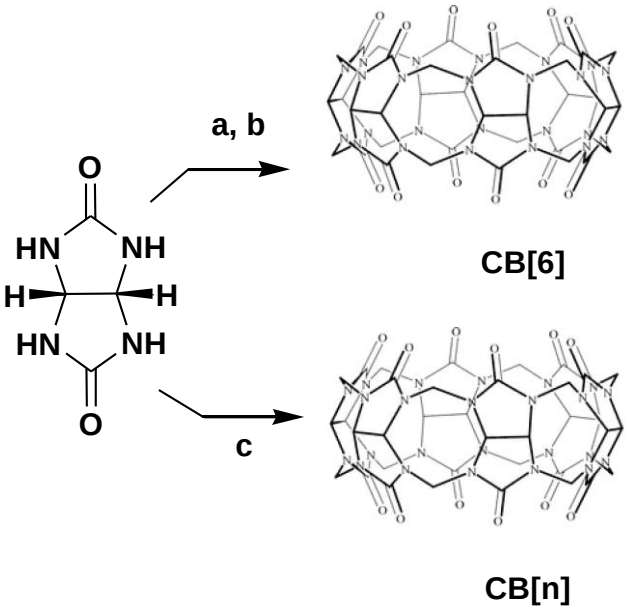

Scheme 4. Synthesis of CB[6] from 1a under forcing conditions and a mixture of CB[n] under milder conditions. a) CH_2O, HCl, heat; b) H_2SO_4; c) CH_2O, HCl, 100°C, 18 h. [38] Reproduced with permission from ref. 38. Copyright 2005 John Wiley and Sons.

It should be noted that all aforementioned time consuming purification methods were bearing a risk of toxicity and limitation in scaling-up; a new approach presented by Scherman group[40], which they called as a "greener" method for purification. This approach consists of ionic liquid binding and solid state metathesis reaction; they used 1-ethyl-3-methylimidazolium bromide reagent to bind CB[7] selectively where CB[5] remained in solution and CB[7]-[C_2mim]PF_6 complex precipitated and resulted in an aqueous solution of pure CB[5]. Then solid CB[7]-[C_2mim]PF_6 complex was converted back to its bromide form via a solid state reaction yielding pure CB[7] with a very high yield (71 %) in a reasonable purification time.

1.1.1.2.3.2 Dimensions and Structure

X-ray crystal structures of the various homologues shown in Figure 7 and Table 2 revealed cavity volumes that were comparable to previous cyclodextrin derivatives, with a potential application as a molecular container.[38]

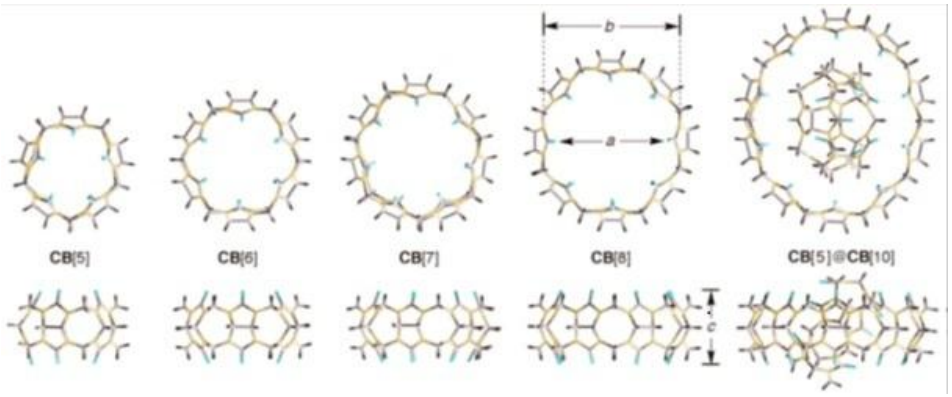

Figure 6. Top and side views of the X-ray crystal structures of CB[5],[7] CB[6],[2] CB[7],[7] CB[8],[7] and CB[5]@CB[10].[9] The various compounds are drawn to scale.[38] Reproduced with permission from ref. 38. Copyright 2005 John Wiley and Sons.

	M_r	a [Å][a]	b [Å][a]	c [Å][a]	V [Å^3]
CB[5]	830	2.4	4.4	9.1	82
CB[6]	996	3.9	5.8	9.1	164
CB[7]	1163	5.4	7.3	9.1	279
CB[8]	1329	6.9	8.8	9.1	479
CB[10][b]	1661	9.0- 11.0	10.7-12.6	9.1	-
α-CD	972	4.7	5.3	7.9	174
β-CD	1135	6.0	6.5	7.9	262
γ-CD	1297	7.5	6.3	7.9	427

Table 2. [a] The values quoted for a, b, and c for CB[n] take into account the van der Waals radii of the relevant atoms. [b] Determined from the X-ray structure of the CB[5]@CB[10] complex.[38] Reproduced with permission from ref. 38. Copyright 2005 John Wiley and Sons.

Other structural features also revealed by Mock et al.[19] after characterization of CB[6] through IR, ^{1}H, ^{13}C NMR. The carbonyl absorption at 1720 cm^{-1} indicated glycouril units while the presence of three signals, a doublet at around 4.5 ppm and a

singlet and a doublet at about 5.5 ppm with equal intensity in the ^{1}H NMR spectrum verified a highly symmetric non aromatic structure. As mentioned before Mock et al. cited that magnetic non-equivalence of the methylene protons arises from endo- and exocyclic orientations as the verification of methylene bridges, a hydrophobic cavity and two identical carbonyl containing portals revealed by X-ray data.

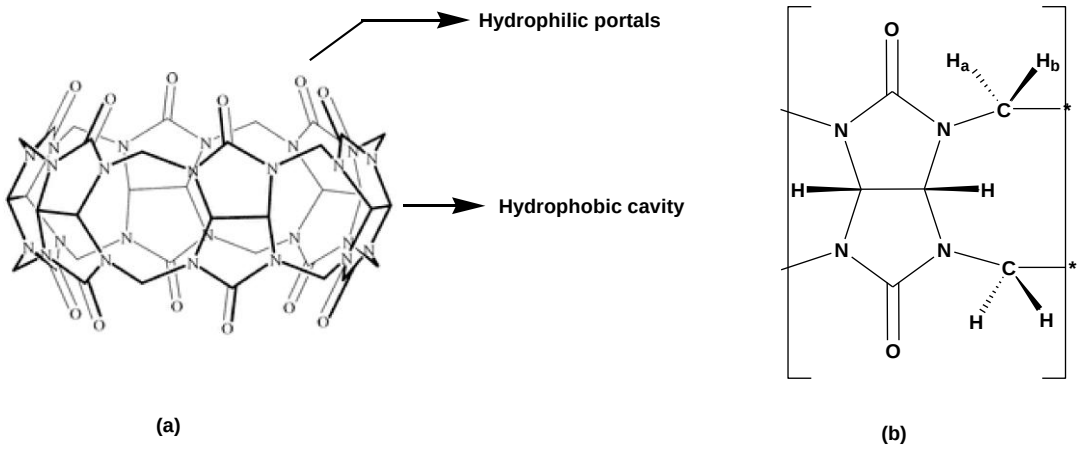

Figure 7. (a) Representation of the different binding regions of CB[6], (b) Endo- and exocyclic methylene protons bearing magnetic non-equivalence.

Electrostatic potential is an important parameter for the molecular recognition properties of a molecule and the map below shows a β–CD and CB[7]; as it can be seen from the Figure 9 portals of CB derivative more negative than cyclodextirn derivative, that makes CB a better molecular recognition agent which resembles a significant preference for cationic guests.[41]

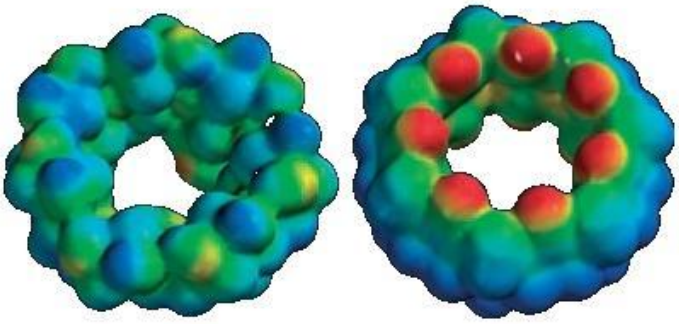

Figure 8. Electrostatic Potential map for (a) α-CD and (b) CB[6] [38] Reproduced with permission from ref. 38. Copyright 2005 John Wiley and Sons.

1.1.1.2.3.3 Physical Properties

Water solubility of CB[n] family is one of the important challenges since CB[6] and CB[8] are insoluble and CB[5] and CB[7] are modestly soluble in water.[38] Solubility of CB[5]-CB[8] in concentrated aqueous acid increase dramatically due to the fact that the pKa value of the conjugate acid of CB[6](pKa values for other homologues were expected to be same.) is 3.02 since the carbonyl groups lining the portals of CB[n] are weak bases.[42-48] Another property of CB[5]-CB[8] homologues was reported as their high thermal stability shown by thermal gravimetric analysis as exceeding 370°C.[48]

1.1.1.2.3.4 Host-guest Chemistry of CB[n]

Due to being the first purely obtained member of CB family, CB[6] host-guest chemistry was known better compared to other family members. First attempt for the study of CB[6] complexes was made by Mock et al. [50] with amines. The structural features of CB[6] (exactly same with other members except that the number of repeating units), consisting carbonyl decorated portals and a hydrophobic cavity resulted in stable complexes according to binding constants with amines and when compared with α-cyclodextrins for their amino complexes' stability, it was reported

by Buschmann et al.[48] and Mock et al.[50] that CB[6] exhibited a better stability. These results were interpreted as the result of electrostatic interactions between CB[6] and guests while CD derivatives lacked in that point. However, another investigation comparing affinities of [18]crown-6 and CB[6] towards several cations resulted in a generally equaling or exceeding manner of CB[6].[52-58]

Studies of Mock et al.[50] also revealed the affinity dependence on chain length as depicted in below Figure 10. Optimum chain length for the most favourable interaction was reported as diaminopentane and diaminohexane for diaminoalkane species while *n*-butylamine as a monoaminoalkane was reported as having the highest affinity for CB[6] due to fulfilment of the spatial arrangement between host and guest for the sake of complementarity.

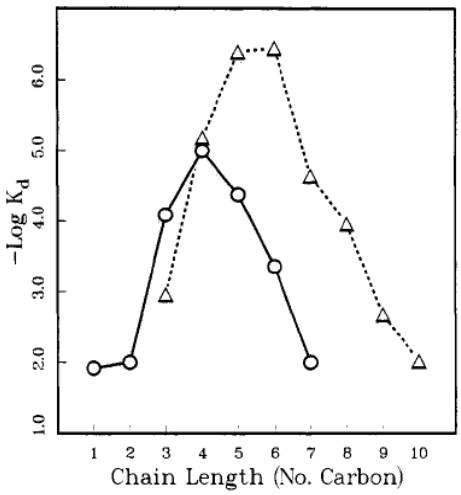

Figure 9. Dependence of strength of binding to CB[6] upon chain length *n*-alkylammonium ions (o-o) and *n*-alkanediammonium ions (Δ-- Δ). Vertical axis proportional to free energy of binding (log K_d).[38] Reproduced with permission from ref. 38. Copyright 2005 John Wiley and Sons.

While CB[6] is compared with its analogic member of α-CD in CD family, CB[7] is compared with β-CD in terms of their volumes and CB[7] is known to be more voluminous than its analogues.[38] This property enables CB[7] to be able to bind a wider number of positively charged aromatic guest including adamantanes and

bicyclooctanes,[59, 60, 61, 62] naphthalene,[63, 64, 65] stilbene,[66] viologen,[67-71] o-carborane,[72] ferrocene,[73] and cobaltocene[73] derivatives .

When compared with γ-CD, CB[8] bears a more complex recognition behaviour due to being capable of binding two aromatic rings simultaneously.[74] This simultaneous binding capability was used by Kim and co-workers as a recognition motif to control intramolecular folding processes.[75] Scherman et al. also contributed this stoichiometry dictated complexes of CB[8] in the field of controlling self-assembled structures and aggregated motifs based on aryl/alkylimidazolium salts in water.[76]

It should be also noted that the remarkable complex of CB[5]@CB[10] as established by X-ray crystallography is reported to resemble a gyroscope and this kind of molecular gyroscopes are classified as potential components of future molecular machines.[38]

1.1.1.2.3.5 The Ability of CB Homologues to Catalyze 1,3-Dipolar Cycloaddition

As it is shown in below Scheme 5 illustrating a particular example, alkynes undergo 1,3-dipolar cycloadditions with alkyl azides, to yield in a mixture of 1,4- and 1,5-regioisomers of 1,2,3-triazole in a considerably slow manner.(k_0 = 1.16 x 10^{-6} M^{-1} s^{-1} in aqueous formic acid at 40 °C) [77] In 1983, Mock et al. reported another remarkable feature of CB[6] as being able to accelerate this 1,3-dipolar cycloaddition by a factor of 5.5 x 10^4 ,in a regiospecific fashion. Mock et al. [77] explained this catalytic effect as a result of the good match between volume of CB[6] cavity and transition state consist of alkyne and alkyl azide at van der Waals distance in a compressed manner, recalling Pauling principle for catalysis. It is important to note that lock and key principle was demonstrated in a nonbiochemical host-guest system for the first time.

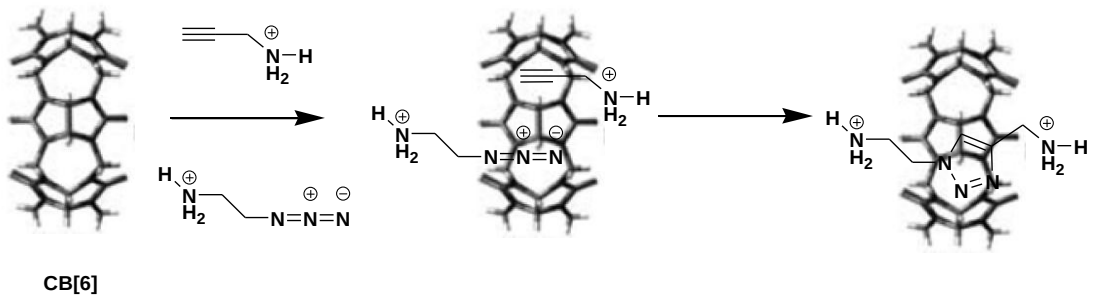

Scheme 5. Catalysis of a [3+2] dipolar cycloaddition inside CB[6].[38] Adopted from ref. 44.

This nonbiochemical host-guest system was resounded with its potential applications in biology after the discovery of Cu^{I} as a catalyst for this 1,3-dipolar cycloaddition in a regiospecific manner.[78] Since Cu^{I} is an undesirable substance for many biological application, CB[6] has been described as a harmless catalytic alternative.[27] This advantage has substantially increased application areas of CB[6] in parallel with the use of click chemistry which was known as a philosophy of tailoring synthetic chemistry tools in a way that is making use of already existing small units in an elegant way to obtain desired products.

Tuncel et al. reported that other CB derivatives also investigated for their catalytic effects on 1,3-dipolar cycloaddition but due to lack of a good match of transition state with the interior volume of the macrocycle, no enhancement was recorded.[27]

1.1.2 Self-Sorting

Self- sorting phenomena [79, 80] is one of the key concepts in molecular recognition and defined as the ability to efficiently distinguish between self and nonself within complex mixtures[81] ; however, previous definition works for the biochemical processes related to proteins, DNA, immune system etc. where high fidelity recognition processes bear a vital role. [82] Self- sorting in biology can be also defined as an ability of a system to respond stimuli and to adapt environment in a manner eventually yields in evolution.[83] For today's chemist, who is seeking answers for the question "Why we cannot make life?"[84] and consequently classifying "adaptability" as one of the pillars of building life and survival, understanding and using tools of

self-sorting is an initial step for the preparation and consequently development of complex molecular systems.[83]

From the supramolecular perspective, self-sorting is classified in two main categories as “narcissistic” and “social” self sorting. While definition of “narcissistic” self-sorting perfectly matches with the biological meaning as distinguishing self from non-self, social self-sorting defines the condition in which more than one kind of hosts and guests exist and more than one host bears tendency to interact for one guest. In social self-sorting condition, binding constants of the hosts with the same guest and stoichiometry is decisive. Stoichiometry controls self-sorting process, if there are two types of hosts (A,B) and two types of guests (X,Y) exist in an equimolar manner; since the host (A) bearing higher binding constant than other host (B) binds to almost all of the guest type (X) which is also desired by other host (B), there will be only other type of guest (Y) remaining and will be available for the host (B) to bind.[85]

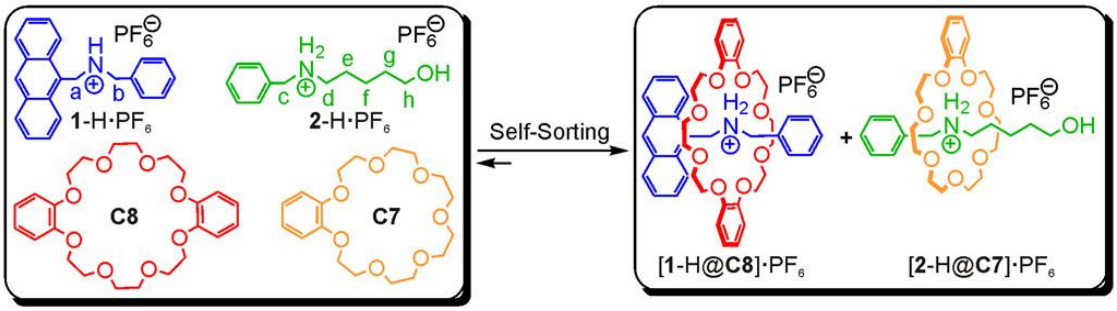

Scheme 6. A 4-component self-sorting system that owes its high fidelity to the following facts: (*i*) benzo-21-crown-7 (**C7**) is not able to pass over a phenyl group under the conditions of the experiment. Thus, the formation of a pseudorotaxane with **1**-H_PF6 is kinetically hindered; (*ii*) the complexation of **2**-H_PF6 with **C7** is thermodynamically more stable than that with dibenzo-24-crown-8 (**C8**); (*iii*) **C8** thermodynamically prefers **1**-H_PF6 over **2**-H_PF6.[80] Reproduced with permission from ref. 80. Copyright 2008 American Chemical Society.

Simultaneous molecular recognition events can occur in one system, yielding a higher level programming language of social self-sorting; this kind of self-sorting is classified as integrative self-sorting in which more than two different subunits are available for two or more recognition events with positional control. Smartness of these integrative systems are based on the fact that orthogonal binding sites do not need to be very different, even quite similar subunits can maintain selectivity as in following examples like metallo-supramolecular trapezoids,[86] multiply threaded pseudorotaxanes on an ammonium ion/crown ether basis or CB derivatives,[87-89] and polymeric aggregates. [90] A self-sorting event can occur either in a thermodynamic or kinetic manner; generally systems are called kinetic self-sorting systems except for those which attain thermodynamic equilibrium.[88]

1.1.3 Molecular Machines

As a modern approach to supramolecular chemistry, molecular machine design is another process. One can describe molecular machines as defined structures composed of discrete number of molecular components that are able to produce specific stimuli dependent quasi-mechanical movements. It is also suggested that this movement should perform a useful function. Molecular machines can be both artificially (a pH driven molecular switch) or naturally (ribosome) formed. Driving force for this assemblies to function is a gradient generated by processes carried on in stimuli; this gradient can be generated by the change in parameters that are also called as chemical fuels, like pH, redox, heat and light.[49]

If we think of everyday life analogs of molecular machines, “motor” of every machine serves as heart for these structures; and motion of molecular machines is controlled by these motors. Controlling the movement is accomplished via design of the molecular machine either to restrain or to overcome or to exploit Brownian motion.[52]

This motors can be classified in two categories as unidirectional rotary and linear motors. A motor can be described as rotary if it can rotate 360° repetitively and

be controlled over directionality after consuming energy, and can be described as linear if one component of the assembly shuttles reversibly along an axel like component, as a result of translational motion as seen in Scheme 9[38] and Scheme 10[123] (as beeing pH-driven molecular machines).

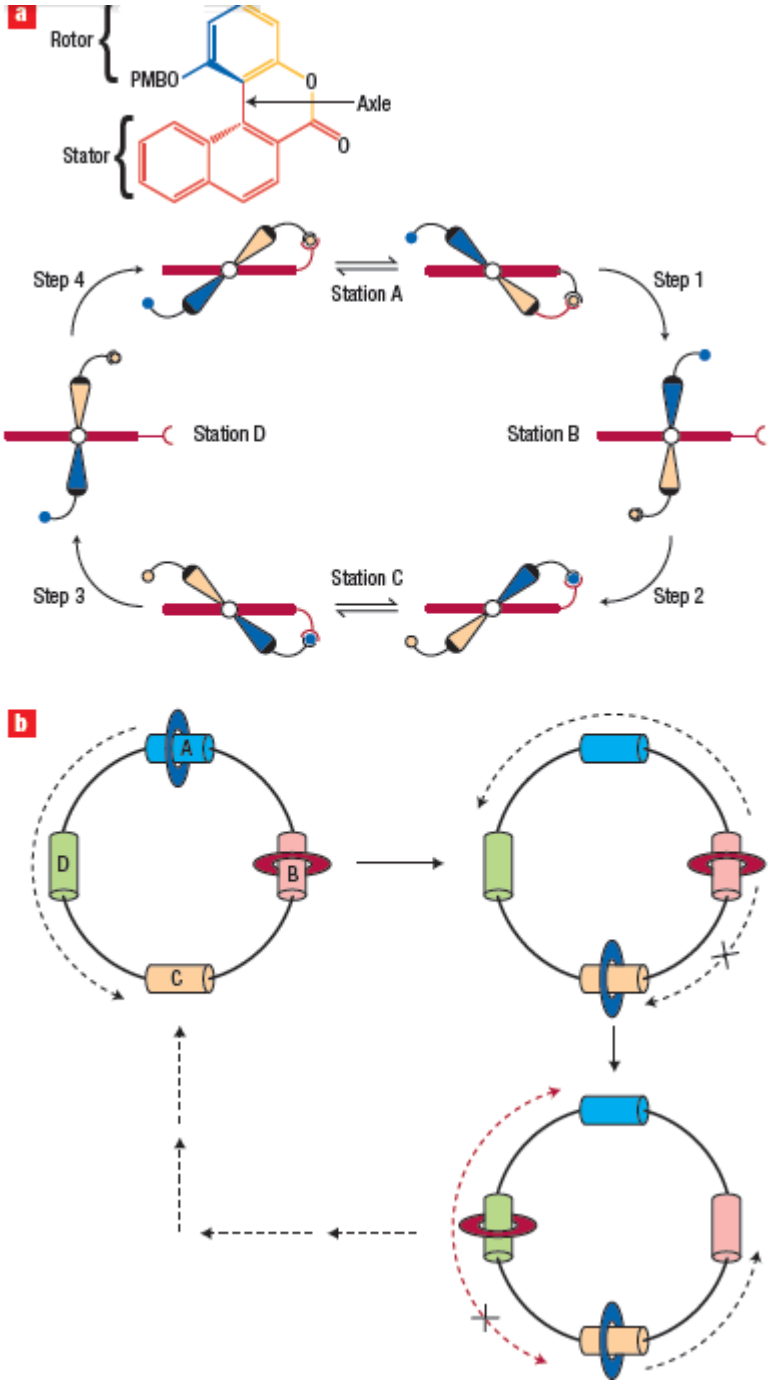

Figure 10 Rotary molecular motors in which a sequence of steps results in a full 360°

unidirectional movement around the central axis. **a**, Molecular structure (station A) of a reversible, unidirectional molecular rotary motor driven by chemical energy and a schematic illustration of the rotary process. The bond-breaking processes rely on chiral non-racemic chemical fuel that discriminates between the two dynamically equilibratinghelical forms, A and C. The bond-making processes between the rotor (yellow/blue) and the stator (red) use the principle that the sequential reactions are selective for either the blue or yellow parts of the rotor unit; that is, either the yellow or the blue end of the rotor can be selectively bound to the stator (red) to form A or C. **b**, A four-station [3]catenane (a molecular assembly in which one or more rings are inter-locked) in which unidirectional movement along the ring is controlled by sequential chemical and photochemical reactions. Adapted with permission from ref 49. Part of the entire rotary process is shown; at each stage one ring blocks the reverse rotation of the other ring ensuring unidirectionality over the entire cycle. Reproduced with permission from ref. 52. Copyright 2006 Nature Publishing Group.

1.1.4 CB[n] Containing Materials

1.1.4.1 Mechanically Interlocked Complexes

Mechanically interlocked molecules are assemblies of molecules through non-covalent interactions as a result of their topologies.[91] These complexes bear mechanical kind of bonding that prevents dissociation of the intrinsically linked complex without cleavage of one or more covalent bonds.[92] Rotaxanes, catenanes, molecular knots and molecular Borromean rings are examples of mechanically interlocked molecular architectures and in this thesis, our scope will be on CB containing rotaxanes.

1.1.4.2 Rotaxanes, Pseudorotaxanes, Polyrotaxanes

The name is build from Latin equivalents of wheel and axle as “rota” and “axis”, *rotaxane*. As the name implies rotaxanes are mechanically interlocked species in which a wheel like structure, a macrocyclic molecule, is threaded along an axle in a

locked manner by bulky stopper units; another structure that only differs from a rotaxane as lacking the stopper units is called a pseudorotaxane. Consequently, polymer analogues of the aforementioned system are called polyrotaxane and polypseudorotaxane, respectively, in which macrocyclic units are threaded onto a subunit of a polymer main chain or side chain (Figure 11).[6]

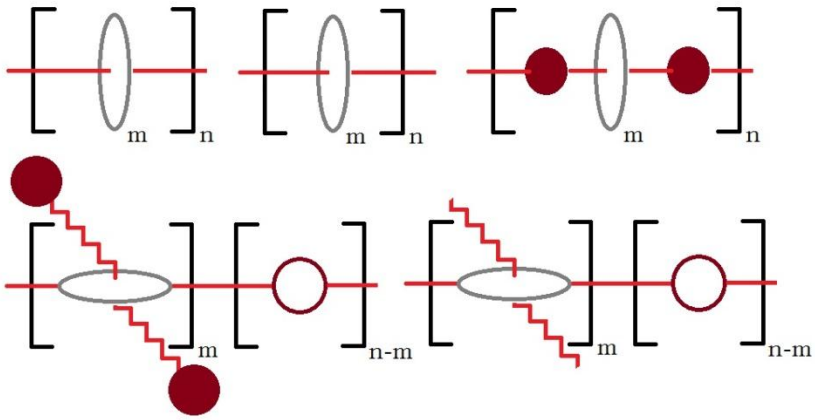

Figure 11. Schematic representation of various types of main chain polyrotaxanes.

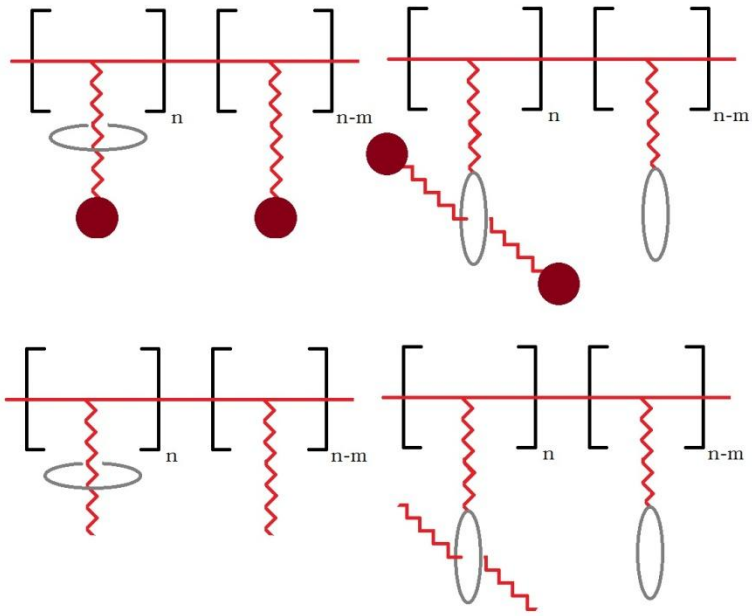

Figure 12. Schematic representation of various types of side chain polyrotaxanes

First example of a [2]rotaxane was reported by Harrison and Harrison, in this system, axle was decane-1,10-diol bis(triphenylmethyl) ether and the macrocycle was 2-hydroxy-cyclotriacontanone.[93] Afterwards, studies of Kim et al. and Schollmeyer et

al. revealed that all pseudo rotaxanes consisting axles bearing functional end groups that can be converted to bulky stopper groups, are potential rotaxanes.[94,95] Buschmann et al. reported another approach for polyrotaxane synthesis as heating a mixture of α,ω-amino acids and CB[6] and formation of a polyrotaxane was observed via condensation reaction that took place between amino- and carbonyl groups.[96] Aforementioned studies were examples for chemical conversion method. (Scheme 6) Another approach is clipping of the macrocycle from linear segments in the presence of axle with stopper groups, or polymer in the case of polyrotaxanes, or slipping of the macrocycle along stopper groups to settle on axle; entering is another way in which axle segment disassembles in the presence of macrocycle. And as the last approach threading consist of settling of the macrocycle along axle and adding stopper groups to the system by a chemical reaction.(Scheme 7)[97-99] In active template method introduced by Leigh et al., macrocycle both catalyse axle formation and after settles on the formed axle.[100]

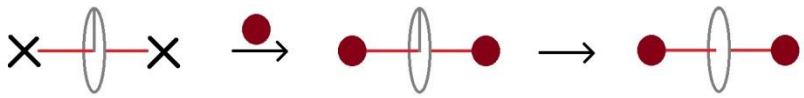

Scheme 7. Chemical conversion method

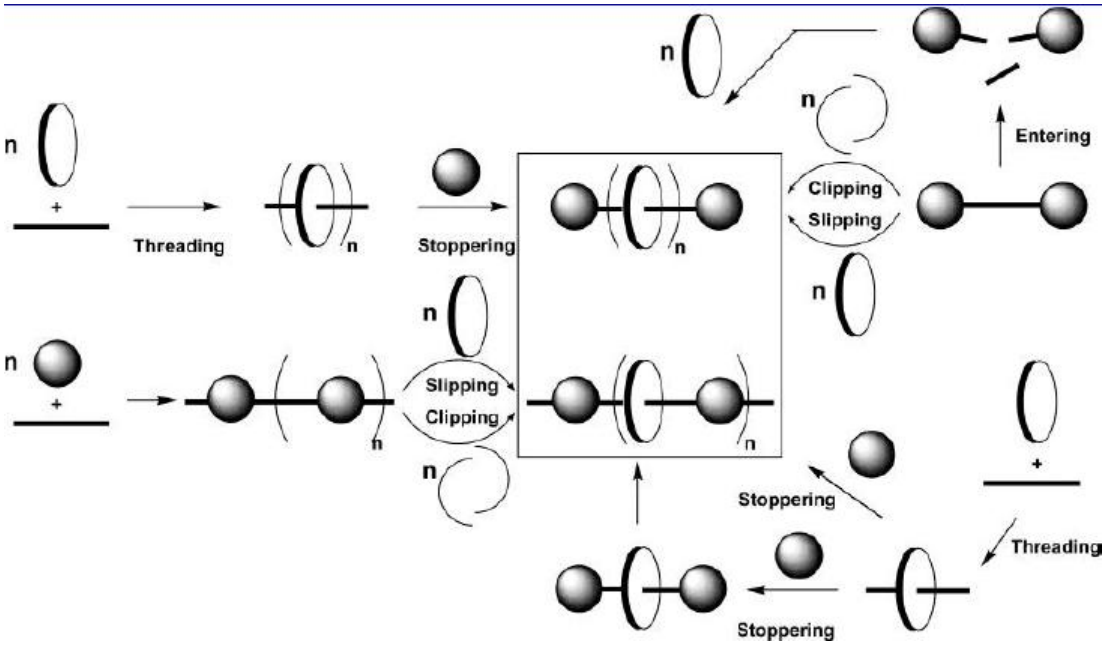

Scheme 8. Schematic representation of the methods for the synthesis of rotaxanes and polyrotaxanes[101] Reproduced with permission from ref. 101. Copyright 2004 American Chemical Society.

All these methods requires a negative ΔH for the favourable settling of macrocycle on the axle thorough non-covalent interactions; however, for the slipping method, an important drawback occurs as the fact that ΔG >0, as a result of negative ΔS and an almost zero ΔH.

Potential applications for polyrotaxanes can be listed as photo-, pH- and thermo-responsive molecular switches[102-107], fiber production[79], PLEDs[110,111] and biodegradable drug delivery vehicles[108,109].

It should be noted that all aforementioned methods for rotaxane synthesis yield in low yields after several steps of purification. In 2004, Tuncel[101] et al. introduced a smart way of rotaxane synthesis as catalytic self-threading, also an example for active template method. Catalytic property of CB[6] in 1,3- Dipolar Cycloaddition was used as a key tool for axle formation from already functionalized monomer units, most important advantage of this method is being able to control the number of macrocycles per repeating units yielding a controlled and well-defined structure. In their studies on pseudopolyrotaxanes formation via post-threading, it was revealed that choice of monomer in terms of sterical concerns is critical in ensuring the catalytic activity of CB[6]. A reduced form of Nylon 6/6 was used for heat and time dependent CB[6] threading experiments and degree of threading was measured via comparison of the threaded to non-threaded methylene protons of the axle and an alternating pattern for threading was suggested as a rationalization of 50% topmost limit for the threading, for a five-fold excess CB[6] addition. It was also suggested that slow threading kinetics were a result of high energy need for the hopping of macrocycle as seen for higher threading ratios in high temperatures and queuing of CB[6] molecules to be threaded, also. It was additionally noted that a side-on complexation can occur and inhibit hopping mechanism.

Consequently, again by Tuncel et al.[101], a new monomer design was performed, consisting stopper groups that enable both functional ends of the monomer can be active without steric hindrance. The crucial importance of CB[6] in polymerization

was tested and starting materials were recovered, completely; polymerization time was also found to be important that leads to an increase in molecular weight. This increase in molecular weight was found to be optimum at 60°C and longer heating times considerably resulted a decrease in molecular weight. Branched polyrotaxanes were also studied by Tuncel[101] et al.; a branched structure was obtained via catalytic effect of CB[6] with a new monomer bearing three functional sides at room temperature.

One of the early examples of a pH-responsive molecular switch was given by Mock [50] et al. in 1990. In this study, a pH dependent CB[6] shuttling along a triamine axle was observed. While CB[6] preferred to reside in the hexanediammonium region at pH values below p*K*a value (6.73) of the anilinium group, it moved to the butanediammonium region that was fully protonated above p*K*a value of the anilinium group.(Scheme 9) In 2001, Kim[23] et al., designed another pH-driven kinetically controlled molecular switch consisting a bistable [2]rotaxane that could switch from state 1 to 2 by pH change while the reverse process requires pH change plus thermal activation.

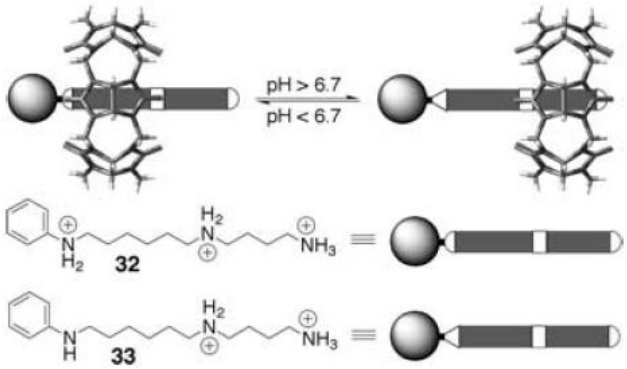

Scheme 9. CB[6]-based molecular switch.[38] Reproduced with permission from ref. 38. Copyright 2005 John Wiley and Sons.

In 2006, Tuncel et al.[123] presented a CB[6] containing water soluble [5]Rotaxane and [4]Pseudorotaxane anchored to a meso-tetraphenyl porphyrin. pH-driven switching properties of these systems were monitored by ^{1}H-NMR via comparison

with a model phorpyhrin that was made free from threaded CB[6]s in basic conditions.

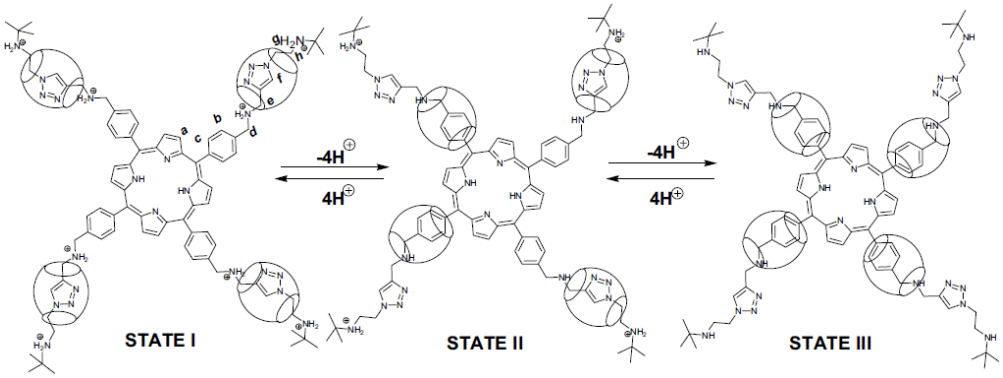

Scheme 10. pH driven states of a porphyrin-based molecular switch.[123] Reproduced with permission from ref. 123. Copyright 2006 Springer.

In a following study by Tuncel et al.[110], a previous work[101] was revisited and catalytic self-threading in which 1,3-dipolar cycloaddition was used in the coupling of diazide and dialkyne monomers for the synthesis of a pH-responsive polypseudorotaxene. In this approach, a longer aliphatic spacer was used due to the fact that CB[6] resemble a lower affinity for binding. Polyrotaxane was synthesized in 80% yield in the form of a colourless film. Number-average molecular weight of this polymer was estimated as 20800 Da by comparing integral intensities of triazole proton threaded. Successful polymerization was also monitored by weak azide peaks of triazole in IR
spectrum after placing one equivalent of triazole in reaction mixture. pH-responsive switcing ability was also tested via ^{1}H-NMR and while up to pH=9 CB[6] was threaded on triazole ring, at higher pH values CB[6]s moved and settled on dodecamethylene spacer.

Beside aforementioned systems, in 2007 Tuncel et al.[124] presented a molecular switch as a bistable [3]rotaxane. This system was also an example of CB[6] catalyzed 1,3-dipolar cycloaddition in rotaxane synthesis in a high yield. As shown in the Scheme11 pH-driven switching of CB[6] molecules along the axle results in a

conformational change and after protonation of –NH- groups following by heating, CB[6] molecules moved back to triazole units, which is thermodynamically more stable state 1. Kinetically controlled behaviour of this molecular switch was also studied in another work of Tuncel et al.[125] and rate constants for shuttling process were also measured over the range 313 to 333 K via the Eyring equation, while propyl spacer consisting axle was too short for accomodation of a CB[6] molecule.

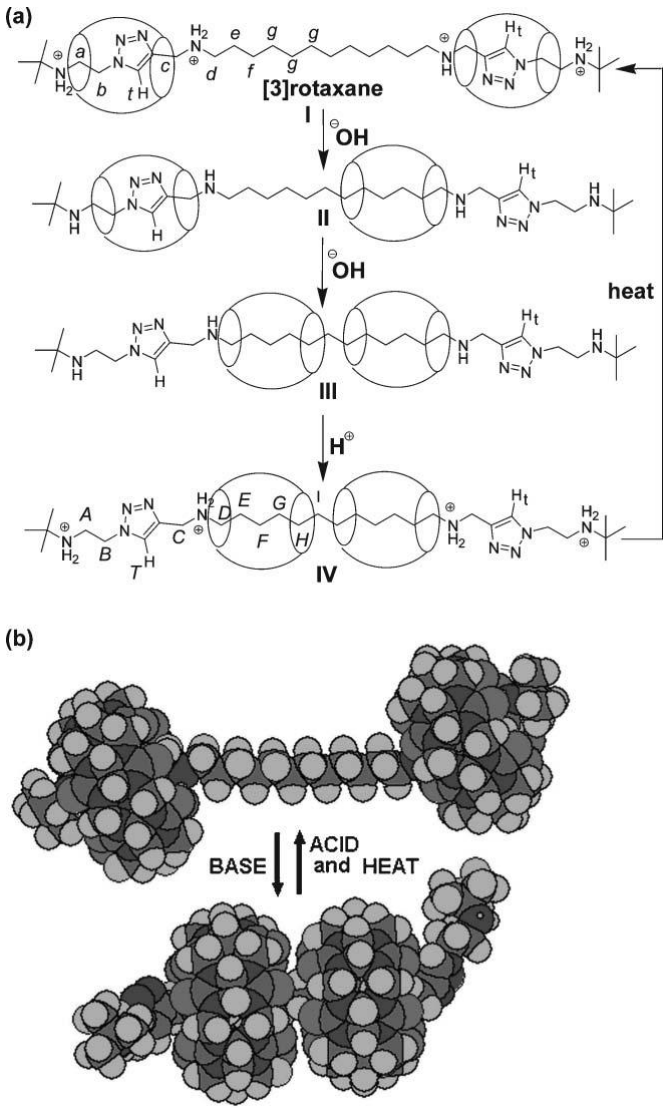

Scheme 11. pH and heat driven CB[6]-based bi-stable molecular switch.[[124] Reproduced with permission from ref. 124. Copyright 2007 Royal Society of Chemistry.

Stoddart[148] et al. in 2009, designed a system for controlled release dependent on the pH and excitation wavelength parameters as an AND logic gate; in which only simultaneous excitation at 448 nm and addition of NaOH causes release of contents due to providing both a light induced dynamic wagging motion of the nanoimpellers and opening the nanovalves upon NaOH addition.

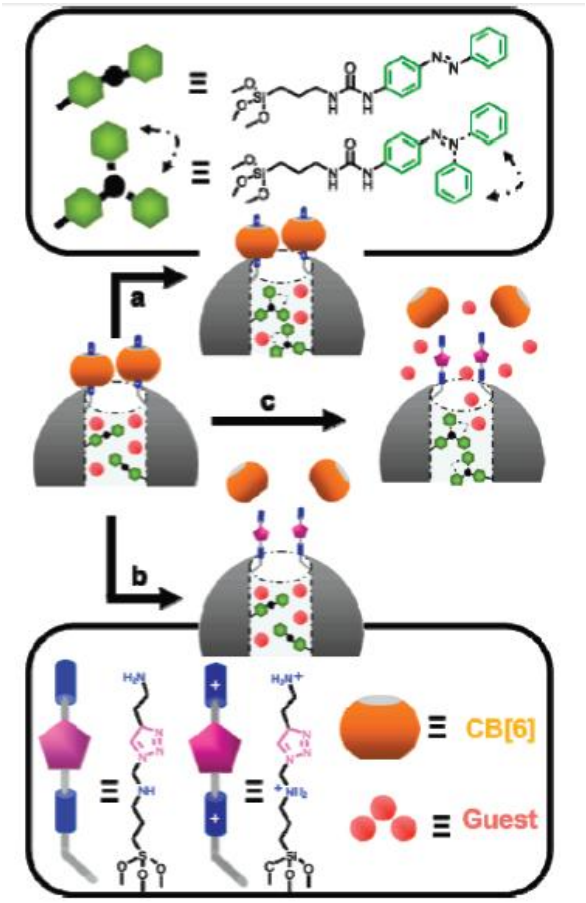

Figure 13. (a) Excitation with 448 nm light induces a the dynamic wagging motion of the nanoimpellers, but the nanovalves remain shut the contents are contained. (b) Addition of NaOH opens the nanovalves, but the static nanoimpellers are able to keep the contents contained. (c) Simultaneous excitation with 448 nm light AND addition of NaOH causes the contents to be released.[148] Reproduced with permission from ref. 148. Copyright 2009 American Chemical Society.

Another application on catalytic property of CB[6] in 1,3- Dipolar Cycloaddition will be visited in this thesis as a hetero[4]pseudorotaxane.[27]

1.1.4.3 Other Examples of CB[n] Containing Materials

1.1.4.3.1 In Frameworks

Controlling a multilayer's thickness precisely in surface modification via layer by layer deposition has become an important issue in the field of materials chemistry due to its industrial applications. Buschmann et al.[96] designed a polyester surface formed from layer of polyacrylic acid and CB[6] complexed with spermine and IR spectra of the material showed that there were no dethreading of CB[6] from the structure. In another layer by layer framework growth study by Buschmann et al.[96], stable CB[6]-spermine and N,N'-bis-(3-carboxyethyl)-1,4-diaminobutane complexes were used in building rigid structures; framework growth was monitored by linear increase at the maximum 704 nm.

1.1.4.3.2 Controlling Supramolecular Aggregates by Using CB[n]

Controlling hydrophobic aggregates by altering self-assembly behaviour is important issue that finds its applications generally ionic liquid containing systems in chemical synthesis, catalysis, preparation of conducting polymers, and fabrication and operation of polymeric electrochemical devices. In 2010, Scherman et al.[40] reported that addition of both CB[7] and CB[8] host molecules to aromatic substituent containing aryl/alkyl molecules in aqueous media can result in unique self-assembly behaviours by forming π-π stacked aggregates. This behaviour is a result of more favourable interactions between aromatic substituents with hydrophobic CB cavity than aqueous media. In their particular work, rather than previously visited rigid, well-defined supramolecular structures, a dynamic interplay between all of the components of the system under thermodynamic control was introduced in aqueous media, as shown in Scheme 11.

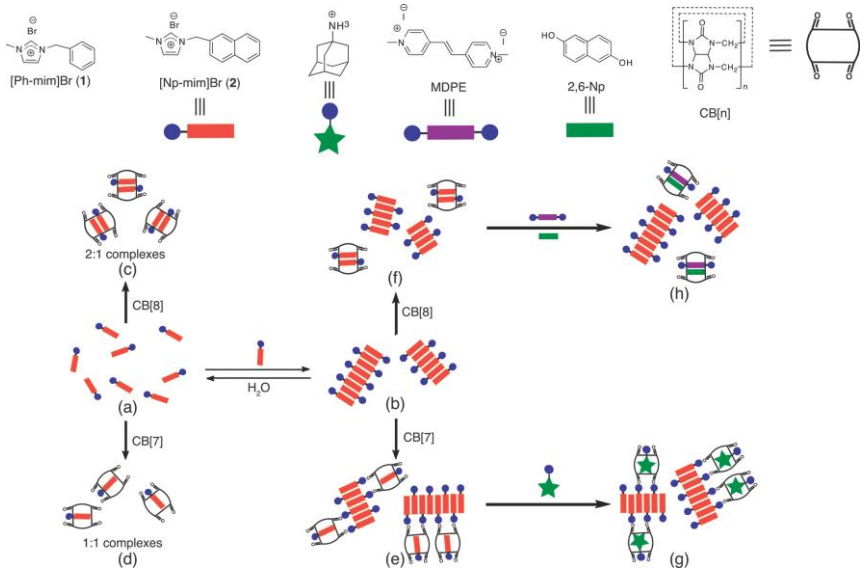

Scheme 12. The π-π stacking can be easily tuned through the addition of the macrocyclic hosts CB[7] and CB[8] as well as select small molecule competitive guests.[40] Reproduced with permission from ref. 40. Copyright 2010 American Chemical Society.

A similar approach for enhancing light emitting properties of fluorene based conjugated polymers via triggering structure of aggregates in aqueous media will be visited in this thesis.[147]

1.1.5 Fluorene Based Conjugated Polymers

Conjugated polymers are a special class of polymers that resemble remarkable electronic and optic properties, besides providing an advantage of processibility. Studies on this special area carried by Alan Heeger[126], Hideki Shirakawa[127] and Alan MacDiarmid[128] also rewarded with 2000 Nobel Prize in chemistry mainly on the discovery of high conductivity in polyacetylene. Today, studies in this area mainly depend on the structural tailoring that yields in various applications as also

visited in this thesis. Beside various applications on display technology[129, 130, 131, 132, 133], biological applications mainly on sensing[134], lasers[135,136] and solar cell applications[137].

It is that the delocalized π molecular orbitals along polymer backbone make these fascinating materials to bear optically and electrically emerging properties. Along the conjugated system π-bonding (HOMO) and π*-antibonding (LUMO) orbitals resemble valence and conduction bands, respectively; an excited electron is promoted from π bonding orbital to π*, since these band gaps are in between 1-3.5 eV[138], transitions can be monitored via UV. In the case of electrical conductivity, one valence e^- resides in all sp^2 hybridized continuous carbon centres and in the case of doping by oxidizing agents these e^-s become mobile along this partially filled conjugated system in one dimensional electronic band.

Early members of conjugated polymer family like polyacetylene was not stable in the presence of oxygen and processing was not feasible and since conjugated polymers should be stable and easily processable, new types of conjugated polymers were invented as shown Figure 14.

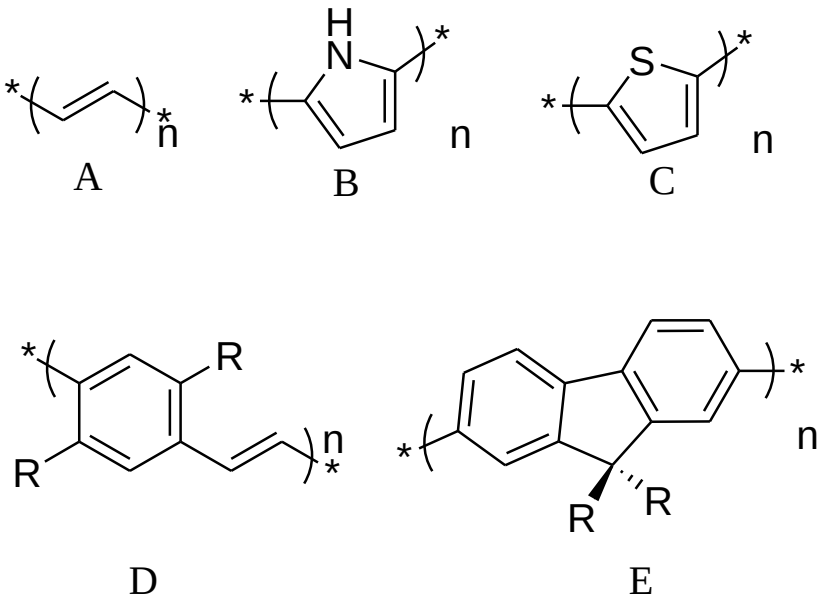

Figure 14 Conjugated polymer examples: A) Polyacetylene, B) Polypyrrole C) Polythiophene D) Poly (phenylene vinylene) E) Polyfluorene

Aforementioned concerns on conjugated polymers are mainly valid for achieving LED applications (Figure 16). A basic LED (OLED) is composed of the parts depicted below; ITO (Indium tin oxide) with a large work function, resembles a p type hole-injecting electrode (anode), conjugated polymers stands for the conducting material in between and cathode is selected as a low work function material like 2A and 3A metals. As injected holes and electrons move along the conjugated polymer to form excitons, a photon emission is observed as a result of decay.[139]

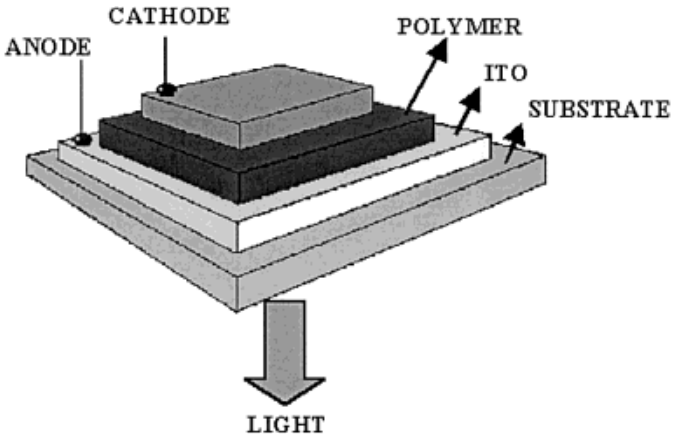

Figure 15 A model OLED.[120] Reproduced with permission from ref. 120. Copyright 2001 John Wiley and Sons.

Among the various conjugated polymers developed, polyfluorene, poly(9, 9-dialkylfluorene), derivatives are received an important attention due to their remarkable properties as possessing a photochemically and chemically stable, rigid biphenyl groups on backbone, easily functionalizable C9 position and resulting blue emission from due to a large band gap.[120] It should be also noted that polyfluorene derivatives resembles a solid state behaviour that opens additional paths for industrial processes.[119] However, important drawbacks related to the solid state is excimer emission caused by dimerised units in the excited state and results in a less energetic emission (red shift) and lower lifetimes[140], keto defect formation because of fluorenone units[141] and cross linking[140].

Yoshimo et al.[142] proposed one of the first examples of substituting side chains to fluorene core increase solubility and coupling via $FeCl_3$ oxidation. Then, further developments enabled high molecular weight polyfluorene derivatives via transition metal-catalyzed couplings including reductive couplings of dihaloaryls introduced by Yamamoto , cross-couplings of aryldiboronic acids and also dihaloaryls by Suzuki and couplings of distannylaryls, dihaloaryls by Stille.[143] (Scheme 13)

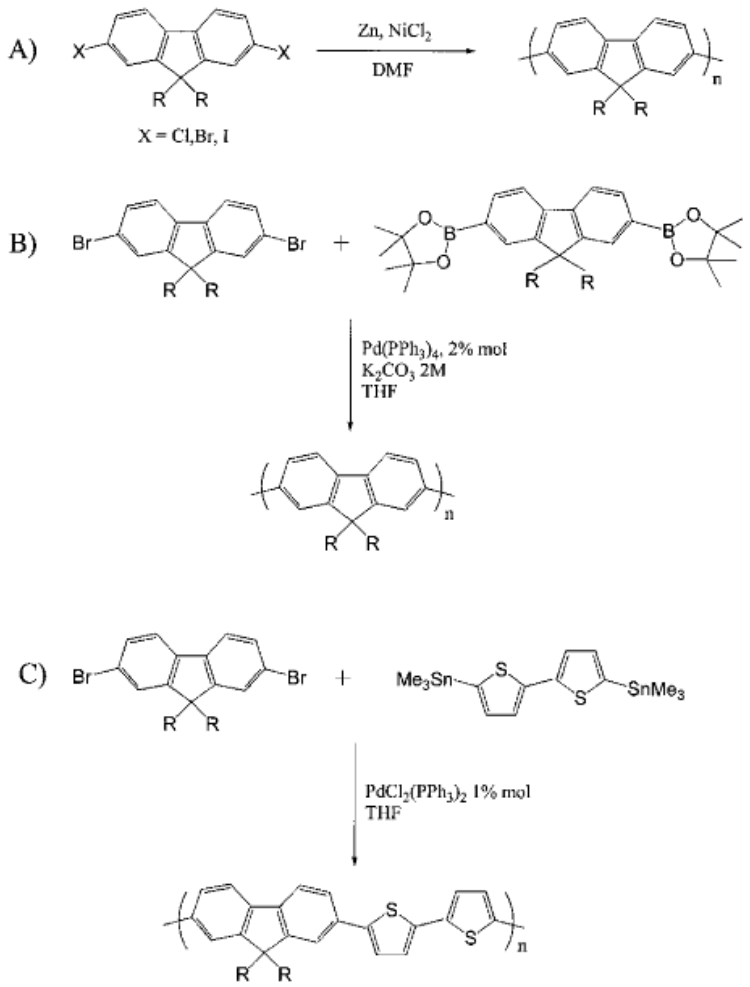

Scheme 13. Yamamoto(A), Suzuki(B) and Stille(C) coupling for polyfluorene synthesis.[120] Reproduced with permission from ref. 120. Copyright 2001 John Wiley and Sons.

Solubility of polyfluorenes in organic solvents can be handled well via adding alkyl containing side chains, however obtaining water soluble polyfluorenes are of great interest since biological applications requires hydrophilic agents as well as optoelectronic applications in aqueous media. Via side chains containing groups as carboxylate, ammonium, phosphate and sulfonate, water soluble polymers can be obtained however, bearing ionic side chains in a biological media causes non-selective interactions. Moreover, fluorene core of polymers cause an intrinsic aggregation as a further resistance to be soluble in water and it should be note that less soluble conjugated polymers yield in lower fluorescent quantum yields, that is not desirable. To disturb this π-π stacking between polymer backbones several solutions has been proposed as interaction with surfactants by Lo´pez-Cabarcos et al.[122] via an alkyl ammonium surfactant addition to poly(thienyl ethylene oxide butyl sulfonate) polymer solution, Jamnik et al.[144] suggested addition of non-ionic amphiphiles to poly{1,4-phenylene-[9,9-bis(4-phenoxy-butylsulfonate)] fluorene-2,7-diyl} solution; incorporation with bulky groups by Bo et al. [121] as dendronized polyfluorenes; encapsulating backbone of the polymer with a suitable macrocycle was also studied by a number of researchers, Durocher et al. [145] and Tanguy et al.[146] presented encapsulation of thiophene based polymers by CD and Tuncel et al. used CB[8] as a backbone encapsulating agent for enhancement in water solubility of poly[9,9-bis{6(N,N-dimethylamino)hexyl}fluoreneco-2,5-thienylene as will be discussed in this thesis further.[147]

Chapter 2

RESULTS AND DISCUSSION

Introduction

This chapter consists of two main sections. First section reports the ability of CB[n] homologues to self-sort and recognise the binding sites of a ditopic guest according to their size, shape and chemical nature as well as the formation of kinetically controlled hetero[4]pseudorotaxane.

In the second section, the effects of CB[n] homologues on the solubility, photo physical properties and the morphology of non-ionic conjugated polymers are reported. The nano-structured supramolecular assembly formed between CBs and conjugated polymers will be discussed.

SECTION 1:

This section was published as "Sequence specific self-sorting of the binding sites of a ditopic guest by cucurbituril homologues and subsequent formation of a hetero[4]pseudorotaxane" Gizem Çeltek, Müge Artar, Oren A. Scherman, Dönüs Tuncel, *Chemistry A European Journal*, 2009, 15, 10360-10363. Reproduced in part with permission from Wiley-VCH Verlag GmbH&Co. KGaA, Weinheim. Copyright 2009 Wiley-VCH Verlag GmbH&Co. KGaA, Weinheim.

In this work, a guest containing two distinct binding sites which differ chemically and geometrically from each other was prepared through a click reaction. The selectivity and recognition behavior of cucurbit[n]uril homologues (where n =6,7 and 8) toward each of the binding sites of these guests were studied. These binding sites are comprised of a flexible and hydrophobic dodecyl spacer and a five-membered triazole ring terminated with ammonium ions. The formation of 1:2, 1:1 and 1:1 complexes between the guest and CB homologues, namely CB[6],[7], and [8] respectively have been confirmed by ^{1}H-NMR spectroscopy and mass spectrometry. Moreover, it was shown that CB[6], CB[7] and CB[8] had the ability to recognize and self-sort the recognition sites according to their chemical nature, size and shape. The formation of hetero[4]pseudorotaxane containing both CB[6] and CB[8] through sequence-specific self-sorting was also observed. Suggested structures after the formation of complexes of CB homologues with **Axle A** are illustrated in the Figure 16.

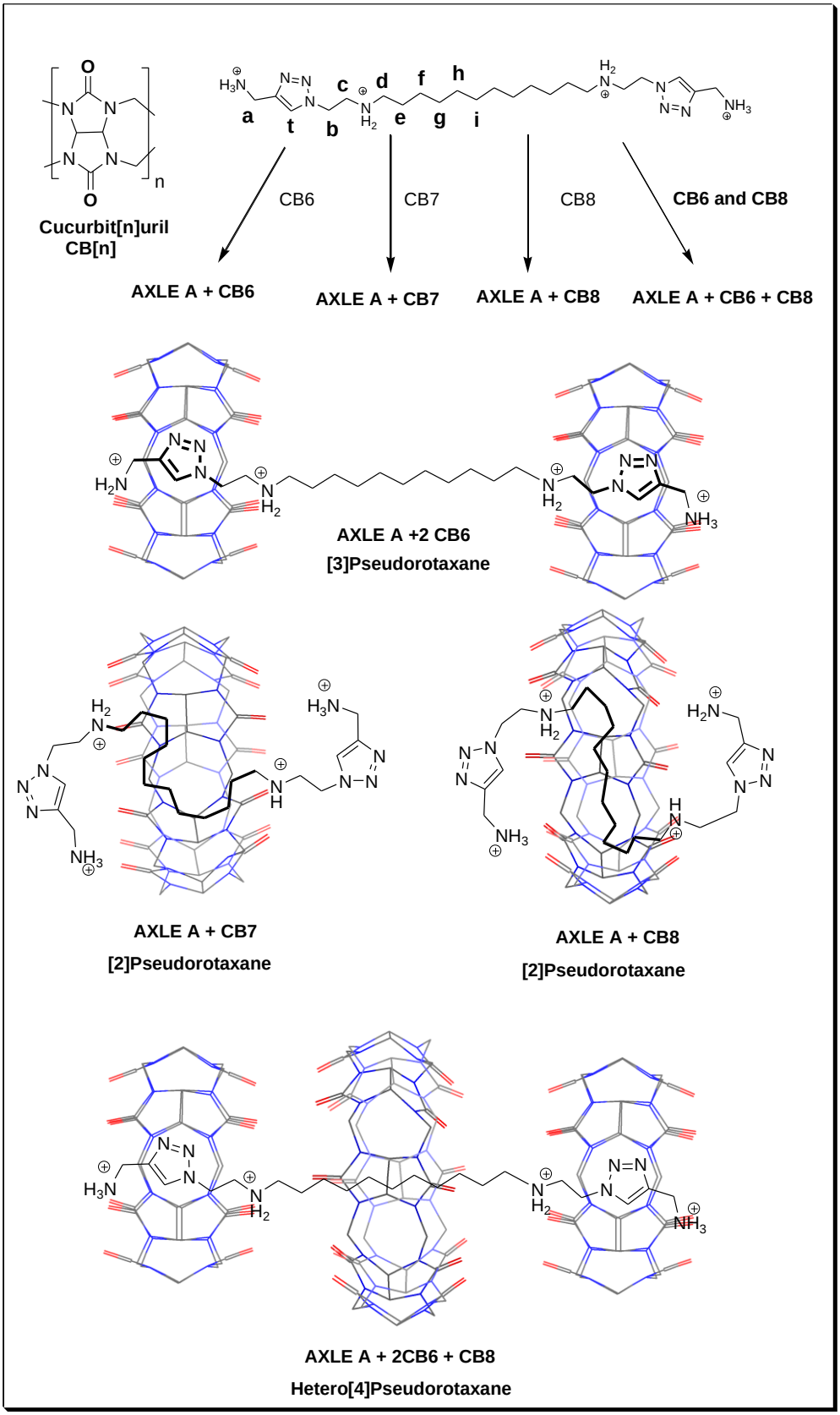

Figure 16. Suggested structures after the formation of complexes of CB homologues with **Axle A**.

2.1.1 Synthesis and Characterization of the Axle A

Axle A was synthesized via Cu^{I}-catalyzed click-chemistry between the hydrochloride salts of N,N'-bis-(2-azido-ethyl)-dodecane-1,12-diamine and two equivalent of propargylammonium chloride monomers in high yield. The reaction scheme for the synthesis of Axle A is shown in Scheme 14.

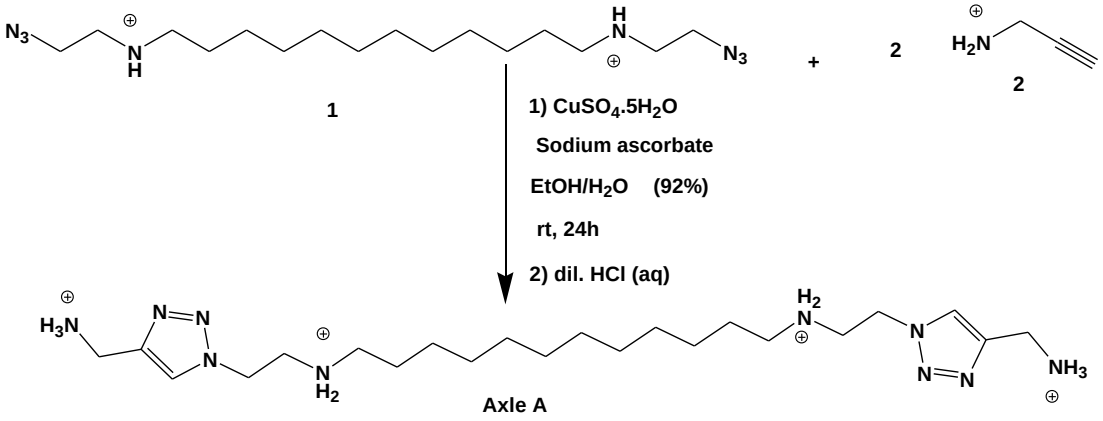

Scheme 14. Synthesis of Axle A (counter ion chlorides are omitted for clarity).

The characterization of the Axle A was carried out by ^{1}H-NMR, ^{13}C-NMR, COSY and elemental analysis. ^{1}H-NMR (Fig. 16) and also COSY (Fig.17) spectra show characteristic signal of triazole proton of H_t at 8.12 ppm as a result of Cu^{I}-catalyzed click-chemistry.

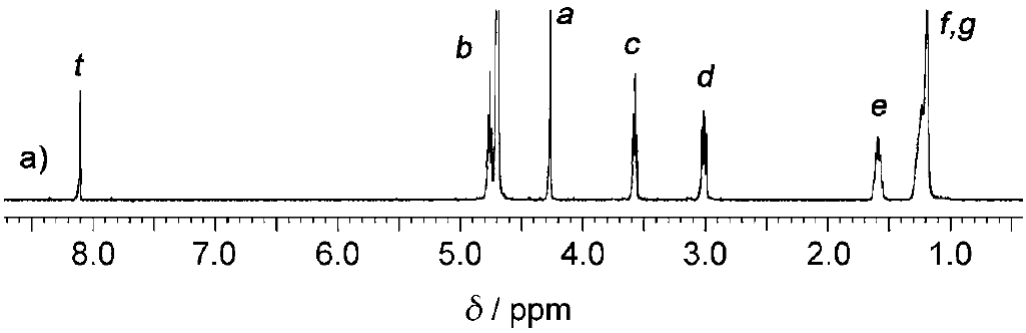

Figure 17. ^{1}H-NMR spectra of Axle A.

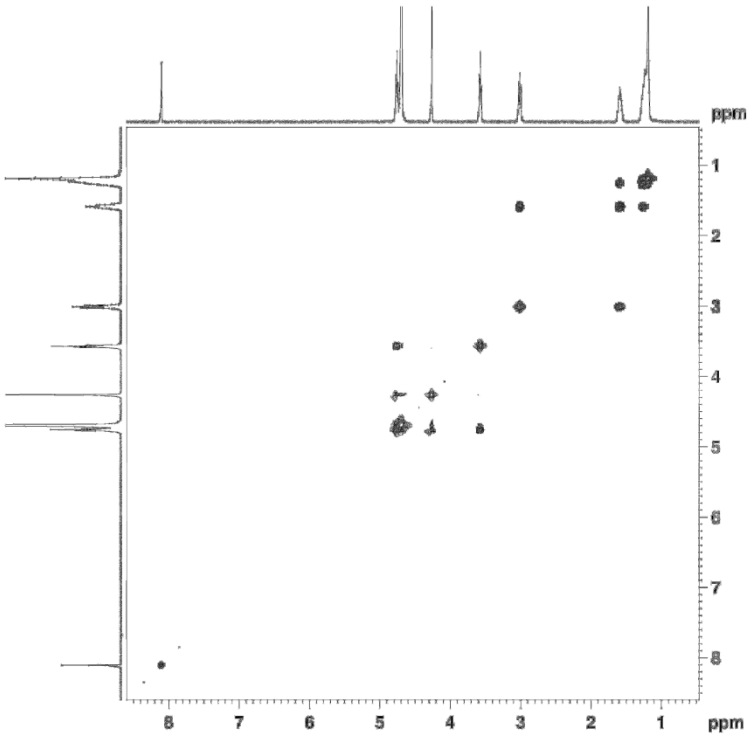

Figure 18. COSY spectra of Axle A.

In this axle, there are two recognition sites which are the dodecyl alkyl chain and the two diammonium triazoles. The complexation behavior of CB[6], CB[7] and CB[8] with Axle A was first investigated by ^{1}H-NMR titration then the resulting pseudorotaxanes were isolated and characterized by 1D, 2D-NMR experiments and MALDI-MS.

It is known from the previous works that CB[6] prefers to bind the diaminotriazole sites rather than the dodecyl spacer.[112] The driving force for this type of complexation is mainly due to the size selectivity as triazole has an appropriate size to fill the cavity of the CB[6] as well as ion-dipole interactions between ammonium ions and the oxygens of the carbonyl portals. Figure 19 shows the ^{1}H-NMR spectrum of [3]pseudorotaxane of CB[6] with **Axle A**. It is evident that triazole units are threaded by CB[6]s and as a result the signal from the triazole proton is shifted 1.7 ppm upfield (from 8.2 ppm to 6.5 ppm); while there are not significant changes in the signals for dodecyl protons indicating this part is not encapsulated by CB[6].

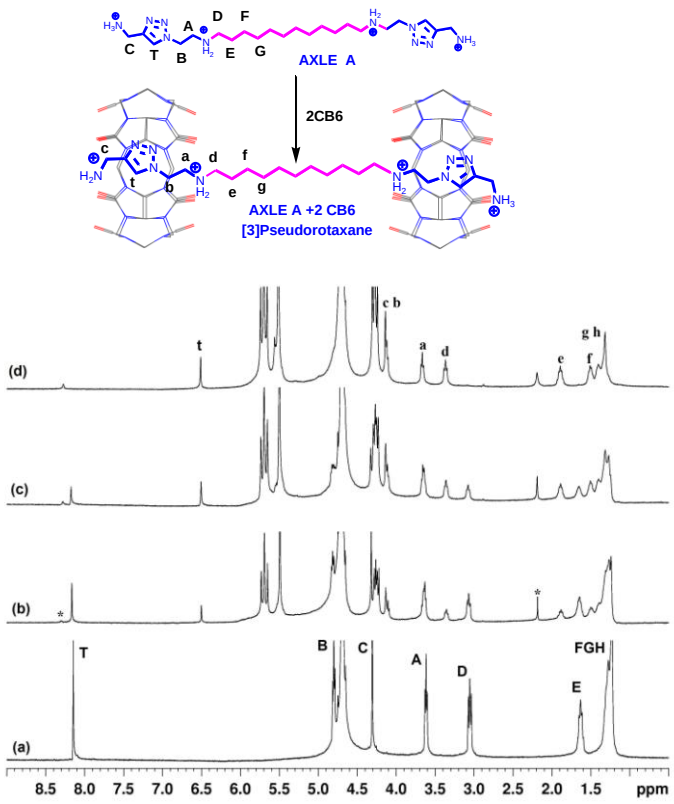

Figure 19. ^{1}H NMR (400 MHz, D_2O, 25 °C) spectra of **Axle A**; the addition of (a) 0 equiv of CB[6] (b) 0.5 equiv of CB[6], (c) 1 equiv of CB[6], (d) 2.2 equiv of CB[6] (* denotes impurities).

Host-guest chemistry and recognition properties of CB[8] toward the same guest were also investigated by ^{1}H-NMR titration. The axle was dissolved in D_2O and 0.5 equiv increments of CB[8] up to 2.1 equiv were added as solid. Although CB[8] is not soluble in water, it dissolves in the aqueous solution of **Axle A**. Just after each addition and dissolving CB[8], a ^{1}H-NMR spectrum was recorded at room temperature. The ^{1}H-NMR spectrum after addition of 0.5 equiv of CB[8] shows two sets of signals due to encapsulated and unencapsulated protons of the guest. This indicates that the exchange of complexed and uncomplexed guest is slow on the NMR time scale. There is a significant upfield shift in the chemical shifts of all dodecyl protons. The signal from the triazole proton is shifted 0.1 ppm downfield. This clearly indicates that CB[8] encapsulates dodecyl protons but not the triazole which is in contrast to CB[6]. Addition of 1 equiv of CB[8] causes the appearance of

only one set of protons and further addition of CB[8] produced similar spectra. Accordingly, a [2]pseudorotaxane of CB[8] with **Axle A** results from a 1:1 inclusion complex of CB[8] with the guest; it was isolated and characterized by 1D, 2D-NMR experiments and MALDI-MS. Figure 20 shows the ^{1}H-NMR spectrum of the [2]pseudorotaxane of CB[8]. As can be seen the signals due to the dodecyl protons are shifted upfield whereas the signal from the triazole proton appears at 8.2 ppm. 2D-NMR experiments provide structural information and based on these we can suggest that the dodecyl spacer is folded to fit inside the cavity of CB[8] to maximize the hydrophobic interactions in an efficient manner as shown in the Figure 20.

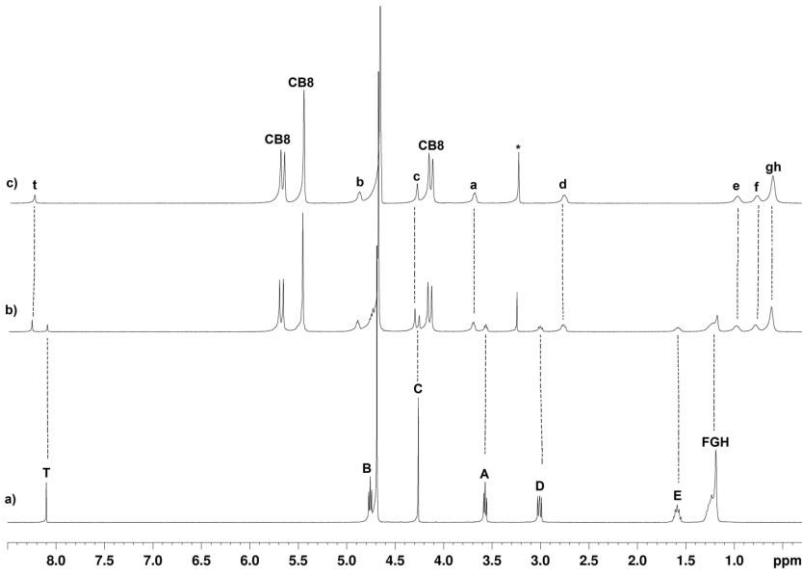

Figure 20. Structure of CB[8]-Axle A and ^{1}H NMR (400 MHz, D_2O, 25 °C) spectra of Axle A; the addition of (a) 0 equiv of CB[8] (b) 0.5 equiv of CB[8], (c) 1.2 equiv of CB[8].

This complex also investigated by MALDI-MS and interpretation of the peak at 1777 as the molecular ion "Axle+CB[8]+4Cl^{-} was verified a 1:1 inclusion complex, shown in Figure 22. In the previous studies on conformational changes of flexible guests within macrocycles for enhanced hydrophobic interactions, several systems were investigated; those observations can be listed as chain length depending conformations (all-trans to s-shaped and helical) of the alkanes upon formation of 2:1 host–guest complexes with p-tert-butylcalix[4]arene[112], the coiling of long alkyl

chains into helices within vase shaped cavitands and cylindrical molecular capsules[113] and U-shaped conformations formed by back- folding in CB[8][114].

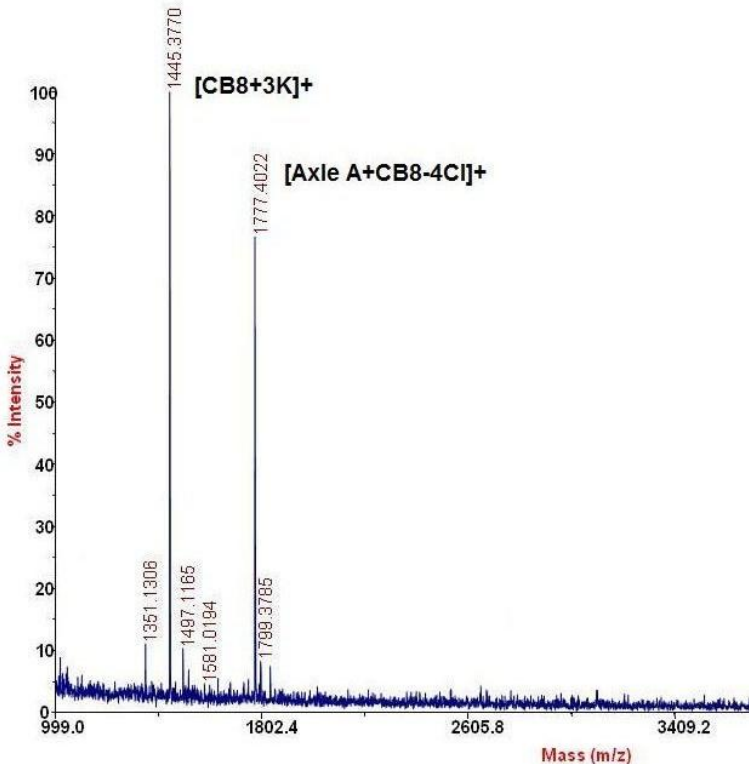

Figure 21. MALDI-mass spectrum of CB[8]-Axle A.

^{1}H-NMR titration experiment with CB[7] is seen in Figure 22. A considerable upfield shift of the peaks for dodecyl spacer protons revealed the encapsulation of this site while there was no shift observed for triazole rings. Due to bearing a smaller cavity, “e” and “d” protons that are far away from centre when compared with “h,g,i” protons, were not buried into CB[7] as can be seen from small upfield shifts of “e” and “d” protons.

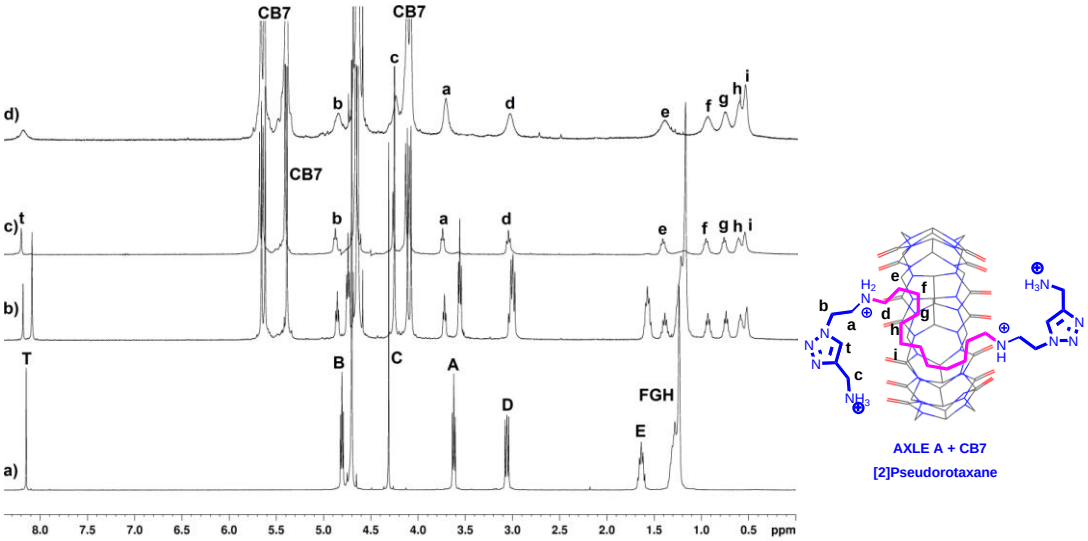

Figure 22. Proposed structure of CB[7]-Axle A and ^{1}H NMR (400 MHz, D_2O, 25 °C) spectra of Axle A; the addition of (a) 0 equiv of CB[7] (b) 0.4 equiv of CB[7], (c) 0.9 equiv of CB[7], (c) 1.3 equiv of CB[7].

It should be noted that a [3]pseudorotaxane containing two CB[7] along dodecyl spacer was observed, as verified by MALDI-tof-MS spectra with two molecular ions matching with 1:1, shown in Figure 23, and 2:1 complex as shown in Figure 22.

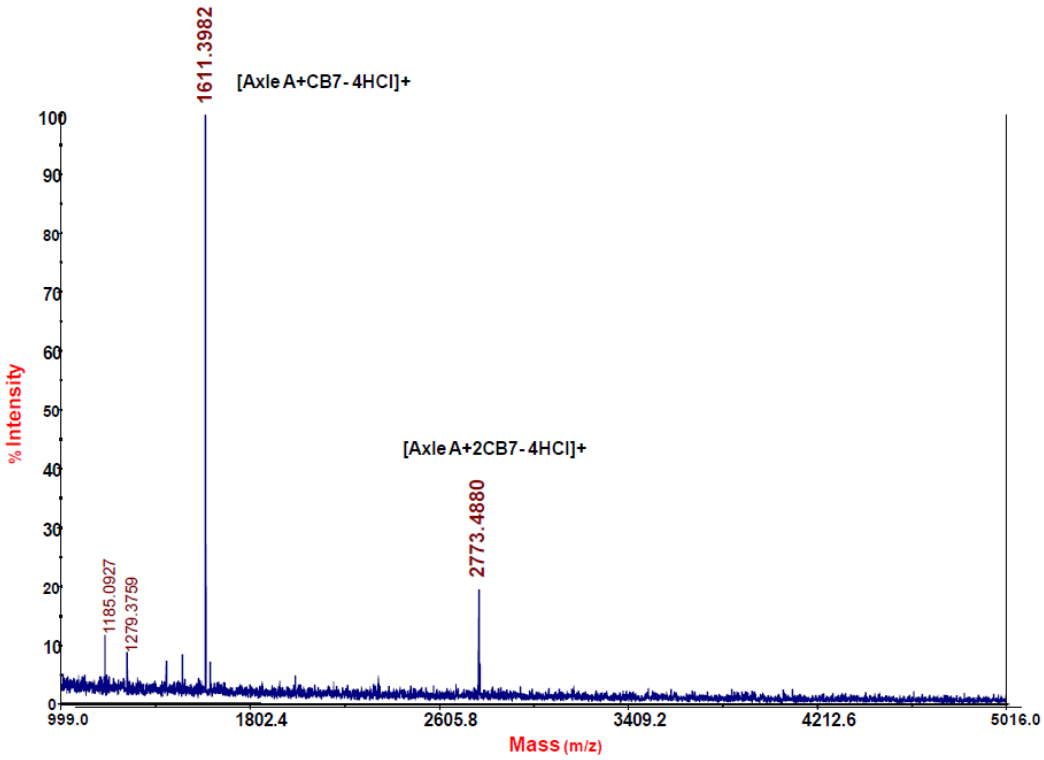

Figure 23. MALDI-mass spectrum of CB[7]-Axle A.

From titration experiments conducted with CB[6], CB[7] and CB[8], different recognition properties due to different cavity sizes were observed as a [3]pseudorotaxane with two CB[6] threaded on triazole rings, [2] and also [3]pseudorotaxane with one or two CB[7] threaded on dodecyl spacer, respectively and a [2]pseudorotaxane with one CB[8] on dodecyl spacer that is in a folded conformation to increase hydrophobic interactions.

2.1.2 Hetero[4]Pseudorotaxane formation via complexation of Axle A with both CB[6] and CB[8] Homologues Simultaneously

Complexation behaviour of Axle A with CB[8] and CB[6] has also been investigated, in a media containing both CB[6] and CB[8]. 2 equivalents of CB[6] was introduced an already formed [2]pseudorotaxane of CB[8] with Axle A and ^{1}H-NMR spectra was recorded at 10 min, 2 h, 24 h and 96 h, as shown in Figure 24. Disappearance of the triazole signal at 8.1 ppm and appearance of new signals at 6.49 and 6.47 ppm together revealed that triazole protons were encapsulated. Appearance of another set of peaks around 1.1-1.8 ppm also revealed that dodecyl centre encapsulated by CB[8] but in a different conformation that yielded in different environments for dodecyl protons. Integrating peaks that belong to [3]pseudorotaxane between δ= 0.4-1.1 ppm and peaks between δ=1.1-1.8 ppm that belong to hetero[4]pseudorotaxane and comparing them, revealed that "hetero[4]pseudorotaxane:[3]pseudorotaxane" ratio was 85:15, 75:25, 45:55 and 30:70 for 10 min, 2 h, 24 h and 96 h, respectively. With the additional verification resulted by ratio of integration of triazole peaks at δ= 6.47 and 6.49 ppm, it was concluded that initially hetero[4]pseudorotaxane forms as a major component after CB[6] addition to CB[8] and Axle A; however, after a certain time when equilibrium starts to be established, [3]pseudorotaxane becomes the major product and hetero[4]pseudorotaxane becomes minor one. Alternatively stated, hetero[4]pseudorotaxane forms as the kinetic product while [3]pseudorotaxane forms as a major thermodynamic product.

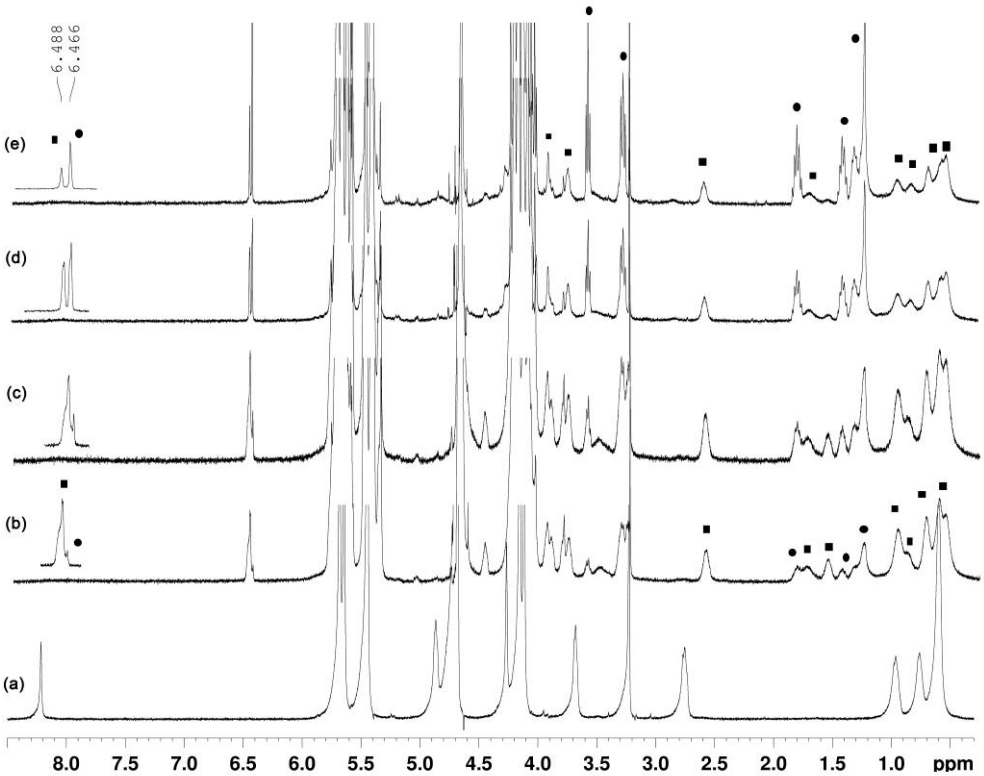

Figure 24. The 1H NMR spectra (400 MHz, 25 8C, D_2O) of a) Axle A+ CB[8]; b) 10 min later after addition of 2 equiv CB[6] to (a); c) 2 h later after addition of 2 equiv CB[6] to (a); d) 24 h later after addition of 2 equiv CB[6] to (a); e) 96 h later after addition of 2 equiv CB[6] to (a). Rectangle and sphere denote protons from hetero[4]pseudorotaxane and [3]pseudorotaxane respectively; the peak at d=3.25 ppm is assigned to MeOH residue.

In another experiment, 1 equivalent of CB[8], 2 equivalents of CB[6] and Axle A mixed in D_2O at the same time and ^{1}H-NMR spectra recorded after 10 minutes, again firstly a kinetic then thermodynamic product as hetero[4]pseudorotaxane and [3]pseudorotaxane was formed, respectively, as MALDI-tof-MS spectra shows with peaks for molecular ions at *m/z*= 2443 for [3]pseudorotaxane (Axle A + 2 CB[6]) and 3772 for hetero[4]pseudorotaxane (Axle A + 2CB[6] + CB[8]) (Figure 25). Even after two weeks of excess addition of CB[8], spectra showed equilibrium was reached via [3]pseudorotaxane formation.

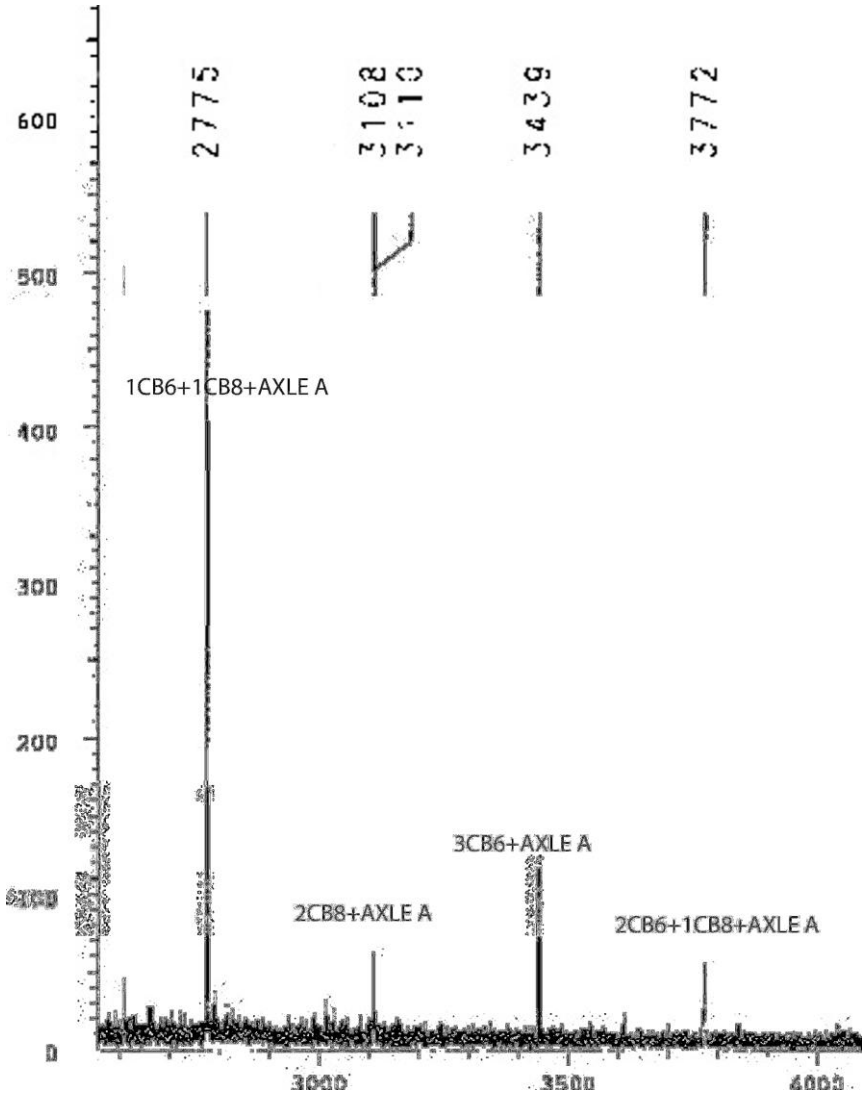

Figure 25. MALDI-mass spectrum of Axle A+1CB[8]+2CB[6].

To sum up, recognition properties of CB[6], CB[7] and CB[8] were investigated by using a two binding site bearing axle that is a product of Cu^{I}-catalyzed click reaction. Formation of complexes in the following ratios as 1:1, 1:1 and 1:2 for CB[8], CB[7] and CB[6], respectively, were investigated via ^{1}H-NMR and mass spectrometry. Beside monitoring the emerging ability of CB[6], CB[7] and CB[8] homologues in recognition of different binding sites of axle, a controllable formation of hetero[4]pseudorotaxane in the means of kinetic and order of addition factors were introduced.

Section 2

This section was published as “The Effect of Cucurbit[n]uril on the Solubility, Morphology, and the Photophysical Properties of Nonionic Conjugated Polymers in an Aqueous Medium” Dönüs Tuncel, Müge Artar, Saltuk B. Hanay, Journal of Polymer Science: Part A: Polymer Chemistry, 2010, 48, 4894–4899. Reproduced in part with permission from Wiley-VCH Verlag GmbH&Co. KGaA, Weinheim. Copyright 2010 Wiley-VCH Verlag GmbH&Co. KGaA, Weinheim.

In this part, the effect of CB[n] homologues on the dissolution and the photo physical properties of non-ionic conjugated polymers in water were investigated. A fluorene-based polymer, namely, poly[9,9-bis{6(N,N dimethylamino)hexyl}fluorene-co-2,5-thienylene (PFT) was synthesized via Suzuki coupling and characterization was performed by spectroscopic techniques including 1D and 2D NMR, UV–Vis, fluorescent spectroscopy, and matrix-assisted laser desorption mass spectrometry (MALDI-MS). The interaction of CB[6], CB[7] and CB[8] with PFT have been investigated and observed that only CB[8] among other CB homologues forms a water-soluble inclusion complex with PFT. Furthermore, upon complex formation a considerable enhancement in the fluorescent quantum yield of PFT in water was observed. The structure of resulting PFT@CB[8] complex was characterized through ^{1}H and selective 1D-NOESY and further investigated by imaging techniques (e.g. AFM, SEM, TEM and fluorescent optical microscopy) to reveal the morphology. The results suggested that through CB[8]-assisted self-assembly of PFT polymer chains vesicle-like nanostructures formed. The sizes of nanostructures were also determined using dynamic light scattering (DLS) measurements.

2.2.1 Synthesis and Characterization of poly[(9, 9-bis (Dimethylamino-hexyl)-9H-fluorene)-benzene] (PFT)

Synthesis of poly[9,9-bis{6-(N,N-dimethylamino)hexyl}fluorene-co-2,5-thienylene (PFT) was performed as shown in the reaction Scheme 15 after the conversion of M1 into M2 via excess dimethylamine solution in THF, by Pd-catalyzed Suzuki coupling of M2 with 2.5-thiophenediboronic acid. (M1 was synthesized according to literature[115])

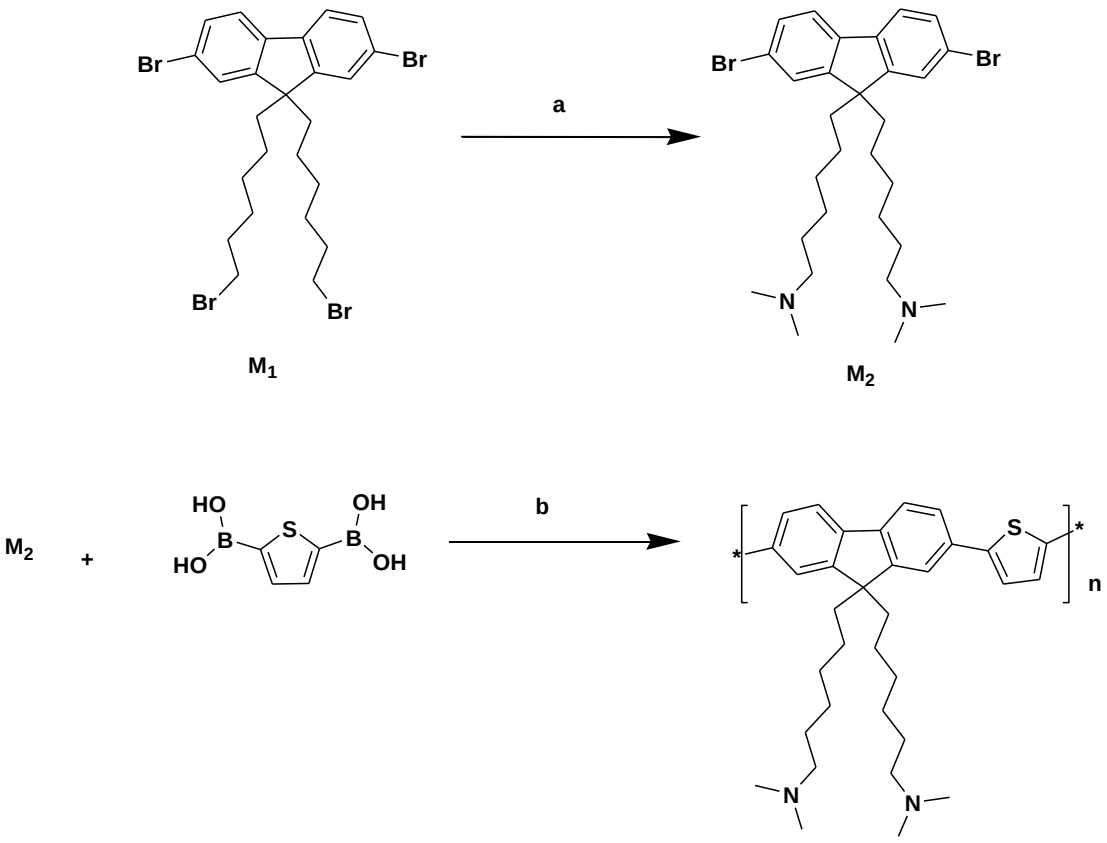

Scheme 15. (a) THF, 94% (b) $PdCl_2$(dppf), K_2CO_3, H_2O/THF, 77%.

^{1}H-NMR spectrum of PFT in $CDCl_3$ shows aromatic protons in between δ=7.75-7.52 ppm while side chain protons give signals in between δ=2.25-0.75 ppm.

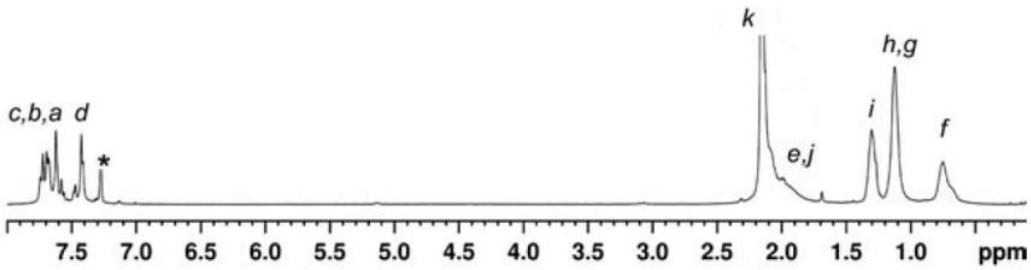

Figure 26. ^{1}H-NMR spectrum of PFT in $CDCl_3$

FT-IR spectrum in Figure 27 of PFT shows amine stretching peak at around 3415 cm^{-1}, alkyl C-H stretching at around 2929 and 2848 cm^{-1}, aromatic C=C bending at around 1606 and 1457 cm^{-1}, aromatic C-H bending at around 796 cm^{-1}. MALDI-MS spectrum is also verified structure as showing peaks that are separated by a mass of ~500 Da corresponding to the mass of one repeating unit.

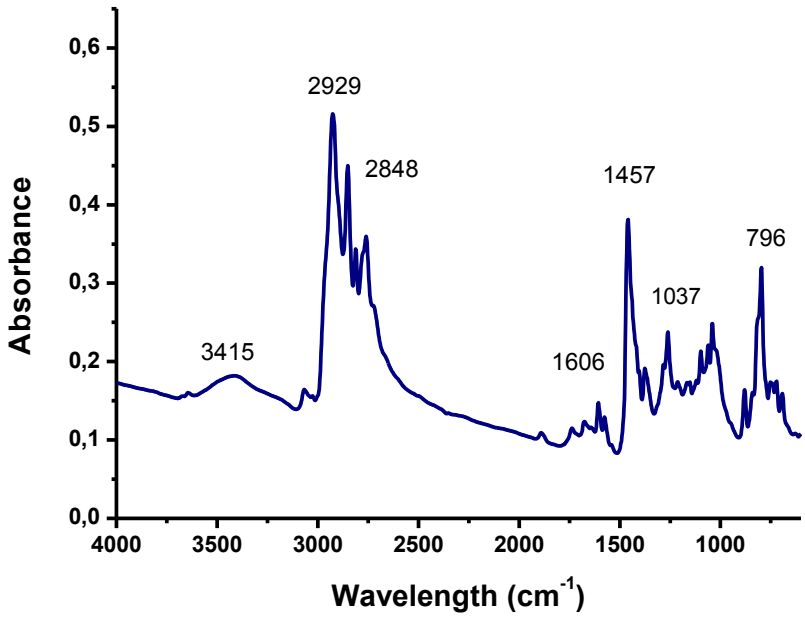

Figure 27. FT-IR spectrum of PFT.

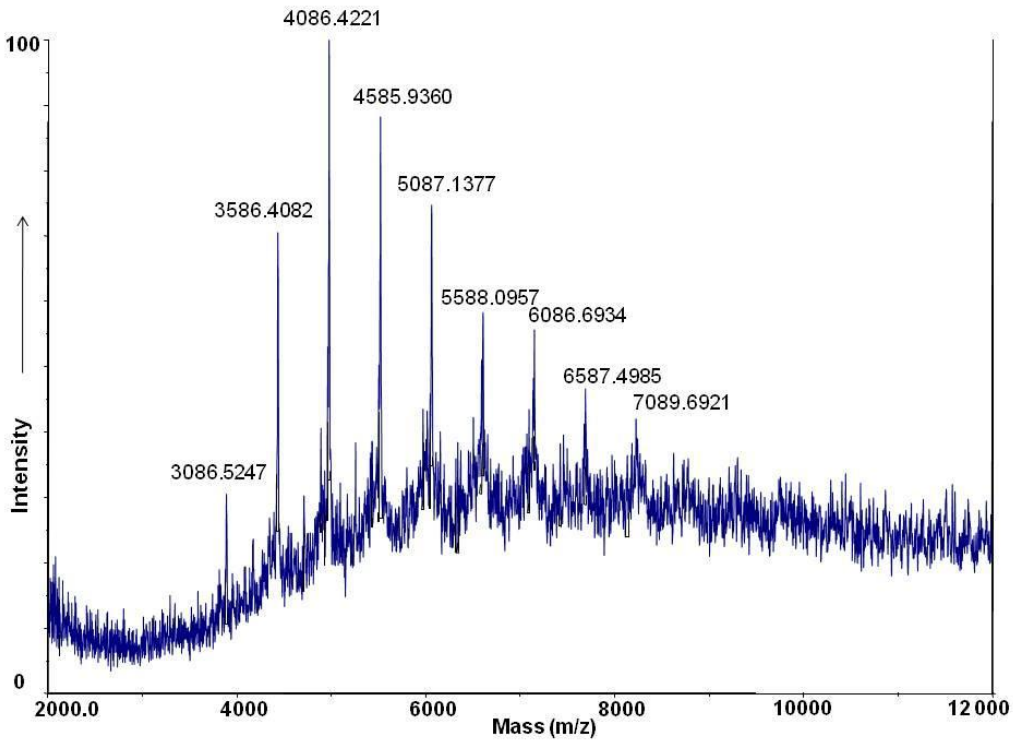

Figure 28. MALDI-TOF mass spectrum of PFT from a trihydroxy acetophenone (THAP) matrix.

2.2.3 Synthesis and Characterization of PFT@CB[8] Complex

PFT@CB[8] complex was prepared in water by adding CB[8] in sonicated PFT solution and stirred overnight; after filtration a bright green emitting solution was obtained. Then the solvent was removed under reduced pressure and a yellow powder was obtained.

PFT is known as soluble in solvents like methanol, THF, $CHCl_3$ and aqueous acid but not in water due to π-π stacking of aromatic backbone causing intrinsic aggregation, low water solubility and consequently low fluorescent quantum yield. However, water solubility for conjugated polymers like PFT is highly desirable due to being applicable in biology, optoelectronics and any other field that requires aqueous media[116,117,118] since as a conjugated light emitting polymer, it bears a high fluorescent quantum yield and high chemical stability.[119,120] Various approaches have been suggested to increase water solubility of this polymers as incorporation of bulky groups[121], interaction with surfactants[122,123] and encapsulating backbone of

the conjugated polymer with a suitable macrocycle[124-126]. In this thesis study, CB[n] derivatives (n=6, 7, 8) were used as macrocycles for enhancing water solubility and consequently fluorescent quantum yield of PFT. Among CB derivatives CB[7] is known as fairly water soluble while CB[6] and CB[8] are not considered as water soluble derivatives. However, only PFT@CB[8] yielded green light emitting bright aqueous solution and enhanced fluorescent quantum yield.

To understand the complex structure, NMR experiments were performed. However, as can seen below (Figure 29) water soluble version of PFT, protonated PFT gives very broad signals that make analysis difficult.

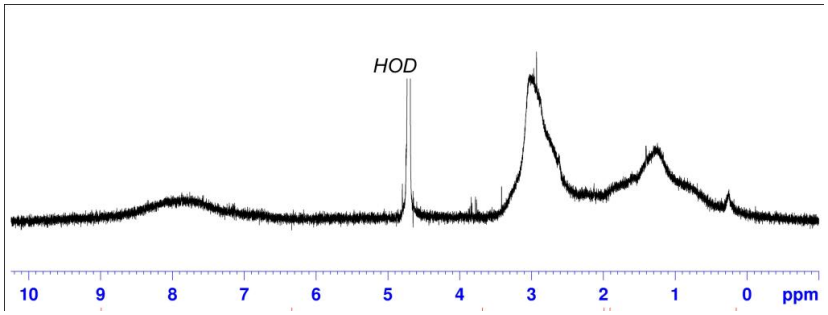

Figure 29.. ^{1}H-NMR (400 MHz, 298 K) spectrum of protonated PFT in D_2O (3 mM).

Therefore, for first ^{1}H-NMR experiment PFT was dissolved in $CDCl_3$ in the absence of CB[8] and compared with the PFT@CB[8] complex in D_2O (Figure 30). It is seen that there are significant changes in the aromatic region as 0.5-1 ppm upfield shift and side chain terminal methyl protons and in the protons next to nitrogen as 0.6 ppm downfield shift. It should be also note that aromatic backbone is interacting with Hx since it gives NOE due to irradiation at 5,73 ppm. Before further interpretation of these spectra, one should think of the possibility of solvent effect due to two different media with different solvents and different polarities consequently.

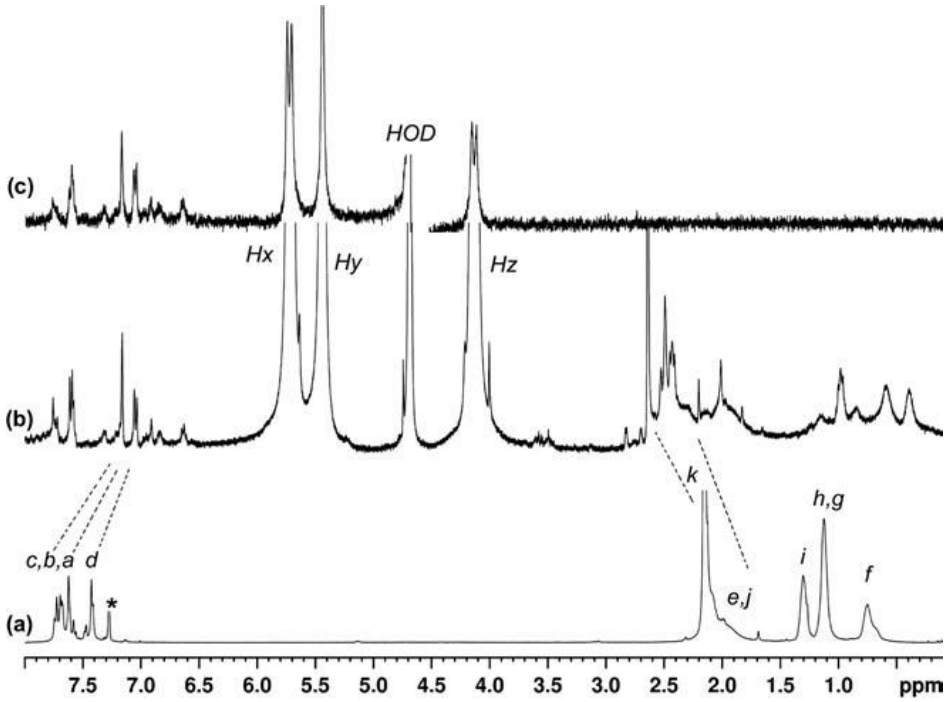

Figure 30.. 1H-NMR (400 MHz, 298 K) spectra of (a) PFT $CDCl_3$, (b) PFT@CB[8] (3 mM) in D_2O, and (c) 1D-NOESY spectrum of PFT@CB[8] in D_2O, proton Hx at 5,73 ppm was irradiated, mixing time D: 100 ms (* for CHCl3).

In the light of aforementioned curiosity, a control ^{1}H-NMR experiment was conducted with using 2,7-Dibromo-9-((3-bromo-hexyl)-dimethylamine)-9H-fluorene (M2) as the prototype of PFT. In the first ^{1}H-NMR experiment with this prototype, M2H-protonated monomer was used in the absence and presence of CB[8] in D_2O, M2 in $CDCl_3$ in the absence of CB[8] and M2 in the presence of CB[8] in D_2O (Figure 31). From a physical point of view, it should be noted that, M2 became water soluble in the presence of CB[8] while it is not in the absence of CB[8]. In the Figure 31-c, a and b proton signals shifted 0.6 ppm upfield while c shifted 0.1 ppm downfield; j proton belongs to side chain also shifted 0.3 ppm upfield in the presence of CB[8].

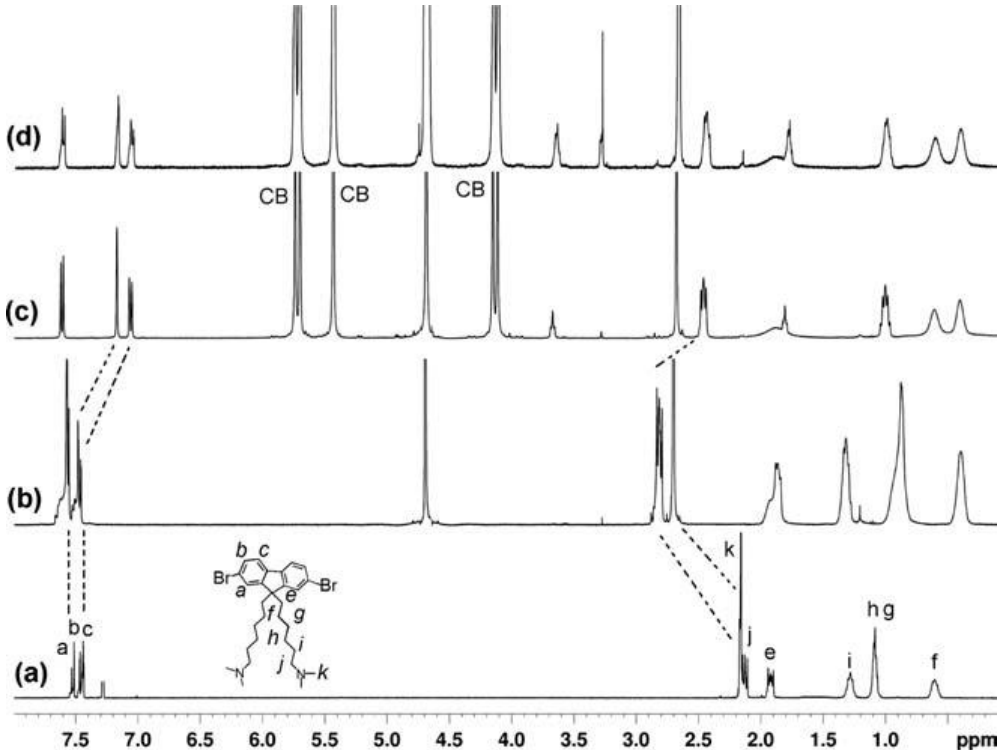

Figure 31. ^{1}H-NMR (400 MHz, 298 K) spectra of (a) M2 in $CDCl_3$, (b) protonated M2 (M2H) in D_2O, (c) M2H (4 mM) in the presence of 1 equiv CB[8] in D_2O, and (d) M2 (4 mM) in the presence of 1 equiv CB[8] in D_2O.

Selective 1D-NOESY NMR experiments were also conducted to monitor nature of the interaction (Figure 32). Firstly, by varying mixing times, all well-resolved peaks were irradiated and all correlation peaks were negative. Then the sample was irradiated at the peaks of fluorene protons, belong aromatic backbone, and large negative NOEs were observed at 5.71 ppm and 5.44 ppm that are resembling Hx and Hy protons of CB[8], respectively. For the further control of CB[8] protons', Hy and Hx, environment, sample was irradiated at 5.71 and 5.44 ppm and parallelly large negative NOEs were obtained from a,b and c protons belong to fluorene backbone; however, no correlations between side chain protons and CB protons were observed except for k protons residing in methyls bonded to nitrogen. A negative strong NOE was observed for k proton, when the sample irradiated at 4.12 ppm. Aforementioned protons bearing negative NOE due to the interaction with protons, Hx and Hy, of CB[8] and also 0.6 ppm upfield shift in b and c protons residing on fluorene backbone revealed the fact that aromatic protons were encapsulated by CB[8]. It should be noted that k protons residing on the methyls also showed negative NOE by

irradiation at 4.12 ppm, belongs to Hz proton of CB[8]. Another point to emphasize is identical k proton shifts of M2H in c and M2 in d, as a result of CB-assisted protonation of M2 in d caused by electron density withdrawing effect of portal carbonyl groups. It can be concluded that shift changes in PFT@CB[8] complex in Figure 30 was not due to solvent effect but caused by interacting species in complex.

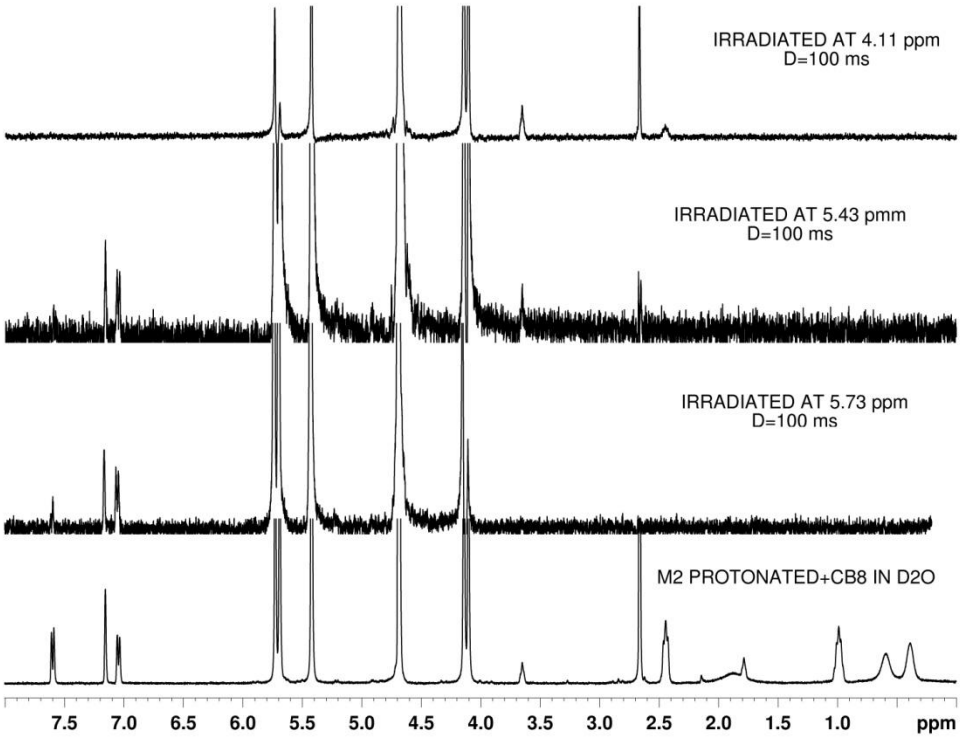

Figure 32.. Selective 1D-NOESY NMR spectra of M2H@CB[8] (400 Mz, D_2O, 25 °C).

After prototype experiments, PFT@CB[8] complex was also analysed by selective 1D-NOESY (Figure 33) and almost same interaction patterns were recorded as following: b and c protons gave negative NOE when Hx, at 5.73 ppm, and Hy, at 5.44 ppm, protons were irradiated; methyl protons, k, gave also negative NOE when Hz proton was irradiated at 4.11 ppm. From all aforementioned results, it can be stated that some part of the aromatic backbone of PFT was encapsulated by CB[8] and methyl protons were in the close proximity with CB[8]. This structure was illustrated in Figure 34.

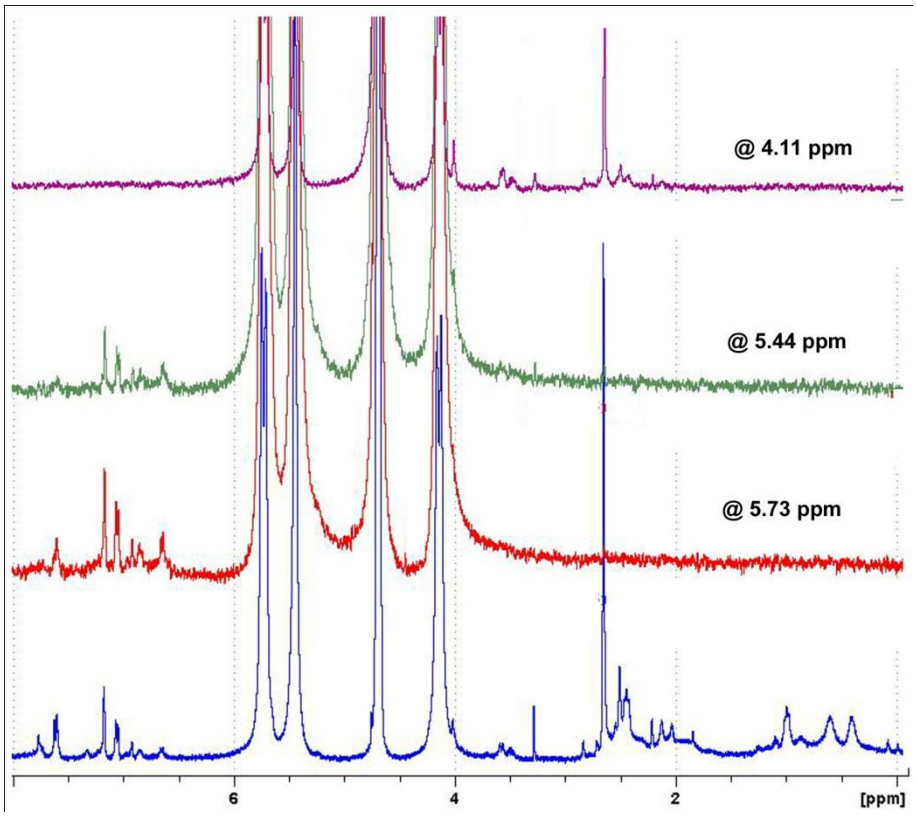

Figure 33. Selective 1D-NOESY NMR spectra of PFT@CB[8] (400 Mz, D_2O, 25 °C), Mixing time D: 100 ms.

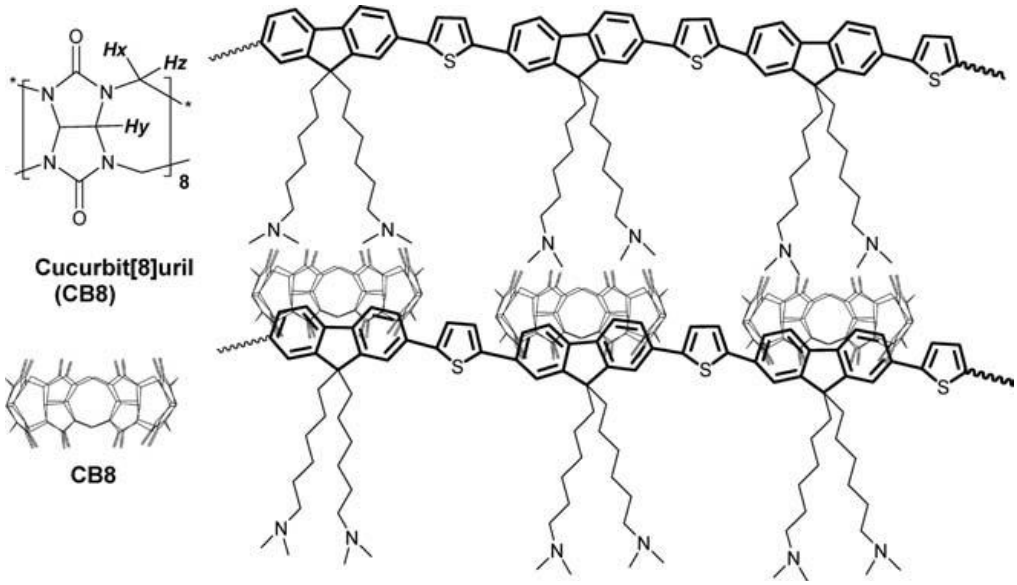

Figure 34. Suggested structure based on the 1H and 1D-NOESY NMR data for the PFT@CB[8] complex formation.

PFT@CB[8] complex exhibited also remarkable optical properties that enable the utilization of this conjugated polymer in the fields where high fluorescent quantum yield properties are required. That was noteworthy to compare absorption and emission properties of PFT in methanol, protonated PFT in water and PFT@CB[8] in water (Figure 35.). Absorbance of PFT protonated in water and PFT@CB[8] were red shifted identically by 3 and 6 nm, respectively, when compared to 436 nm maximum with 457 nm absorption of PFT in methanol. Emission of PFT in methanol was at 479 nm maximum and two vibronic bands at 511 and 549 whereas protonated PFT emitted at 485 nm with two vibronic bands at 519 and 558 nm. Finally, PFT@CB[8] exhibited an emission at 483 nm maximum with two vibronic bands at 515 and 552 nm; and as can be realised PFT @CB[8] emission was red-shifted by 4 nm relative to PFT in methanol and 2 nm blue shifted relative to protonated PFT.

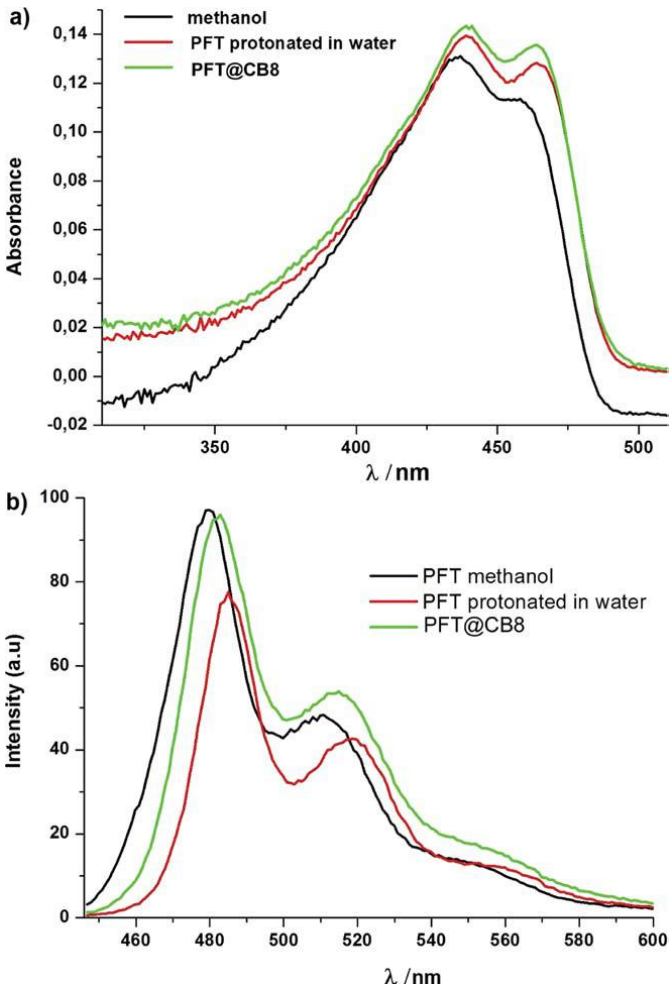

Figure 35. (a) UV–Vis absorption, (b) emission spectra of PFT in methanol, protonated PFT in water and PFT@CB[8] in water.

One of the most remarkable feature of PFT@CB[8] complex was considerably enhanced fluorescent quantum yield as 35% in water, when compared with 45% quantum yield of PFT in methanol and moreover 8% for protonated PFT in water (Table 4).

	λ_{max}abs [nm]	λ_{max}em [nm]	Φ_f[a] [%]	ε_{max}[c] [10^4 $M^{-1}cm^{-1}$]
PFT in MeOH	436, 457(sh)	479, 511, 549	45	4.2
Protonated PFT[b]	439, 464	485, 519, 558	8	2.2
PFT@CB[8][b]	439, 463	483, 515, 552	35	2.1

[a] Quantum yields were measured relative to quinine sulfate 0.1M H_2SO_4 (Φ_f = %55).
[b] Spectra were recorded in water. [c] Per repeat unit.

Table 4. Photophysical data for PFT in methanol, protonated PFT and PFT@CB[8].

Morphology of the complex was also investigated to gain a further understanding of the structure yielding in that much enhancement in emitting properties. Dynamic light scattering experiments in water showed aggregate formation in solution with a diameter of 700 nm, then after filtration by 0.45 μm syringe filter, a particle size around 200 nm was recorded (Figure 36).

Results

		Diam. (nm)	% Intensity	Width (nm)
Z-Average (nm): 651.1	Peak 1:	714.7	100	120.6
PDI: 0.202	Peak 2:	0	0	0
Intercept: 0.8239	Peak 3:	0	0	0

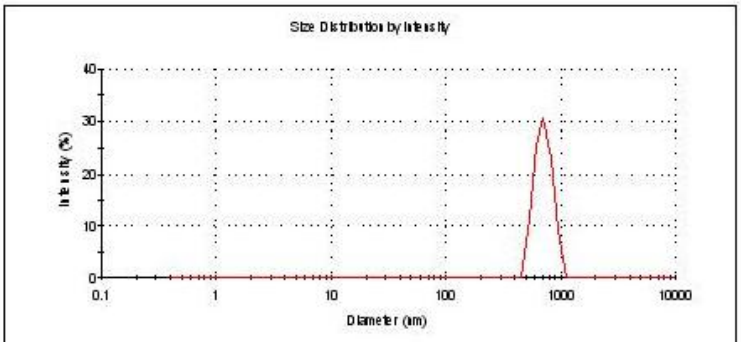

Results

		Diam. (nm)	% Intensity	Width (nm)
Z-Average (nm): 276.3	Peak 1:	238.3	100	57.56
PDI: 0.278	Peak 2:	0	0	0
Intercept: 0.6086	Peak 3:	0	0	0

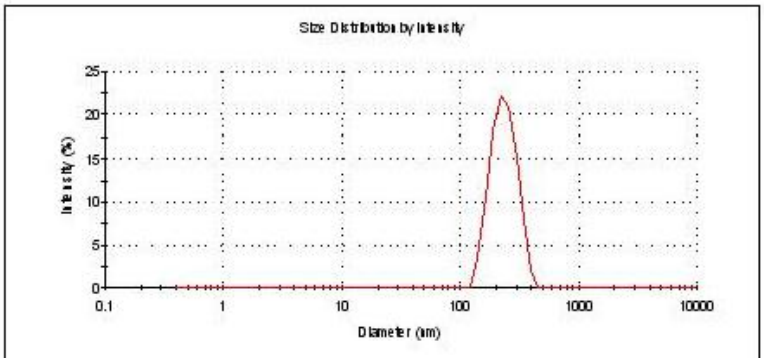

Figure 36. DLS results of PFT@CB[8] before and after filtration

Further investigation on morphology of the aggregates was performed by atomic force microscopy (AFM) (Figure 37), scanning electron microscopy (SEM) (Figure 3.25), transmission electron microscopy (TEM) (Figure 39) and fluorescent optical microscopy (FOM) (Figure 40). All of the investigations verified a spherical structure. AFM image showed particles ranging from 50 nm to 1μm, while SEM image revealed the defleated and collapsed structure and TEM showed formation of vesicle like structure that emits in green as FOM image shows.

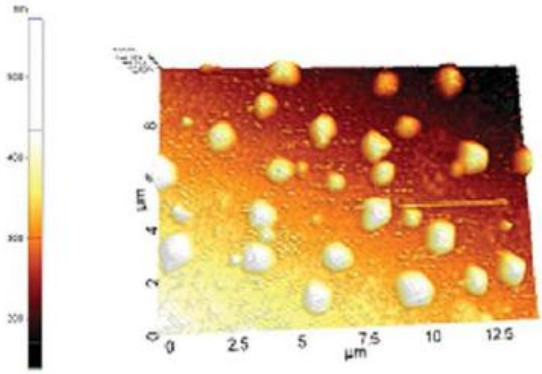

Figure 37. AFM image of PFT@CB[8].

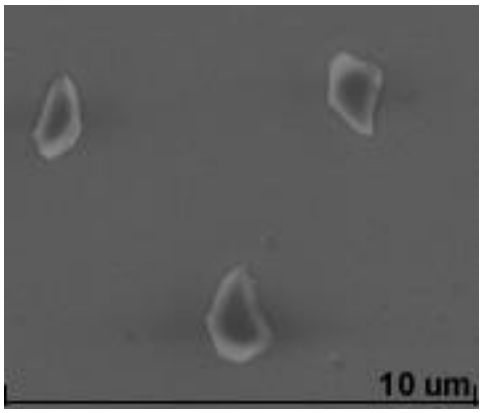

Figure 38. SEM image of PFT@CB[8].

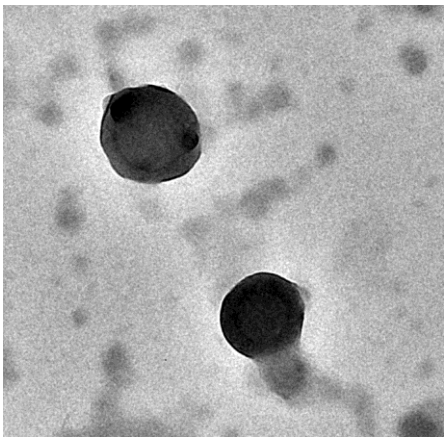

Figure 39. TEM image of PFT@CB[8].

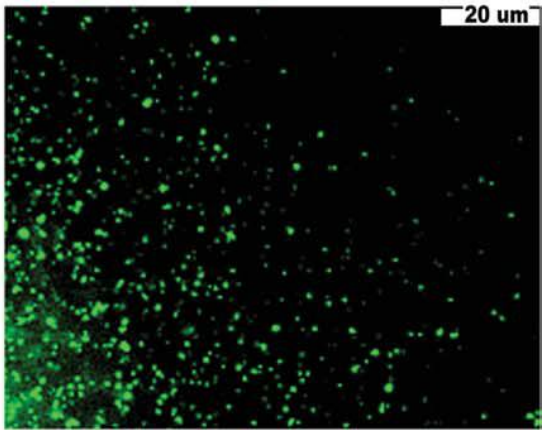

Figure 40. FOM (40x magnification) image of PFT@CB[8].

In the light of all those investigations, CB[8]-triggered vesicle formation was revealed, even formation mechanism is not clear, in a manner that a part of aromatic backbone is encapsulated by CB[8] and another layer's side chain methyl groups also interacting with CB[8] portals and portals of CB[8] in one side interacting with water to yield a water dispersed complex as illustrated in Figure 41. Consequently, this vesicle like somehow ordered structure hinders intrinsic aggregation and enhanced fluorescent quantum yield.

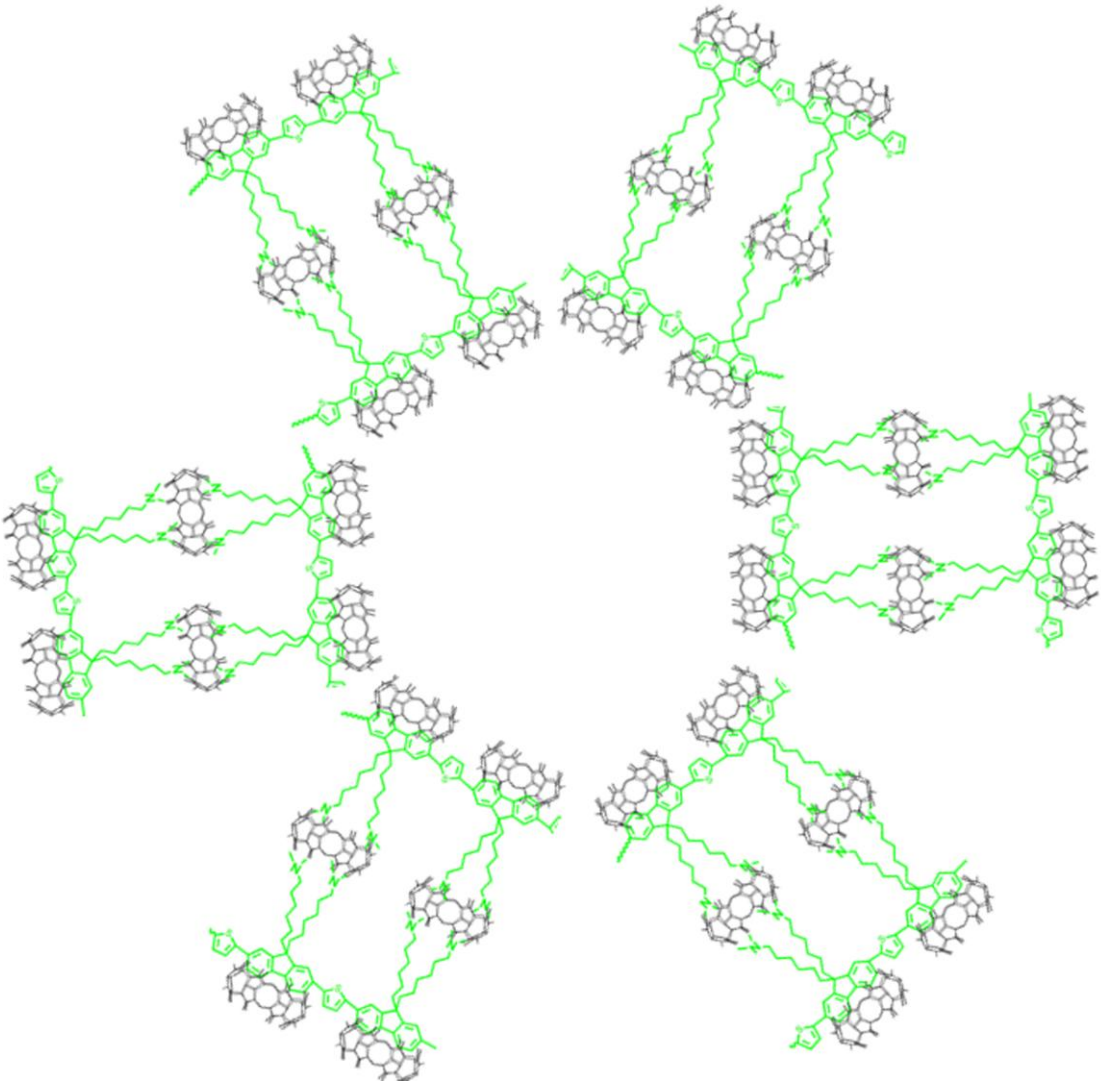

Figure 41. Suggested structure for the vesicles formation.

Chapter 3

CONCLUSION

In the first part of this thesis study synthesis and the characterization of an axle molecule N,N'-Bis-[1-(2-amino-ethyl)-1H-[1,2,3]triazol-4-ylmethyl]-dodecane-1,12-diamine bearing two binding sites and CB[n] (n= 6, 7, 8) derivatives were described; complexation behaviour of CB[6], CB[7] and CB[8] with the axle synthesized was covered and subsequently, isolation and characterization of the resulting pseudorotaxanes was introduced.

Aforementioned investigations were yielded in emerging recognition properties of CB[6], CB[7] and CB[8] that were investigated by using a two binding site bearing axle that is a product of Cu^{I}-catalyzed click reaction. Formation of complexes between CB[8] and axle in the following ratios as 1:1, 1:1 and 1:2 for CB[8], CB[7] and CB[6], respectively, were investigated via ^{1}H-NMR and mass spectrometry. Beside monitoring the emerging ability of CB[6], CB[7] and CB[8] homologues in recognition of different binding sites of axle, a controllable formation of hetero[4]pseudorotaxane in the means of kinetic and order of addition factors were introduced.

In the second part of the thesis, synthesis and characterization of the necessary conjugated polymer and macrocycles were described and characterization of the structure of conjugated polymer-macrocycle complex that yielded in a dissolved, fluorescent aqueous solution was covered.

A CB[8]-triggered vesicle formation was revealed by techniques consisting ^{1}H-NMR, 1D-NOESY, UV-Vis, Fluorescence, Scanning electron, Transmission electron, atomic force and mass spectrometry, and also Dynamic Light Scattering. Moreover, this vesicle like, somehow ordered structure enhanced fluorescent quantum yield via hindering intrinsic aggregation.

Chapter 4

EXPERIMENTAL SECTION

4.1 Materials

Literature procedures were used for the preparation of Azide 1[110] and CB[6], CB[7] and CB[8][109]. Unless noted, all solvents and reagents were in the commercial reagents grade and no further purification step was applied. Silica gel (Kieselgel 60, 0.063-0.200 mm) was used for column chromatography. Silica gel plates (Kieselgel 60 F254, 1mm) were chosen for thin layer chromatography (TLC).

4.2 Instrumentation

Bruker Avance DPX-400 MHz spectrometer was used for Nuclear magnetic resonance (NMR) spectra recordings. D_2O with DSS (3(trimethylsilyl)- 1-propanesulfonic acid sodium salt) was used as an external standard for sample preparation. For 1D-NOESY NMR experiments, selgonp is used and mixing time (D) is varied at 25 °C. Mass spectra were taken on Applied Bio systems MALDI-TOF MS mass spectrometer, equipped with a YAG-Laser (λ = 335 nm) at 10^{-7} Torr, was used and 300 ns delayed extraction mode was used by changing the laser intensity, when necessary. A potential of 20 kV acceleration was used for the reflector mode and average of 60 laser shots were applied and consequently, transferred data to a personal computer was processed further. The MALDI matrix was 2,4,6- Trihydroxyacetophenone (THAP). As scanning electron microscope, Quanta 200 FEG was used and a FEI (model Tecnai G2F30) TEM was used with accelerating voltage of 200 kV. For sample preparation, a copper grid was used and after dropping PFTCB[8] in water, carbon membrane was coated. XE-100E PSIA model microscope was used for AFM imaging, and PFT@CB[8] was drop casted on a silicon wafer. DLS measurements were conducted using Malvern NanoS spectrometer at 633 nm as light source was used and with the angle of 173°.

4.3. Synthesis

4.3.1 Synthesis of N,N'-Bis-[1-(2-amino-ethyl)-1H-[1,2,3]triazol-4-ylmethyl]-dodecane-1,12-diamine:

N,N'-Bis-(2-azido-ethyl)-dodecane-1,12-diamine.2HCl (150 mg, 0.36 mmol), propargylamine.HCl (83 mg, 0.91 mmol) were dissolved in an ethanol-water mixture (5 ml, 2:3, v/v). Consequently, $CuSO_4.5H_20$ (4.5 mg, 0.015 mmol) and sodium ascorbate (7.5 mg, 0.036 mmol) were added. Mixture was stirred at RT overnight, then poured into water (5 ml) and 1M NaOH solution (2 ml) was added. It was stirred for 30 min and extracted with chloroform. Organic phase was collected and the solvent was removed under reduced pressure. The remaining solid residue was suspended in water and stirred further 30 min. Then precipitates (white) were collected by filtration and 3h dried under high vacuum.

Yield: 170 mg, (92%).

M.p. 122-123 °C

Elemental Analysis for $C_{22}H_{44}N_{10}$

Calc.: C, 58, 90; H, 9, 89; N, 31, 22; found: C, 58, 63; H, 10.01; N, 31.07

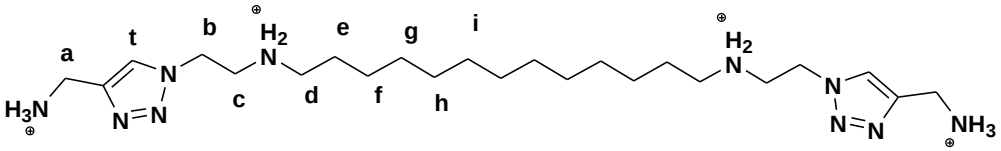

Axle A

^{1}H NMR (400 MHz, $CDCl_3$, 25 °C): δ= 1.18 (m, 8H, **F,G,H**), 1.38 (m, 2H, **E**), 1.51 (m, 6H, -N**H**), 2.54 (t, 2H,$^3J_{HH}$ = 7.2 Hz, **D**), 3.03 (t, 2H, $^3J_{HH}$ = 5.9 Hz, **A**), 3.92 (s, 2H, **C**), 4.37 (t, 2H, $^3J_{HH}$ = 5.9 Hz, **B**), 7.47 (s, 1H, **T**); ^{13}C NMR (100 MHz, D_2O, 25 °C): δ=27.4, 29.6, 29.7, 30.2, 37.7, 49.6, 49.7, 50.4, 122.8 (triazole, = CH), 148.8 (triazole, = CR).

By dissolving it in diluted HCl solution, hydrochloride salt of the ditriazole **Axle A** compound was prepared. After stirring overnight at rt, the solvent was removed under reduced pressure and the solid residue was washed with THF. It was dried under high vacuum 5h. (180 mg, 95%).

^{1}H NMR (400 MHz, $CDCl_3$, 25 °C): δ= 1.30 (m, 8H, **F,G,H**), 1.65 (m, 2H, **E**), 3.05 (t, 2H,$^{3}J_{HH}$ = 7.2 Hz, **D**), 3.56 (t, 2H, $^{3}J_{HH}$ = 5.9 Hz, **A**), 4.35 (s, 2H, **C**), 4.85 (t, 2H, $^{3}J_{HH}$ = 5.9 Hz, **B**), 8.12 (s, 1H, **T**).

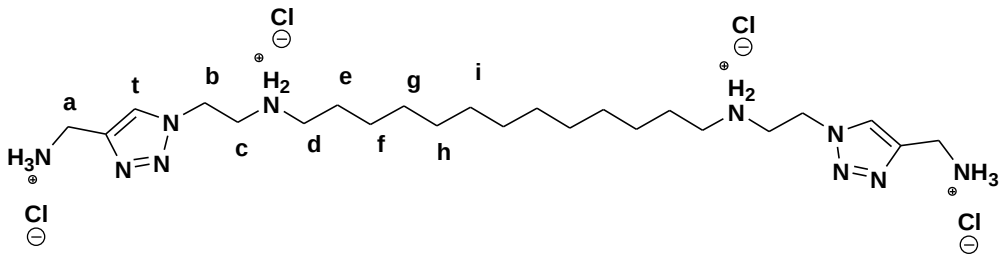

HCl salt of Axle A

4.3.2 Synthesis of {6-[2,7-Dibromo-9-(6-dimethylamino-hexyl)-9H-fluoren-9-yl]-hexyl}-dimethyl-amine:

Firstly, 2,7-Dibromo-9,9-bis(6-bromo-hexyl)-9H-fluorene (1 g, 1.54 mmol) and THF (5 mL) are placed in flask then degassed with argon. Then solution is cooled down to -78°C by liquid nitrogen. And then 2M solution of dimethylamine in THF 10 mL is put under Argon. This mixture is kept under room temperature (RT) for 24 hrs. After reaction is terminated, THF is removed under reduced pressure and added 0.1M NaOH (5 mL) and $CHCl_3$ (10 mL). The mixture is stirred for 30 min; then organic layer is taken and dried over $MgSO_4$. The solvent was removed under reduced pressure. Then flash chromatography on silica gel (ethylacetate/MeOH/NEt_3, 88:10:2) was applied for purification.

Yield : 0.85 g (94%)

^{1}H-NMR (400 MHz,$CDCl_3$, δ): 0.62 (m, 2H, f), 1.08 (m, 4H, h), 1.26 (m, 2H, e), 1.95 (m, 2H, j), 1.09 (m, 8H, g, h), 7.47-7.59 (m, 3H, a, b, c) ppm.
^{13}C-NMR (100 MHz, $CDCl_3$, δ): 145.12 (l), 135.43 (d), 132.21 (c), 130.23 (a), 127.80 (b), 122.50 (n), 56.67 (m), 43.43 (j), 42.90 (e), 41.43 (k), 30.60 (g), 29.32 (i), 28.10 (h), 24.12 (f) ppm .

Elemental analysis:

Calculated for $C_{29}H_{42}Br_2N_2$: C 60.21, H 7.32, N 4.84; found: C 60.05, H 7.23, N 4.75.

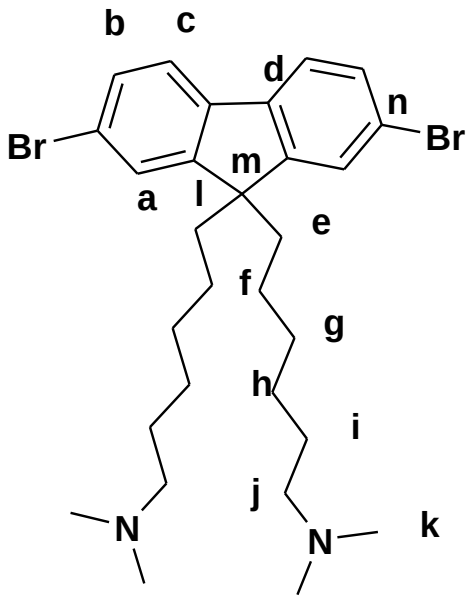

{6-[2,7-Dibromo-9-(6-dimethylamino-hexyl)-9H-fluoren-9-yl]-hexyl}-dimethyl-amine

4.3.3 Synthesis of Poly [9, 9-bis{6-(*N*,*N*-dimethylamino)hexyl}fluorene-*co*-2,5-thienylene] (PFT):

Firstly, {6-[2,7-Dibromo-9-(6-dimethylamino-hexyl)-9H-fluoren-9-yl]-hexyl}-dimethyl-amine (400 mg, 0.691 mmol), 2,5-thiophenediboronic acid (119 mg, 0,692 mmol), $PdCl_2$ (10 mg) and potassiumcarbonate (0.500 g, 3.61 mmol) are mixed in flask under argon. Then a mixture of water (3 mL) and THF (5 mL) are flushed with argon then added to reaction mixture. The mixture is stirred at 80°C, under vacuum for 24 hours and with a continuous flow of argon. After reaction terminates, the mixture is poured into water to have precipitated product. After filtration, residue is redissolved in THF and then precipitated into water. Then solid residue is filtered and polymers are dried for 12 hours; then ^{1}H NMR is applied.
Yield: 400 mg (77 %)

IR (KBr, pellet): 3445 cm^{-1}(m), 2930 cm^{-1}(m), 2850 cm^{-1}(m), 1600 cm^{-1}(m), 1475 cm^{-1}(m), 1043 cm^{-1}(m), 800 cm^{-1}(s).

^{1}H-NMR (400 MHz, $CDCl_3$, δ): 7.75 (m, 6 H, c, b, a), 7.52 (m, 2 H, d), 2.25 (br, 20 H, k, e, j), 1.45 (br, 4 H, i), 1.15 (br, 8 H, h, g), 0.75 (br, 4 H, f) ppm .

^{13}C-NMR (100 MHz, $CDCl_3$, δ): 145.40 (d), 141.93 (r), 138.12 (s), 133.52 (l), 130.63 (d), 128.87 (n), 127,2 (c,a,b), 121.6 (p,o), 58.55 (j), 43.54 (m), 42.91 (e), 41.50 (k), 29.62 (g), 29.40 (i), 28.55(h), 25.11(f) ppm.

UV-Vis: Abs (max) 436 nm

Fluorescence: Emission (max) 479 nm

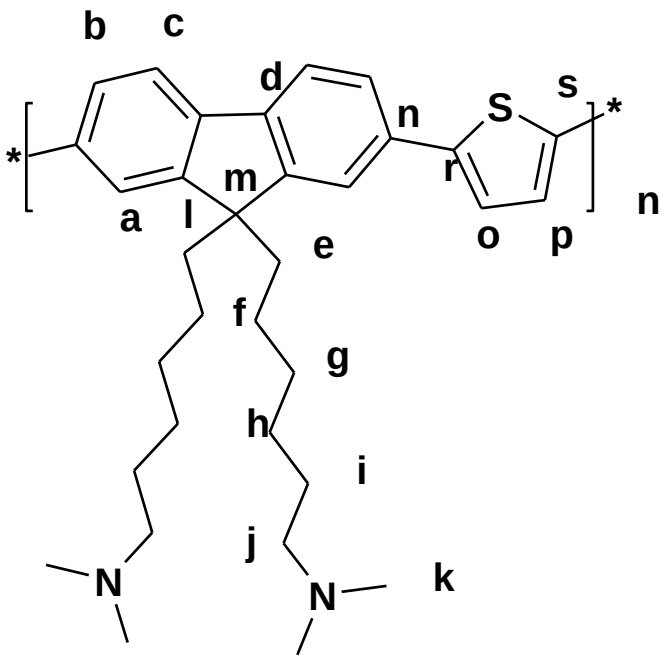

PFT

4.3.4 Synthesis of PFT@CB[8] Complex:

PFT (10 mg, 0.02 mmol) was suspended in 10 mL of water and then sonicated for 10 min and consequently CB[8] (40 mg, 0.03 mmol) was suspended into solution; the mixture was stirred overnight and undissolved particles were removed by suction filtration to obtain bright green emitting solution. The solvent was removed under reduced pressure and yellow powder was obtained.

REFERENCES

[1] D. J. Cram, Nobel Lecture, the Design of Molecular Hosts, Guests, and Their Complexes, Nobel Lecture, 8 December 1987

[2] J-M. Lehn, Nobel Lecture, Supramolecular Chemistry – Scope and Perspective

Molecules – Supermolecules - Molecular Devices, December 8, 1987

[3] C. J. Pedersen, Nobel Lecture, The Discovery of Crown Ethers, December 8, 1987

[4] J. F. Stoddart, *Nature Chem.* , 2009, **1**, 14-15.

[5] http://en.wikipedia.org/wiki/Supramolecular_chemistry

[6] J. W. Steed, D. R. Turner, K.J. Wallace, Core Concepts in Supramolecular Chemistry and Nanochemistry, Wiley, 2007.

[7] J. W. Steed, J. L. Atwood, Supramolecular Chemistry, Second Edition, 2009.

[8] H.M. Powell, P. Riesz, *Nature*, 1948, **161**, 52-53.

[9] A. R. Far, D. M. Rudkevich, T. Haino, J. Rebek, *J. Org. Lett.*, 2000, **2**, 22.

3465-3468.

[10] a] R.M. Izatt, K. Pawlak, J.S. Bradshaw, *Chem Rev*, 1991, **91**, 1721-2085. B] R.M. Izatt, J.S. Bradshaw, S.A. Nielsen, J.D. Lamb, J.J. Christensen, *Chem Rev.*, 1985, **85**, 271-339

[11] D. Tzalis, Y. Tor, *Tetrahedron*, 1996, **37**, 8393-8296.

[12] S. Roelens, R. Torriti, *Supramolecular Chem.*, 1999,**10**, 225-232.

[13] P.C. Kearney, L.S. Mizoue, R.A. Kumpf, J.E. Forman, A. McCurdy, D.A. Dougherty, *J. Am Chem Soc*,1993,**115**, 9907-9919.

[14] (a) A. Ikeda, S. Shinkai, *Chem Rev.*,1997, **97**, 1713-34; (b) A. Ikeda, S. Shinkai, *J Am Chem Soc*,1994, **116**, 3102-3110.

[15] S. Kumar, G. Hundal, D. Paul, M.S. Hundal, H. Singh, *J Org Chem*, 1999, **64**, 7717-7726.

[16] A.Villiers, Compt. Rend. Fr., *Acad. Sci.* 1891, **8**, 435.

[17] A. Harada, *Acc. Chem. Res.*, 2001, **34**, 456–464.

[18] R. Behrend, E. Meyer, F. Rusche, *Justus Liebigs Ann. Chem.*, 1905, **1**, 339.

[19] W.A. Freeman, W.L. Mock, N.-Y. Shih, *J. Am. Chem.*, 1981, **103**, 7367-7368.

[21] A. L. Koner, C. Marquez, M. H. Dickmann, W.M. Nau, *Angew. Chem.*, 2011, **123**, 567-571; *Angew. Chem. Int. Ed.*, 2011, **50**, 545-548.

[22]H.-J. Buschmann, A. Wego, E. Schollmeyer, D. Döpp, *Supramol. Chem,*. 2000, **11**, 225-231.

[23]K.Kim, *Chem.Soc.Rev*., 2002, **31**, 96-107.

[24]U. Rauwald, O.A. Scherman, *Angew. Chem,*. 2008, **120**, 4014-4017; *Angew. Chem. Int. Ed.,* 2008, **47**, 3950-3953.

[25]E.A. Appel, U. Rauwald, S. Jones, J. M. Zayed, O.A. Scherman, *J.Am. Chem. Soc.* 2010,**132**, 14251-14260.

[26]D. Das, O. A. Scherman, *Isr. J.Chem.* 2011, **51**, 537-550.

[27]D. Tuncel, Ö. Ünal, M. Artar, *Isr. J. Chem.* 2011, **51**, 525-532.

[28]A. R. Urbauch, V. Ramalingam, *Isr. J. Chem.* 2011, **51**, 664-678.

[29]Y. H. Ko, I. Hwang, D.-W. Lee, K. Kim, *Isr. J. Chem.* 2011, **51**, 506-514.

[30] D. H. Macartney, *Isr. J. Chem.* 2011, **51**, 600-615.

[31]L. BiczoK, V. Wintgens, Z. Miskolczy, M. Megyesi, *Isr. J. Chem.* 2011, **51**, 625-633.

[32] A. C. Bhasikuttan, S. D. Choudhury, H. Pal, J. Mohanty, *Isr. J. Chem.* 2011, **51**, 634-645.

[33] G. Parvari, O. Reanya, E. Keinan, *Isr. J. Chem.* 2011, **51**, 646-663.

[34]H.- J. Buschmann, *Isr. J. Chem.* 2011, **51**, 533-536.

[35]Y. Chen, Y.-M. Zhang, Y. Liu, *Isr. J. Chem.* 2011, **51**, 559-577.

[36]F. Yang, D.V. Dearden, *Isr. J. Chem.* 2011, **51**, 551-558.

[37] A. I. Day, R. J. Blanch, A. P. Arnold, S. Lorenzo, G. R. Lewis, I. Dance, *Angew. Chem.* 2002, **114**, 285 – 287; *Angew . Chem. Int. Ed.* 2002, **41**, 275 – 277.

[38] J. Lagona, P. Mukhopadhyay, S. Chakrabarti, L. Isaacs, *Angew. Chem. Int. Ed.* 2005, **44**, 4844 – 4870

[39] W.-H. Huang, P.Y. Zavalij, L. Isaacs, *J.Am. Chem. Soc.* 2008, **130**, 8446-8454.

[40] D. Jiao, N. Zhao, O. A. Scherman, *Chem. Commun.* 2010, **46**, 2007-2009.

[41] B. Honig, A. Nicholls, *Science*, 1995, **268**, 1144 – 1149.

[42] P. Germain, J. M. Letoffe, M. P. Merlin, H.-J. Buschmann, *Thermochim. Acta,* 1998, **315**, 87 – 92.

[43] H.-J. Buschmann, E. Cleve, E. Schollmeyer, *Inorg. Chim. Acta*, 1992, **193**, 93 – 97.

[44] J. Szejtli, *Chem. Rev.* 1998, **98**, 1743 – 1753.

[45] F. Trotta, M. Zanetti,G. Camino, *Polym. Degrad. Stab.* 2000, **69**, 373 – 379.

[46] H.-J. Buschmann, K. Jansen, C. Meschke, E. Schollmeyer, *J. Solution Chem.* 1998, **27**, 135 – 140.

[47] G.-L. Zhang, Z.-Q. Xu, S.-F. Xue, Q.-J. Zhu, Z. Tao, Wuji Huaxue Xuebao, *Acta Phys Chim Sin*, 2003, **19**, 655 – 659.

[48] K. Jansen, H.-J. Buschmann, A.Wego, D. DWpp, C. Mayer, H. J. Drexler, H. J. Holdt, E. Schollmeyer, *J. Inclusion Phenom. Macrocyclic Chem.* 2001, **39**, 357 – 363.

[49] R. Ballardini, V. Balzani, A. Credi, M.T. Gandolfi, M. Venturi, *Acc. Chem. Res.* 2001, **34**, 6: 445–455.

[50] W.L. Mock, N.-Y. Shih, *J. Org. Chem.* 1986, **51**, 4440-4446

[51] http://en.wikipedia.org/wiki/File:Cyclodextrin.svg

[52] Browne W. R., Feringa B. L., Nature Nano., 2006, 1, 25-35.

[53] K. Jansen, H.-J. Buschmann, A.Wego, D. DWpp, C. Mayer, H. J. Drexler, H. J. Holdt, E. Schollmeyer, *J. Inclusion Phenom. Macrocyclic Chem.* 2001, **39**, 357 – 363.

[54] K. N. Houk, A. G. Leach, S. P. Kim, X. Zhang, *Angew. Chem.* 2003, **115**, 5020 – 5046; *Angew. Chem. Int. Ed.* 2003, **42**, 4872 –4897.

[55]M. V. Rekharsky, Y. Inoue, *Chem. Rev*. 1998, **98**, 1875 – 1917.

[56] H.-J. Buschmann, K. Jansen, E. Schollmeyer, *Thermochim. Acta* 2000, **346**, 33 – 36.

[57] H. Fujiwara, H. Arakawa, S. Murata, Y. Sasaki, *Bull. Chem. Soc. Jpn.* 1987, **60**, 3891 – 3894.

[58] R. M. Izatt, R. E. Terry, B. L. Haymore, L. D. Hansen, N. K. Dalley, A. G. Avondet, J. J. Christensen, *J. Am. Chem. Soc.* 1976, **98**, 7620 – 7626.

[59] J. W. Lee, S. Samal, N. Selvapalam, H.-J. Kim, K. Kim, *Acc. Chem. Res.* 2003, **36**, 621 – 630.

[60] Y. Shen, S. Xue, Y. Zhao, Q. Zhu, Z. Tao, *Chin. Sci. Bull.* 2003, **48**, 2694 – 2697

[61] P. Mukhopadhyay, A. Wu, L. Isaacs, *J. Org. Chem.* 2004, **69**, 6157 – 6164.

[62] P. Ma, J. Dong, S. Xiang, S. Xue, Q. Zhu, Z. Tao, J. Zhang, X. Zhou, *Sci. China Ser. B* 2004, **47**, 301 – 310.

[63] B. D. Wagner, N. Stojanovic, A. I. Day, R. J. Blanch, *J. Phys. Chem. B* 2003, **107**, 10 741 – 10746.

[64]K.-C. Zhang, T.-W. Mu, L. Liu, Q.-X. Guo, *Chin. J. Chem.* 2001, **19**, 558 – 561.

[65] J. Kim, I.-S. Jung, S.-Y. Kim, E. Lee, J.-K. Kang, S. Sakamoto, K. Yamaguchi, K. Kim, *J. Am. Chem. Soc.* 2000, **122**, 540 – 541.

[66] S. Choi, S. H. Park, A. Y. Ziganshina, Y. H. Ko, J.W. Lee, K. Kim, *Chem. Commun.* 2003, 2176 – 2177.

[67] H.-J. Kim, W. S. Jeon, Y. H. Ko, K. Kim, *Proc. Natl. Acad. Sci.* 2002, **99**, 5007 – 5011.

[68] W. Ong, M. GZmez-Kaifer, A. E. Kaifer, *Org. Lett.* 2002, **4**, 1791 – 1794.

[69]W. Ong, A. E. Kaifer, *Angew. Chem.* 2003, **115**, 2214 – 2217; *Angew. Chem. Int. Ed.* 2003, **42**, 2164 – 2167.

[70] W. Ong, A. E. Kaifer, *J. Org. Chem.* 2004, **69**, 1383 – 1385.

[71] K. Moon, A. E. Kaifer, *Org. Lett.* 2004, **6**, 185 – 188.

[72] R. J. Blanch, A. J. Sleeman, T. J.White, A. P. Arnold, A. I. Day, *Nano Lett.* 2002, **2**, 147 – 149

[73] W. Ong, A. E. Kaifer, *Organometallics* 2003, **22**, 4181 – 4183.

[74] T. W. Mu, L. Liu, K. C. Zhang, Q. X. Guo, *Chin. Chem. Lett.*2001, **12**, 783 – 786.

[75] J. W. Lee, K. Kim, S. Choi, Y. H. Ko, S. Sakamoto, K.Yamaguchi, K. Kim, *Chem. Commun.* 2002, 2692 – 2693.

[76]D. Jiao, F. Biedermann, F. Tiang, O. A. Scherman, *J. Am. Chem. Soc.* 2010, **132**, 15734-15743.

[77] W. L. Mock, N.-Y. Shih, *J. Org. Chem.* 1983,**48**,3619-3620

[78]V. V. Rostovtsev, L. G. Green, V. V. Fokin, K. B. Sharpless, *Angew. Chem. Int. Ed.* 2002, **41**, 2596

[79] W. M. Nau, O. A. Scherman, *Isr. J. Chem.*, 2011, **51**, 492-494.

[80] W. Jiang, C.A. Schalley, *PNAS*, 2009, 106, **26**, 10425-10429.

[81] P. Mukhopadhyay, A.-X. Wu, L. Isaacs, *J. Org. Chem.* 2004, **69**, 6157 – 6164.

[82]Stryer, L. Biochemistry; 4th ed.; W. H. Freeman: New York, 1995.

[83] P. Mukhopadhyay, A.-X. Wu, L. Isaacs, *J. Org. Chem.* 2004, **69**, 6157 – 6164.

[84]Tedxtalks brainport TEDxBrainport - Bert Meijer – “Why we cannot make life?”

[85] W. Jiang, Q. Wang, I. Linder, F. Klautzsch, C. A. Schalley, *Eur. J. Chem.*,2011, **17**, 8

[86] K. ER, Leigh DA, Zerbetto F, 2007, *Angew. Chem. Int. Ed.*, **46**, 72–191.

[87] GM,Whitesides, JP,Mathias, CT, Sedo,1991, *Science*, **254**, 1312–1319.

[89] G. Celtek, M. Artar, O. A. Scherman, D. Tuncel, *Chem. Eur. J.*, 2009, **15**, 10360-10363.

[90] J-M,Lehn, *Science*, 2002, **295**, 2400–2403.

[91]G. A. Breault, C. A. Hunter and P. C. Mayers, *Tetrahedron* , 1999,**55**, 17, 5265–5293.

[92] J. F. Stoddart, Nagoya Award Lecture, The Nature of the Mechanical Bond, 4 August 2004.

[93] I. T.,Harrison, S.,Harrison, *J. Am. Chem. Soc.* 1967, **89**, 5723.

[94] D. Whang, Y.-M. Jeon, J. Heo, K. Kim, *J. Am. Chem. Soc.* 1996, **118**, 11333-11334.

[95] C. Meschke, H.- J. Buschmann, E. Schollmeyer, *Macromol. Rapid Commun.* 1998, **19**, 59-63.

[96] H.-J. Buschmann, *Isr. J. Chem.*,2011, **51**, 533-536.

[97] F. Aricó, J. D. Badjic, S. J. Cantrill, A. H. Flood, K. C.-F. Leung, Y. Liu, and J. F. Stoddart, *Topics in Current Chemistry*, 2005, **249**, 203–259.

[98] I. Yoon, M. Narita, T. Shimizu, and M. Asakawa, *J. Am. Chem. Soc.*, 2004,**126**, 51, 16740–16741.

[99] N. Kameta, K. Hiratani and Y. Nagawa, *Chem. Commun.* , 2004, **51**, 466–467.

[100]V. Serreli, C.-F. Lee, E. R. Kay, D. A. Leigh, *Nature*, 2007, **445**, 7127, 523–527.

[101] D.Tuncel, J. H. G. Steinke, *Macromolecules*, 2004, **37**, 289.

[102] T. Ooya, N. Yui, *Crit. Rev. Ther. Drug Carrier Syst.*, 1999, **16**,289.

[103] H. Fujita, T. Ooya, N. Yui, *Macromol. Chem. Phys.*, 1999, **200**,706.

[104] H. Fujita, T. Ooya, N. Yui, *Macromolecules*, 1999, **32**, 2534.

[105] T. Ikeda, N. Watabe, T. Ooya, N. Yui, *Macromol. Chem. Phys.*1999,**32**,2534.

[106] T. Ikeda, T. Ooya, N. Yui, *Polym.J.*1999,**31**,658.

[107] T. Ooya, N. Yui, *ACS Symp. Ser*. 2000, **752**,375.

[108] T. Ooya, N. Yui, H. Tomita, W. K. Lee, K. M. Huh, *Macromol. Rapid Commun.*, 2002, **23**, 179.

[109] J. Kim, I-S Jung, S-Y Kim, E. Lee, J-K Kang,S. Sakamoto, K. Yamaguchi,K. Kim,*J. Am. Chem. Soc.* 2000**, 122**, 540-541.

[110] D.Tuncel, H.B.Tiftik, B Salih, *J. Mater.Chem.*, 2006, **16**, 3291- 3296.

[111] A. I. Day, A. P. Arnold, R. J. Blanch and B. Snushall, *J. Org. Chem.*, 2001, **66**, 8094-8100.

[112]K. A. Udachin, G. D. Enright, E. B. Brouwer, J. A. Ripmeester, *J. Supramol. Chem.* 2001, **1**, 97 –100.

[113] a) L. Trembleau, J. Rebek, Jr., *Science* 2003, **301**, 1219 – 1220; b) A. Scarso, L. Trembleau, J. Rebek, Jr., *J. Am. Chem. Soc*. 2004, **126**, 13512 – 13518; c) M. P. Schramm, J. Rebek, Jr., *Chem. Eur. J*. 2006, **12**, 5924 –5933; d) B. W. Purse, J. Rebek, Jr., *Proc. Natl. Acad. Sci*. 2006, **103**, 2530 – 2534.

[114]Y. H. Ko, Y. Kim, H. Kim, K. Kim, *Chem. Asian J.* 2011, **6**, 652 – 657.

[115] G. Merino, T. Heine, G. Seifert, *Chem. Eur. J.* 2004, **10**, 4367-4371.

[116] Hoven, V., Garcia, A., Bazan, G. C., Nguyen, T.-Q. *Adv Mater* 2008, **20**, 3793–3810.

[117]Liu, B., Bazan, G. C. *Chem Asian J* 2007, **2**, 499–504.

[118) Ho, H.-A., Be` ra-Abe` rem, M., Leclerc, M. *Chem Eur J* 2005, **11**,1718–1724.

[119] Scherf, U., List, E. J. W. *Adv Mater* 2002, **14**, 477–487.

[120]Leclerc, M. *J Polym Sci Part A: Polym Chem* 2001, **39**, 2867–2873.

[121] Zhu, B., Han, Y., Sun, M., Bo, Z. *Macromolecules* 2007, **40**, 4494–4500.

[122] Laurenti, M., Rubio-Retama, J., Garcia-Blanco, F., Cabarcosm, E. L. *Langmuir,* 2008, **24**, 13321–13327.

[123] D. Tuncel, N. Cindir, Ü. Koldemir, *J. Inc. Phen. Macrocyclic Chem.* 2006, **55**, 373-380.

[124] D. Tuncel, Ö. Özsar, H. B. Tiftik, B. Salih, *Chem. Commun.* 2007, 1369-1371.

[125] D. Tuncel, M. Katterle, *Chem. Eur. J.* 2008, **14**, 4110-4116.

[126] A. Heeger, Nobel Lecture, Semiconducting and Metallic Polymers: The Fourth Generation of Polymeric Materials, 8 December 2000.

[127] H. Shirakawa, Nobel Lecture, The Discovery of Polyacetylene Film: The Dawning of An Era of Conducting Poylmers, 8 December 2000.

[128]A. MacDiarmid, Nobel Lecture, “Synthetic Metals”: A Novel Role for Organic Polymers,8 December 2000.

[129] Burroughes, J. H., Bradley, D. D. C., Brown A. R., Marks, R. N.; Mackay, K.;

Friend, R. H., Burns, P. L., Holmes, A. B., *Nature*, 1990, **347**, 539–541

[130] Kraft, A., Grimsdale, A. C., Holmes, A. B., *Angew. Chem. Int. Ed.*, 1998, **37**, 402

[131]- Friend, R. H., Gymer, R. W., Holmes, A. B., Burroughes, J. H., Marks, R. N.,

Taliani, C., Bradley, D. C. C., Dos Santos, D. A., Brdas, J. L., Lgdlund, M.,

Salaneck, W. R., *Nature*, 1999, **397**, 121

[132] Bernius, M.T., Inbasekaran, M., O’Brien, J., Wu, W., *Adv. Mater*., 2000, **12**, 1737

[133] Mitschke, U., Bauerle, P. J. J., *Mater. Chem.*, 2000, **10**

[134] McQuade, D.T., Pullen, A. E., Swager, T. M., *Chem. Rev.*, 2000, **100**, 2537-2574

[135] Tessler, N., Denton, G. J., Friend, R. H., *Nature*,1996, **382**, 695-697

[136] McGehee, M. D., Heeger, A. J., *Advanced Materials*, 2000, **12**, 1655.

[137]Sariciftci, N.S., Braun, D., Zhang, C., Sardanov, V., Heeger, A.J., Stucky, G., Wudl, F., *Appl. Phys. Lett.*, 1993, **62**, 585

[138] http://cms.tnw.utwente.nl/polymers/conj_pol.htm

[139] http://en.wikipedia.org/wiki/Conductive_polymer

[140] Lemmer, U., Heun, S., Mahrt, R.F., Scherf, U., Hopmeier, M., Siegner, U., Gobel,E.O., Mullen, K., Bassler, H., *Chem. Phys. Lett.*, 1996, **240**, 373

[141] List, E. J. W., Gaal, M., Guentner, R., de Freitas, P. S., Scherf, U., *Synth. Met.*,

2003, **139**, 759

[142] M. Fukuda, K. Sawada, K. Yoshimo, *J. Polym. Chem.* 1993, **31**, 2465

[143] U. Scherf, E. J. W. List, *Adv. Mater.* 2002, **14**, 7, 477-487.

[144] H. D. Burrows, M. J. Tapia, S M. Fonseca, S.Pradhan, U. Scherf, C. L. Silva, A. A. C. C. Pais, A. J. M. Valente, K. Schillen,V. Alfredsson, A. M. Carnerup, M. Tomsic, A. Jamnik, *Langmuir* 2009, **25**, 10, 5545-5556.

[145]X. Shen, M. Bellette, G. Durocher, *Chem. Phys. Lett.* 1998, **298**, 201 – 210.

[146] C. Lagrost, K. I. C. Ching, J.-C. Lacroix, S. Aeiyach, M. Jouini, P.-C. Lacaze, J. Tanguy, *J. Mater. Chem.* 1999, **9**, 2351 – 2358.

[147] D. Tuncel, M. Artar, S.B. Hanay, *J. Polymer Sci.: Part A* 2010, **48**, 21, 4894-4899.

[148] S. Angelos, Y.-W. Yang, N. M. Khashab, J. F. Stoddart, J. I. Zink, *J. Am. Chem. Soc.*, 2009, **131**, 11344–11346.